

**Some pages of this thesis may have been removed for copyright restrictions.**

If you have discovered material in AURA which is unlawful e.g. breaches copyright, (either yours or that of a third party) or any other law, including but not limited to those relating to patent, trademark, confidentiality, data protection, obscenity, defamation, libel, then please read our [Takedown Policy](#) and [contact the service](#) immediately

VOLUME 1

DIAGENETIC PROCESSES IN ORE FORMATION WITH SPECIAL  
REFERENCE TO THE ZAMBIAN COPPERBELT AND  
PERMIAN MARL SLATE  
( 2 VOLUMES )

BY

MICHAEL ALEXANDER SWEENEY

Thesis submitted for the degree of  
Doctor of Philosophy

at the

University of Aston in Birmingham

February 1985



## Dedication

To my parents and family

## ACKNOWLEDGEMENTS

I am greatly indebted to my supervisors Drs. P. Turner and D. Vaughan for the help, encouragement and guidance they have given me at all stages of this work. I also acknowledge the debt owed to Dr. R. Ixer for his constant encouragement and for fruitful discussion. Dr. A. Chambers is thanked for his assistance with X-Ray Fluorescence Analysis. Special thanks are due to the technical staff of the Department of Geological Sciences, whose friendly help made my work so much easier, Eric Hartland and Beverley Parker are particularly thanked in this respect. Mrs. C. Jakeman of the Chemistry Department is thanked for assistance with carbon analysis, and Mr. R. Howell of the Department of Production is thanked for his technical assistance with electron optics. Dave Plant and Tim Hopkins of the Department of Geology, Manchester University are thanked for their help with electron-probe microanalysis. Helen Turner is thanked for the patience she showed while typing the thesis.

Much of the analytical data presented in this thesis are the result of periods of work at the Geochemistry Division (London), of the British Geological Survey. I am particularly indebted to J. Rouse, P. Greenwood and B. Spiro of the Stable Isotope Unit for their unwavering help and infectious enthusiasm, which made my times at Grays Inn Road so happy and productive. Jane Evans, also of the

Geochemistry Division, is thanked for her assistance with Rb/Sr analysis, and H. Attenbrough for his guidance with fluid inclusion analysis. Dr. D. B. Smith of the Newcastle branch of the British Geological Survey is thanked for his help in the field and for providing Marl Slate core material. Dr. J. Johnson, of the National Coal Board, is also thanked for providing Marl Slate core material for study.

The staff of the Department of Geology, Konkola Division of Z.C.C.M. Limited, are thanked for the help and encouragement they showed me while working with them. I am particularly indebted to Chris Tompkins and Dai Pascoe, both of whom taught me a great deal. The Management of Z.C.C.M. Limited, particularly Dr. P. Freeman, are thanked for their permission to work on material collected at Konkola, and other Copperbelt mines.

Finally, I would like to thank Professor D. D. Hawkes in whose department much of this work was performed, and the Natural Environment Research Council for financial support.

THE UNIVERSITY OF ASTON IN BIRMINGHAM

DIAGENETIC PROCESSES IN ORE FORMATION WITH SPECIAL  
REFERENCE TO THE ZAMBIAN COPPERBELT  
AND PERMIAN MARL SLATE  
(2 Volumes)

MICHAEL ALEXANDER SWEENEY

Submitted for the degree of  
Doctor of Philosophy  
February 1985

Summary

This thesis is concerned with the role of diagenesis in forming ore deposits. Two sedimentary 'ore-types' have been examined; the Proterozoic copper-cobalt orebodies of the Konkola Basin on the Zambian Copperbelt, and the Permian Marl Slate of North East England.

Facies analysis of the Konkola Basin shows the Ore-Shale to have formed in a subtidal to intertidal environment. A sequence of diagenetic events is outlined from which it is concluded that the sulphide ores are an integral part of the diagenetic process. Sulphur isotope data establish that the sulphides formed as a consequence of the bacterial reduction of sulphate, while the isotopic and geochemical composition of carbonates is shown to reflect changes in the compositions of diagenetic pore fluids. Geochemical studies indicate that the copper and cobalt bearing mineralising fluids probably had different sources. Veins which crosscut the orebodies contain hydrocarbon inclusions, and are shown to be of late diagenetic lateral secretion origin. Rb/Sr dating indicates that the Ore-Shale was subject to metamorphism at  $529 \pm 20$  myrs.

The sedimentology and petrology of the Marl Slate are described. Textural and geochemical studies suggest that much of the pyrite (framboidal) in the Marl Slate formed in an anoxic water column, while euhedral pyrite and base metal sulphides formed within the sediment during early diagenesis. Sulphur isotope data confirm that conditions were almost "ideal" for sulphide formation during Marl Slate deposition, the limiting factors in ore formation being the restricted supply of chalcophile elements. Carbon and oxygen isotope data, along with petrographic observations, indicate that much of the calcite and dolomite occurring in the Marl Slate is primary, and probably formed in isotopic equilibrium. A depositional model is proposed which explains all of the data presented and links the lithological variations with fluctuations in the anoxic/oxic boundary layer of the water column.

Keywords

ZAMBIAN COPPERBELT, MARL SLATE, DIAGENESIS,  
GEOCHEMISTRY, STABLE ISOTOPES



## CONTENTS

Page No.

### VOLUME I

Title Page	i
Acknowledgements	ii
Summary	iv
Contents	v

#### CHAPTER 1

#### PROJECT AIMS, APPROACH TO THE INVESTIGATION AND PLAN OF THE THESIS

1.1	Project Aims	1
1.2	Approach to the Investigation	2
1.3	Plan of the Thesis	3

#### CHAPTER 2

#### GEOCHRONOLOGY, STRUCTURE AND EVOLUTION OF THE COPPERBELT DEPOSITORY

2.1	Introduction	8
2.2	Geochronology and Structural Evolution of the Copperbelt.	8
2.2.1	The Basement Complex	8
2.2.1	The Age of the Lower Roan Sediments	10
2.2.3	Deformation of the Roan Sediments	11

2.2.4	The Age of the Lufilian Orogeny	16
2.3	Whole Rock Rb/Sr Age Determination at Konkola	16
2.4	Structural Geology of the Konkola Mine Area	17
2.5	Plate Tectonic Setting of the Copperbelt Depository	20
2.6	Conclusions and Summary	23

### CHAPTER 3

#### SEDIMENTARY AND FACIES INTERPRETATION OF THE MINDOLA CLASTICS FORMATION AND THE COPPERBELT OREBODY MEMBER

3.1	Introduction	25
3.2	Sedimentology of the Bancroft Clastics Member	26
3.2.1	Boulder Conglomerate	26
3.2.2	Pebble Conglomerate	26
3.2.3	Lower Porous Conglomerate	27
3.2.4	Footwall Quartzite	27
3.2.5	Argillaceous Sandstone	28
3.3	Facies Interpretation of the Bancroft Quartzite Member	29
3.4	Sedimentology of the Kafue Arenites Member	32
3.4.1	Porous Conglomerate	32
3.4.2	Footwall Sandstone	33
3.4.3	Footwall Conglomerate	34
3.5	Facies Interpretation of the Kafue Arenites Member	34

3.6	Sedimentology of the Copperbelt Orebody Member	36
3.7	Facies Interpretation of the Copperbelt Orebody Member	38
3.8	Sedimentology and Facies Interpretation of the Nchanga Quartzite Member.	41

#### CHAPTER 4

#### DIAGENESIS OF THE COPPERBELT OREBODY MEMBER AND THE FOOTWALL CONGLOMERATE AND FOOTWALL SANDSTONE UNITS

4.1	Introduction	42
4.2	Post Diagenetic Effects	42
4.3	Diagenetic Features of the Footwall Conglomerate and the Footwall Sandstone	43
4.3.1	Mechanical Infiltration of Clays	44
4.3.2	Dissolution and Replacement Features	44
4.3.3	Authigenic Minerals	45
4.3.3a	Accessory Minerals	45
4.3.3b	Dolomite	46
4.3.3c	Quartz	48
4.3.3d	Feldspars	48
4.3.3e	Sulphides	49
4.4	Paragenetic Sequence of Diagenetic Events in the Footwall Conglomerate and Footwall Sandstone	51

4.5	Diagenetic Features of the Copperbelt Orebody Member	53
4.5.1	Authigenic Minerals	54
4.5.1a	Accessory Minerals	54
4.5.1b	Dolomite	55
4.5.1c	Quartz	58
4.5.1d	Feldspars	59
4.5.1e	Sulphides	63
4.6	Paragenetic Sequence of Diagenetic Events in the Copperbelt Orebody Member	66
4.7	Summary and Conclusions	68

## CHAPTER 5

### REVIEW OF ISOTOPE VARIATION IN GEOLOGICAL SYSTEMS

5.1	Introduction	73
5.2	Fractionation Processes	73
5.3	Sulphur Isotope Fractionation	75
5.3.1	Equilibrium Fractionation	75
5.3.2	Kinetic Fractionation	76
5.3.3	Factors Affecting the Magnitude of Kinetic Fractionation	78
5.3.4	Factors Affecting the Isotopic Composition of Initial Sulphate	80
5.4	Carbon Isotope Fractionation	81
5.4.1	Equilibrium Fractionation	81



6.3.3	Geochemistry of Dolomite Samples	109
6.3.4	Discussion of Dolomite Isotope Data	110
6.3.5	Malachite Results	115
6.3.6	Discussion of Malachite Isotope Data	116
6.4	Geothermometry and Silicate Oxygen Isotope Results	118
6.5	Summary and Conclusions	119

## CHAPTER 7

### COPPERBELT GEOCHEMISTRY WITH SPECIAL REFERENCE TO THE KONKOLA BASIN

7.1	Introduction	122
7.2	Trace Element Geochemistry	124
7.2.1	Analysis of Trace Element Results	131
7.3	Vein Occurrences	133
7.3.1	Vein Geochemistry	136
7.4	Conclusions	140

## CHAPTER 8

### DISCUSSION AND CONCLUSIONS CONCERNING COPPERBELT ORE DEPOSITION WITH PARTICULAR REFERENCE TO THE KONKOLA BASIN

8.1	Tectonic Setting	143
8.2	Effects of Metamorphism (with particular reference to isotopic composition)	144

5.4.2	Kinetic Fractionation	82
5.4.3	Carbon Reservoirs	84
5.4.4	Variations in the Carbon Isotope Composition of Marine Water	85
5.5	Oxygen Fractionation	86
5.5.1	Equilibrium Fractionation	86
5.5.2	Temperature Determination	86
5.5.3	Oxygen Reservoirs	88
5.6	Conclusions	89

## CHAPTER 6

### STABLE ISOTOPE RESULTS FROM THE KONKOLA BASIN

6.1	Introduction	90
6.2	Sulphur Isotope Results	92
6.2.1	Discussion of Sulphate Source and its Isotopic Composition	92
6.2.2	Ore-Shale Results	93
6.2.3	Discussion of Ore-Shale $\delta^{34}\text{S}$ Values	95
6.2.4	Footwall Result and Discussion	98
6.2.5	Conclusions	99
6.3	Carbonate $\delta^{18}\text{O}$ and $\delta^{13}\text{C}$ Isotope Results	100
6.3.1	Discussion of Factors Affecting the Interpretation of Precambrian Carbonate Isotope Values	101
6.3.2	Dolomite Results	106

6.3.3	Geochemistry of Dolomite Samples	109
6.3.4	Discussion of Dolomite Isotope Data	110
6.3.5	Malachite Results	115
6.3.6	Discussion of Malachite Isotope Data	116
6.4	Geothermometry and Silicate Oxygen Isotope Results	118
6.5	Summary and Conclusions	119

## CHAPTER 7

### COPPERBELT GEOCHEMISTRY WITH SPECIAL REFERENCE TO THE KONKOLA BASIN

7.1	Introduction	122
7.2	Trace Element Geochemistry	124
7.2.1	Analysis of Trace Element Results	131
7.3	Vein Occurrences	133
7.3.1	Vein Geochemistry	136
7.4	Conclusions	140

## CHAPTER 8

### DISCUSSION AND CONCLUSIONS CONCERNING COPPERBELT ORE DEPOSITION WITH PARTICULAR REFERENCE TO THE KONKOLA BASIN

8.1	Tectonic Setting	143
8.2	Effects of Metamorphism (with particular reference to isotopic composition)	144

8.3	Palaeoenvironment of the Mindola Clastics	
	Formation and the Copperbelt Orebody Member	145
8.4	Diagenetic Events	147
8.5	Transportation and source of copper and cobalt	155
8.5.1	Transportation of Copper and Cobalt	156
8.5.2	Source of Copper and Cobalt	158

## CHAPTER 9

### INTRODUCTION, REGIONAL SETTING, SEDIMENTOLOGY AND PETROGRAPHY OF THE MARL SLATE

9.1	Introduction	167
9.2	Pre-Marl Slate Geological Setting	168
9.3	Mid-Permian (Zechstein) Marine Transgression	171
9.4	The Sedimentology and Petrography of the Marl Slate	173
9.4.1	Water depth and Marl Slate Thickness	173
9.4.2	Petrography of the Marl Slate	174
9.4.3	Cathodoluminescence Observations on the Marl Slate and the Transition Zone	176
9.4.4	Sulphide Forms in the Marl Slate and the Transition Zone	178

CHAPTER 10

GEOCHEMISTRY OF THE MARL SLATE

10.1	Introduction	181
10.2	Previous Work	181
10.3	Trace Element Geochemistry	183
10.4	Variation in the Organic Carbon content of the Doncaster Core	186
10.5	Calcite, Dolomite and Quartz Content and Carbonate Composition of the Doncaster Core	187
10.6	Discussion of Geochemical Results	189
10.7	Pyrite Formation and Marl Slate Geochemistry	190
10.7.1	C/S Ratios in the Marl Slate	194
10.7.2	Degree of Pyritization in the Marl Slate	195
10.7.3	Pyrite Compositional Variations Within the Marl Slate	197
10.8	Summary	198

CHAPTER 11

STABLE ISOTOPE RESULTS FROM THE MARL SLATE

11.1	Introduction	201
11.2	Carbon and Oxygen Isotope Results from Borehole J1000	204



11.3	Stable Isotope Results from the Marl Slate	
	Section of the Doncaster Core	205
11.3.1	Carbon Isotope Results	205
11.3.2	Oxygen Isotope Results	206
11.3.3	Sulphur Isotope Results	207
11.4	Discussion of the Stable Isotope Results from	
	the Marl Slate Section of the Doncaster Core	208
11.5	Stable Isotope Results from the Transition	
	Zone Section of the Doncaster Core	212
11.5.1	Carbon Isotope Results	212
11.5.2	Oxygen Isotope Results	212
11.5.3	Sulphur Isotope Results	213
11.6	Discussion of the Stable Isotope Results of	
	the Transition Zone of the Doncaster Core	214
11.7	Summary and Conclusions	217

## CHAPTER 12

### THE MARL SLATE : DISCUSSION AND CONCLUSIONS

12.1	Summary	222
12.1.1	Marl Slate Regional Setting and	
	Petrography	222
12.1.2	Geochemical Observations	224
12.1.3	Isotopic Observations	227
12.1.4	Textural and Compositional Observations	230
12.1.5	Conclusions	233

	<u>Page No.</u>
12.2 Proposed Model for Marl Slate Formation	236
12.3 Implications of the Proposed Model to Marl Slate Mineralization.	139
REFERENCES	244

## VOLUME II

	<u>Page No.</u>
Title Page	i
Contents	ii

### FIGURES

Figure 2.1	Location of the Copperbelt in relationship to tectonic structures, showing the different shear senses and movement directions (Modified after Coward and Daly, 1984).	2
Figure 2.2	Geological Map of the Zambian Copperbelt.	3
Figure 2.3	Re-interpretation of Copperbelt structures in terms of a thrusting model (after Coward and Daly, 1984).	4
Figure 2.4	Rb-Sr isochron diagram for samples of Ore-Shale.	5
Figure 2.5	Geological Map of the Konkola Mine Area.	6
Figure 2.6	Isopach map of the Hangingwall Quartzite (Nchanga Quartzite Member) after Naish, 1973.	7
Figure 2.7	Generalised chronology and effect of tectono-thermal events.	8
Figure 2.8	Reconstruction of events leading to the formation of the Lufilian Arc (after Unrug, 1983).	9



Figure 3.1	Diagrammatic log of the Mindola Clastic and Lower Kitwe Formations.	10
Figure 3.2	Schematic diagram of the depositional environment of units of the Bancroft Quartzite Member.	11
Figure 4.1	Suggested paragenetic sequence of diagenetic events in Footwall Rocks.	12
Figure 4.2	Correlation between carbon and copper (Borehole CP337).	13
Figure 4.3	Plot of cobaltiferous pyrite, chalcopyrite and carrollite compositions.	14
Figure 4.4	Suggested paragenetic sequence of diagenetic events in the Copperbelt Orebody Member (Ore-Shale).	15
Figure 4.5	Summary of the diagenetic stages in the formation of the Copperbelt Orebody Member and the Footwall Conglomerate and Sandstone.	16
Figure 4.6a	The System Cu-Fe-S-O-H at 25°C, 1 atm and total dissolved sulphur (after Garrels and Christ, 1965).	17
Figure 4.6b	Summary of the Eh-pH field for waters pertinent to Copperbelt Orebody Member and 'footwall rocks' diagenesis (after Becking et al., 1960).	
Figure 5.1	The reservoir effect: showing schematically successive aliquots in equilibrium with the reservoir (after Coleman, 1977).	18

Figure 5.2	Variation of $\delta^{34}\text{S}$ as a function of $f_{\text{O}_2}$ and $p_{\text{H}}$ (after Ohmoto, 1972)	19
Figure 5.3	Variation of $\delta^{34}\text{S}$ with sulphide/sulphate ratio (after Coleman, 1977).	20
Figure 5.4	Diagenetic zones of carbonate formation during sediment (Mudstone) burial (after Curtis, 1977; Irwin et al, 1977; and Benmore, 1983).	21
Figure 6.1	Histogram showing the frequency of Orebody $\delta^{34}\text{S}$ values.	22
Figure 6.2	Combined $\delta^{34}\text{S}$ values plotted against lithology.	23
Figure 6.3	Plot of $\delta^{18}\text{O}$ versus $\delta^{13}\text{C}$ results for Footwall and Ore-Shale samples.	24
Figure 6.4	Plot of $\delta^{13}\text{C}$ and ppm Sr against lithology for samples from Borehole CP197.	25
Figure 6.5	Plot of $\delta^{18}\text{O}$ against lithology for samples from Borehole CP197.	26
Figure 6.6	Carbon and oxygen isotope compositions for corrected Precambrian calcite values (modified after Hudson, 1977).	27
Figure 6.7	Plot of $\delta^{18}\text{O}$ versus $\delta^{13}\text{C}$ for Malachite samples.	28
Figure 6.8	Temperature distribution No. 1 Shaft (calculated from coexisting mineral pairs).	29
Figure 7.1	Location plan of sample Boreholes.	30
Figure 7.2	Element dendograms for samples from the footwall and unit A of the Ore-Shale.	31

Figure 7.3	Element dendograms for samples from units B and C of the Ore-Shale.	32
Figure 7.4	Element dendograms for samples from units D and E of the Ore-Shale.	33
Figure 7.5	Element dendogram for samples from the Hangingwall Quartzite.	34
Figure 7.6	Plot of normalised cation totals for quartz vein fluid inclusions from the Ore-Shale and Footwall.	35
Figure 9.1	Generalised sketch map of the western parts of the Zechstein basin showing the location of boreholes sampled (adapted from Smith, 1980).	36
Figure 9.2	Schematic block diagram of the Southern Permian Basin and Central North Sea system of highs at the time of the Zechstein transgression. (after Glennie and Buller, 1983).	37
Figure 9.3	Possible reaction pathways to framboidal and euhedral pyrite (after Raiswell, 1982).	38
Figure 10.1	Vertical profiles of geochemical parameters of the Marl Slate section of the Doncaster Core.	39
Figure 10.2	Vertical profiles of geochemical parameters of the Transition Zone section of the Doncaster Core.	40
Figure 10.3	Dendograms for samples from the J1000 and 49/26-4 cores.	41



Figure 10.4	Dendograms for samples from the Transition Zone and Marl Slate Sections of the Doncaster Core.	42
Figure 10.5	Dendograms for samples from the different lithologies of the Transition Zone core.	43
Figure 10.6	Plot of weight percent carbon versus weight percent pyrite sulphur for freshwater normal marine and anoxic sediments (adapted from Leventhal, 1983; Berner and Raiswell, 1983).	44
Figure 10.7	Organic carbon and pyrite sulphur plots for samples from the Doncaster Core.	45
Figure 10.8	Degree of pyritization against organic carbon content for the Marl Slate section of the Doncaster Core.	46
Figure 11.1	Plot of $\delta^{18}\text{O}$ and $\delta^{13}\text{C}$ values against height for Borehole J1000.	47
Figure 11.2	Plot of $\delta^{13}\text{C}$ , $\delta^{18}\text{O}$ , $\delta^{34}\text{S}$ and percentage dolomite in the carbonate phase for the Marl Slate section of the Doncaster Core.	48
Figure 11.3	Plot of percentage dolomite in the sample carbonate phase versus $\delta^{18}\text{O}$ and $\delta^{13}\text{C}$ values for the Marl Slate Section of the Doncaster Core.	49
Figure 11.4	Plot of $\delta^{13}\text{C}$ , $\delta^{18}\text{O}$ , $\delta^{34}\text{S}$ and percentage dolomite in the carbonate phase for the Transition Zone section of the Doncaster Core.	50
Figure 11.5	Plot of $\delta^{18}\text{O}$ versus $\delta^{13}\text{C}$ with lithology for the Transition Zone core.	51

Figure 11.6	Plot of $\delta^{18}\text{O}$ versus $\delta^{34}\text{S}$ with lithology for the Transition Zone core.	52
Figure 12.1	Proposed model of Marl Slate formation.	53
Figure 12.1	Concentration of dissolved and particulate iron and manganese in the Black Sea (after Brewer and Spencer, 1974).	54
Figure A3.1	Flow chart for sample preparation for Copperbelt Samples.	90
Figure A4.1	Linear regression plots for repeat carbonate samples.	94
Figure A6	Schematic diagram of equipment used in the analysis of fluid inclusion Gas/Liquid phases.	99
Figure A6.1	Fluid inclusion Gas/Liquid phase geochemistry - Footwall Sample 1 South.	101
Figure A6.2	Fluid inclusion Gas/Liquid phase geochemistry - Footwall Sample 2 South.	102
Figure A6.3	Fluid inclusion Gas/Liquid phase geochemistry - Ore-Shale 1 South.	103
Figure A6.4	Fluid inclusion Gas/Liquid phase geochemistry - Ore-Shale 2 South.	104
Figure A6.5	Fluid inclusion Gas/Liquid phase geochemistry - Ore-Shale 3 North.	105
Figure A8.1	Borehole AP644. (Appendix 8 and 10 in	
Figure A8.2	Borehole AP643. back pocket of thesis)	

Figure 11.6	Plot of $\delta^{18}\text{O}$ versus $\delta^{34}\text{S}$ with lithology for the Transition Zone core.	52
Figure 12.1	Proposed model of Marl Slate formation.	53
Figure 12.1	Concentration of dissolved and particulate iron and manganese in the Black Sea (after Brewer and Spencer, 1974).	54
Figure A3.1	Flow chart for sample preparation for Copperbelt Samples.	90
Figure A4.1	Linear regression plots for repeat carbonate samples.	94
Figure A6	Schematic diagram of equipment used in the analysis of fluid inclusion Gas/Liquid phases.	99
Figure A6.1	Fluid inclusion Gas/Liquid phase geochemistry - Footwall Sample 1 South.	101
Figure A6.2	Fluid inclusion Gas/Liquid phase geochemistry - Footwall Sample 2 South.	102
Figure A6.3	Fluid inclusion Gas/Liquid phase geochemistry - Ore-Shale 1 South.	103
Figure A6.4	Fluid inclusion Gas/Liquid phase geochemistry - Ore-Shale 2 South.	104
Figure A6.5	Fluid inclusion Gas/Liquid phase geochemistry - Ore-Shale 3 North.	105
Figure A8.1	Borehole AP644. (Appendix 8 and 10 in	
Figure A8.2	Borehole AP643. back pocket of thesis)	

Figure A8.3 Borehole AP647.

Figure A8.4 Borehole BV25C.

Figure A8.5 Borehole BV26C.

Figure A8.6 Borehole BP58N.

Figure A8.7 Borehole BP55N.

Figure A8.8 Borehole AP674.

Figure A8.9 Borehole AP646.

Figure A8.10 Borehole AP629.

Figure A8.11 Borehole AD203.

Figure A8.12 Borehole AP982.

Figure A8.13 Borehole CP197.

Figure A8.14 Borehole CP337.

Figure A8.15 Borehole AP978.

Figure A8.16 Borehole AP972.

Figure A10.1 Borehole J1000.

Figure A10.2 Borehole 49/26-4.

Figure A10.3 Borehole Marl Slate (D.C.).

Figure A10.4 Borehole Transition Zone (D.C.).



## LIST OF TABLES

		<u>Page No.</u>
Table 2.1	Stratigraphic succession of the Konkola Basin (classification modified after Clemmey, 1976).	56
Table 3.1	Summary of sedimentary features in the Copperbelt Orebody Member (Ore-Shale).	57
Table 4.1	Energy dispersive microprobe data for euhedral Footwall dolomites (all metals calculated as percent carbonate).	58
Table 4.2	Electron probe microanalysis of Carrollites.	59
Table 4.3	Electron probe microanalysis of feldspar grains (g) and authigenic overgrowths (A) from the Ore-Shale.	60
Table 6.1	Sulphur isotope results for samples from Borehole AP978.	61
Table 6.2	Sulphur isotope results from Ore-Shale and Footwall rock samples.	62
Table 6.3	Carbon and Oxygen isotope results for Konkola carbonates.	63
Table 6.4	Carbonate isotope results for whole rock samples from Borehole CP197.	64
Table 6.5	Atomic absorption analysis results of Footwall and Ore-Shale lenticle dolomites, and EPMA analysis of lenticle rim and core samples.	65
Table 6.6	Compositional and isotopic data for mine waters at Konkola.	66



Table 6.7	Isotope results of Malachite samples (in descending stratigraphic order).	67
Table 6.8	Silicate oxygen isotope results.	68
Table 7.1	Electron probe micro-analysis of fine grained and lenticular chalcopyrite.	69
Table 7.2	Electron probe micro-analysis of fine grained and lenticular bornite.	70
Table 7.3	Electron probe micro-analysis of rutile and zircon.	71
Table 7.4	Correlation between elements at the 95% confidence limit for combined borehole samples (n=243).	72
Table 7.5	Results of energy dispersive analysis of decrepitation products from Footwall and Ore-Shale Quartz veins.	73
Table 7.6	Normalised cation totals for decrepitated Ore-Shale and Footwall sample fluid inclusions.	74
Table 10.1	Mean trace element composition of Marl Slate Borehole samples.	75
Table 10.2	Normalised carbonate compositional data and percentage calcite/dolomite for the Doncaster Core.	76
Table 10.3	Compositional variation of pyrite from the Doncaster Core.	77
Table 11.1	Carbon and oxygen isotope results from Borehole J1000.	78

Table 11.2	Carbon, oxygen and sulphur isotope results from the Marl Slate section of the Doncaster Core.	79
Table 11.3	Carbon, oxygen and sulphur isotope results from the Transition Zone section of the Doncaster Core.	81
Table 12.1	Characteristic features of different lithological types associated with the Marl Slate.	82
Table A7.1	Correlation coefficients for all element pairs in Borehole AP644.	107
Table A7.2	Correlation coefficients for all element pairs in Borehole AP643.	108
Table A7.3	Correlation coefficients for all element pairs in Borehole AP647.	109
Table A7.4	Correlation coefficients for all element pairs in Borehole BV25C.	110
Table A7.5	Correlation coefficients for all element pairs in Borehole BV26C.	111
Table A7.6	Correlation coefficients for all element pairs in Borehole BP58N.	112
Table A7.7	Correlation coefficients for all element pairs in Borehole BP55N.	113
Table A7.8	Correlation coefficients for all element pairs in Borehole AP674.	114

Table A7.9	Correlation coefficients for all element pairs in Borehole AP646.	115
Table A7.10	Correlation coefficients for all element pairs in Borehole AP629.	116
Table A7.11	Correlation coefficients for all element pairs in Borehole AD203.	117
Table A7.12	Correlation coefficients for all element pairs in Borehole AP982.	118
Table A7.13	Correlation coefficients for all element pairs in Borehole CP197.	119
Table A7.14	Correlation coefficients for all element pairs in Borehole CP337.	120
Table A7.15	Correlation coefficients for all element pairs in Borehole AP978.	121
Table A7.16	Correlation coefficients for all element pairs in Borehole AP972.	122
Table A7.17	Correlation coefficients for all element pairs in all Boreholes.	123
Table A9.1	Correlation coefficients for all element pairs in Borehole J1000.	124
Table A9.2	Correlation coefficients for all element pairs in Borehole 49/26/4.	127
Table A9.3	Correlation coefficients for all element pairs in the Marl Slate section of the Doncaster Core.	128

Table A9.4	Correlation coefficients for all element pairs in the Transition Zone section of the Doncaster Core.	129
------------	--	-----

LIST OF PLATES (not numbered)		83
-------------------------------	--	----

Plate 3.1	Sedimentary structures.	
Plate 3.2	Sedimentary structures.	
Plate 3.3	Carbonate pseudomorphs.	
Plate 3.4	Sedimentary structures.	
Plate 4.1	Diagenetic features - feldspars.	
Plate 4.2	Diagenetic features - 'clay' coatings.	
Plate 4.3	Diagenetic features - replacement features.	
Plate 4.4	Diagenetic textures - carbonates.	
Plate 4.5	Diagenetic textures - carbonates.	
Plate 4.6	Diagenetic textures - sulphides/silicates.	
Plate 4.7	Diagenetic textures - sulphides/silicates.	
Plate 4.8	Diagenetic features - cathodoluminescence micrographs.	
Plate 4.9	Diagenetic textures - ore minerals.	
Plate 7.1	Fluid inclusions - salinit variation.	
Plate 7.2	Fluid inclusions - solid phases.	



Plate 7.3	Fluid inclusions - hydrocarbon.	
Plate 9.1	Field relationships - Yellow Sands.	
Plate 9.2	Field relationships - Yellow Sands.	
Plate 9.3	Algal coated clasts - Yellow Sands.	
Plate 9.4	Petrographic observations - Marl Slate.	
Plate 9.5	Petrographic observations - Marl Slate.	
Plate 9.6	Petrographic observations - Marl Slate.	
Plate 9.7	Cathodoluminescence observations - Marl Slate.	
Plate 9.8	Dolomite nodules - Marl Slate.	
Plate 9.9	Cross-cutting veins - Marl Slate.	
Plate 9.10	Pyrite forms - Marl Slate.	
Plate 9.11	Sulphide textures - Marl Slate.	
APPENDICES		84
Appendix 1	Cathodoluminescence Techniques	85
Appendix 2	Method of Determination of Whole-Rock Carbonate Carbon and Organic Carbon Content	86
Appendix 3	Technical Details of Sulphur Isotope Analysis and Sample Preparation	87
Appendix 4	Technical Details of Carbonate Isotope Analysis and Sample Preparation	91

Appendix 5	Trace Element Determination by X-Ray Flourescence	95
Appendix 6	Sample Preparation and Analysis of Fluid Inclusion Gas/Liquid Phases	98
Appendix 7	R-Mode Correlation Matrices for Borehole Element Pairs Copperbelt Boreholes	106
Appendix 8	Trace Element Concentration Profiles Copperbelt Borehole Cores	124
Appendix 9	R-Mode Correlation Matrices for Borehole Element Pairs Marl Slate Boreholes	125
Appendix 10	Trace Element Concentration Profiles Marl Slate Borehole Cores	130
Appendix 11	Electron Microprobe Analysis	131

## CHAPTER 1

### PROJECT AIMS, APPROACH TO THE INVESTIGATION

#### AND PLAN OF THE THESIS

##### 1.1 PROJECT AIMS

This work is fundamentally concerned with investigating the role of diagenesis in forming ore deposits. Two sedimentary "ore-types" have been examined, namely the stratiform copper-cobalt orebodies of the Konkola Basin on the Zambian Copperbelt (Chapters 2 - 8), and the marginally (copper, lead, and zinc-bearing) Marl Slate (Kupferschiefer equivalent) of Central England, (Chapters 9 - 12).

A knowledge of diagenetic processes active in metalliferous sediments should aid our understanding of the genesis of these "orebodies" and of similar deposits throughout the world.

It was not an original aim of this project to study the geology of the Konkola Mine Area in detail. However, for a number of reasons, primarily the delay in obtaining unweathered Marl Slate drillcore material, an investigation of samples from Konkola was initiated. The samples studied were those brought back by the author on his return from a period of employment in Zambia. Although these samples were representative of the Konkola

Orebodies (being from 16 Orebody drillcore intersections), other associated lithologies are not well represented, and further collection was not possible for logistic reasons.

A further consequence of this situation was a lack of detailed sedimentological logs; consequently, the facies analysis presented in Chapter 3 is not as rigorous as the author would wish.

A major difficulty in investigating the effects of diagenesis on the Konkola Basin sediments is the problem of distinguishing between diagenetic textures and structures, and those produced by later deformation and metamorphism. No such difficulties were encountered in studying the Marl Slate samples, which have remained unmetamorphosed and relatively underformed since their deposition.

## 1.2 APPROACH TO THE INVESTIGATION

The general approach in this work has been firstly to review the geology of the two "ore types" in their regional context, including their tectonic and metamorphic histories. A general model for the depositional environment, deduced from facies analysis, has then been constructed. Petrographic observations, supplemented by electron microprobe analysis and scanning electron microscopy (Appendix 11) has then been used to determine



the sequence of diagenetic events for each "ore type". Geochemical studies, mainly using X-ray fluorescence analysis, were undertaken to link base metal concentrations to host lithology, and in an attempt to define the pattern of mineralization and determine the means by which base metals were introduced. A limited amount of fluid inclusion geochemistry was also undertaken. The results of carbon, oxygen and sulphur stable isotope analyses have been used extensively throughout this study to complement the sedimentological and textural observations, and further refine the diagenetic models. In the case of the Konkola Basin deposits, stable isotopes (sulphur and silicate oxygen) were also used in an attempt to determine metamorphic temperatures, and Rb/Sr analyses were used to determine the age of metamorphism.

### 1.3 PLAN OF THE THESIS

Chapters 2 - 8 are concerned with the study of the Konkola Basin, while the results of the Marl Slate investigation are presented in Chapters 9 - 12. All of these chapters, along with the list of references cited, appear in volume 1 of the thesis. Volume 2 contains all figures, tables and photographic plates (in chapter order), along with the appendices. Figures and tables which appear in appendices are prefixed with the letter A. The figures for appendices 8 and 10 are housed in the back of Volume II.

Chapter 2 outlines the regional structural evolution of the Copperbelt and places it in a plate tectonic setting. The structural geology of the Konkola Mine Area is then outlined, and new Rb/Sr age determinations presented, along with a brief review of the stratigraphy.

In Chapter 3, the sedimentology of the Konkola Basin is described with particular reference to the Ore-Shale and its footwall rocks. The results of a facies analysis are presented, and palaeographic reconstructions and sedimentation processes are discussed.

Chapter 4 outlines the diagenetic events that occurred in both the Ore-Shale and the immediate footwall rocks. A paragenetic sequence of authigenic minerals is recognised in both of these units. The formation of sulphides is shown to be an integral part of the diagenetic processes active within the sediments. From the data presented, speculations are made concerning the changing chemistry of interstitial solutions during the early diagenesis of these units.

In Chapter 5, the processes of fractionation with respect to sulphur, carbon and oxygen isotopes are briefly reviewed. Variation in the isotopic composition of the reservoirs of these elements and factors that may effect their degree of fractionation in geological systems are also discussed.

Stable isotope data from the Konkola Basin are presented in Chapter 6. The variation in sulphur isotope values is linked with changes in sedimentary environment as deduced from facies analysis. The variation in isotopic composition of dolomite and malachite samples is shown to reflect changes in the isotopic composition of porewater, which are compatible with the sequence of diagenetic events established in Chapter 4. An attempt is made to determine the temperature of metamorphism using the oxygen isotope results from co-existing silicates.

In Chapter 7 an attempt is made to link trace element geochemistry with host rock mineralogy. Certain elements are shown to be associated with minerals of a detrital origin, while others are associated with minerals of probable 'marine' origin. Statistical analysis of the data implies that copper and cobalt may have had different sources. The geochemistry of the solid, liquid and gaseous phases of fluid inclusions from veins which cross-cut the Ore-Shale confirms the lateral secretion origin for these veins, and also the presence of hydrocarbons in the vein-forming fluids.

In Chapter 8 the data presented in previous chapters are combined to establish the overall sequence of diagenetic events which have affected the Konkola Orebodies. The problems of ore genesis are discussed with



reference to this sequence of diagenetic events. The sources of copper and cobalt, and their possible means of transportation are considered. A model using all available evidence is then proposed to explain the genesis of the Konkola orebodies.

In Chapter 9, the regional setting and evolution of the Zechstein Basin, and the conditions leading to the Mid-Permian marine transgression are outlined. The sedimentology and petrography of the Marl Slate are described, particular reference being made to the forms of the sulphides and to observations made using cathodoluminescence.

In Chapter 10, geochemical data from the Marl Slate are presented. Using organic carbon and pyrite sulphur concentration along with degree of pyritization measurements, Marl Slate geochemistry is shown to reflect the environment of pyrite formation.

In Chapter 11, the results of detailed carbon, oxygen and sulphur isotope analyses are presented, and their implications for Marl Slate formation and basin evolution are discussed.

In Chapter 12, the data from the previous three chapters are combined to propose a model of Marl Slate formation. Evidence is presented which implies that much



of the calcite and dolomite occurring in the Marl Slate is primary and formed in isotopic equilibrium. It is shown that over most of the Zechstein Basin, conditions were suitable for sulphide formation, the limiting control on sulphide formation being the lack of suitable chalcophile elements. Finally, possible sources of base metals, and thus potential sites of ore formation, are briefly discussed.

It was intended to devote a chapter to comparing the two "ore types" studied. However, as this work progressed, it became apparent that the environment and processes of ore formation in the Marl Slate and in the Zambian Copperbelt have only a superficial resemblance, and a comparison has therefore not been made.

CHAPTER 2  
GEOCHRONOLOGY, STRUCTURE AND EVOLUTION  
OF THE COPPERBELT DEPOSITORY

2.1 INTRODUCTION

In this chapter pertinent geochronological data are reviewed and new data presented. The local structural geology of the Konkola Mine area is discussed. Finally, the regional structural evolution of the Copperbelt Depository is examined, and put into a plate tectonic context.

2.2 GEOCHRONOLOGY AND STRUCTURAL EVOLUTION OF THE COPPERBELT

Copperbelt tectono-thermal evolution from the Basement Complex (= 2000 Ma) to the Lufilian Orogeny (456 Ma), and its effect on Katangan sediments is discussed below. The main structural trends of the region are shown in Figure 2.1.

2.2.1 The Basement Complex

The Basement Complex consists of the Muva and Lufuba Groups (Table 2.1; stratigraphic classification after Clemmey, 1976) together with older granites, including

those forming the core of the Kafue Anticline. The granites have yielded ages of 1702 Ma for the Roan Antelope granite (Cahen et al., 1970a), and 2018 Ma for the Mufulira granite (Cahen et al., 1970b). More recently, Cliff and Clemmey (1974) have obtained an age of  $2000 \pm 100$  Ma from muscovite of a pegmatitic complex which cross-cuts the Basement at Mindola mine, Kitwe. An exception to these Basement granite ages is the Nchanga Red Granite which yields a Rb/Sr age of  $570 \pm 40$  Ma (Snelling et al., 1964) and a k/Ar age of  $490 \pm 20$  Ma. More recent U/Pb dating has given a 1100 My age (see Clemmey, 1976). Cahen and Snelling (1984) suggest an age of between 1100 - 1200 Ma for the Nchanga Red Granite, which is more in keeping with the field relationships, and conclude that the younger ages represent a partial metamorphic re-equilibration event.

The Lufuba 'schists' are thought by Cahen and Snelling (1984) to have been deposited just prior to the Ubendian (1800 Ma) tectono-thermal event, which resulted in the formation of a series of N-NW trending valleys, (e.g. Mimbula, Nchanga). The Muva quartzites and schists were deformed (Cahen, 1974) and metamorphosed along with the Lufuba schists during the Kibaran orogeny ( $1310 \pm 25$  Ma), to produce a series of north-easterly trending folds, (Garlick, 1961) with culminations forming in the Kafue Anticline (after Fleischer et al.) see Figure 2.2.



The Basement structure has had a marked controlling influence on Roan sedimentation. Lower Roan sediments commonly pinch out against Basement palaeo-highs, and on a localised scale Basement topography commonly controls palaeocurrent direction (see individual mine descriptions in Mendelsohn, 1961 and Clemmey, 1976). Basement topography (up to 300 m elevation differences) has also closely controlled the disposition of fold axes in the Katangan sediments which were induced by later deformation (Voet and Freeman, 1972).

#### 2.2.2 The Age of the Lower Roan Sediments

The transgression which marks the base of the Roan group is thought to be younger than 1130 Ma (Cahen and Snelling, 1984) and is certainly post-Kibaran. The northeastern limit of the Copperbelt Orebody transgression is shown in Figure 2.2.

The Bushimay Group (Mbuji Mayi Group in Cahen and Snelling, 1984), see Figure 2.1, is considered chronologically equivalent to the Roan Group by Cahen (1974). This is on the grounds that it lies stratigraphically between a similar Basement complex to the Roan and the Grand Conglomerate marker horizon (a tillite), and also has a similar sedimentation history. The Bushimay Group is sandwiched between lavas of  $948 \pm 20$  Ma and folded metasediments of Kibaran age. An



intermediate age of 1055 Ma from syngenetic galena is also substantiated by the results of studies on stromatolites as discussed by Cahen (1974).

The oldest ages obtained from the Roan are  $840 \pm 40$  Ma on the Zambian Copperbelt and  $882 \pm 42$  Ma in Shaba, both ages are from vein mineralization and are therefore minimum ages. The Ore-Shale horizon (Copperbelt Orebody member) is post-Kibaran and pre-882 Ma, but probably in the region of 1055 Ma, if the Bushimay and Roan Groups are chronologically equivalent.

### 2.2.3 Deformation of the Roan Sediments

The rocks of the Lower Roan Group have been subjected to three tectono-thermal events; the Lomamian orogeny, the Lusakan folding and the Lufilian orogeny (Cahen and Snelling, 1984).

The Lomamian orogeny slightly deformed the lavas above the Bushimay group, and is therefore post  $948 \pm 20$  Ma. On the Zambian Copperbelt, the orogeny has produced recumbent folds at Chingola (Garrard, 1965) (Figure 2.2) and at Luanshya (Hickman, 1974), and in the Lusaka area (Barr, et al., 1978). Drysdall, et al. (1972) have pointed out that the form of the Lufilian Arc is controlled by structures younger than this recumbent folding.

Cahen and Snelling (1984) consider the pegmatite veins discussed above to have formed just prior to the Lusakan folding event, and therefore providing a minimum age of 822 Ma for this event, which has otherwise no marked effect in the mine areas.

The Lufilian orogeny has been sub-divided into three different phases by Cahen (1974) and Francois (1974), and was extended to five phases by Cahen and Snelling (1984). This work refers mainly to the tectonic evolution in Shaba, no such detailed subdivision has yet been documented on the Zambian Copperbelt. The orogeny deformed both the Basement and the overlying Katangan cover, and produced the major structural features of the area, the Lufilian Arc (Figure 2.1). The Lufilian Arc is defined by foliation trends and fold axes which swing from north-east near the Angolan border to north-west on the Zambian Copperbelt where the Kafue Anticline forms a dominant structure.

On the north-eastern flank of the anticline, relevant folds have axial planes dipping north-east and parallel to the Kafue anticlinal axis while on the south-west flank, folds are arranged en echelon and trend east-south-east, with axial planes dipping *south-westerly*. In the exterior of the Lufilian Arc (in Zaire), nappes of mineralised Lower Roan have been thrust over the Kundelungu rocks, and

subsequently refolded with them. It has been suggested that the main phase of deformation may have been earlier in central and southern Zambia than in the north (Drysdaal et al., 1972).

The Lufilian Arc was considered by Garlick (in Mendelsohn, 1961) to have formed by the north-eastwards push of Katangan sediments between the Kibaran massif to the west, and the Bangweulu massif to the east (Figure 2.1). More recently Coward and Daly (1984) have interpreted the Lufilian Arc to be the product of an ENE verging thrust package, with the Kafue Anticline being interpreted as a hangingwall ramp (Figure 2.3c), the final structure representing some 50% shortening. This reinterpretation is based primarily on the following observations.

(1) The intensity of Basement deformation increases upwards and south-west away from the core of the dome (Kafue Anticline), and shows no simple symmetry as expected from diapiric uplift. However, since 1940 when Garlick demonstrated that the Roan sediments were younger than the granites, the structure of the Kafue Anticline and its flanking sediments has been considered to be the result of folding events, as previously discussed, and not due to diapiric uplift.

(2) Sheared gneissic Basement has been thrust into the



sediments of the Lower Roan (Figure 2.3a,b). However, in the actual mine company report (Diederix, 1977) there is no mention of the Basement being sheared as shown in Figure 2.3a, and the folding shown agrees with its position as part of an anticline separating the major Chingola and Chabwanyama synclines. More importantly, the arkose formation which contains the ore wedges out against the anticline, and contains conglomerate beds with gneiss and red granite pebbles suggestive of the existence of an adjacent palaeohigh during arkose deposition and prior to deformation by folding (Voet and Freeman, 1972). Copper and cobalt mineralization extends into Basement rocks immediately below the arkose. The field relationships in this example are not consistent with the thrusting origin suggested.

(3) Coward and Daly (1984) state; "The major domes are a result of culminations above thrust ramps at depth,.... many of the domes are aligned approximately in the thrust transport direction and are possibly culminations with the culmination walls aligned above lateral ramps". Although deformed during the Lufilian, many of the domes were palaeohighs which affected Lower Roan sedimentation; for example, the Lower Roan pinchout at Chililabombwe (Figure 2.2) and the incomplete sedimentation at the Konkola dome (Cailteux, 1974). Thus, at least some of the granite domes were in existence and affecting sedimentation long before the thrusting events took place.



(4) Bedding-parallel thrust and decoupling planes are recorded by a number of authors (McKinnon and Smith, 1961; Jordaan, 1961). Intense asymmetric and disharmonic folding occurs above some such decoupling zones and may explain the zones of mud and rubble found when drilling in the highly deformed Hangingwall Aquifer at Konkola (M. Coward, pers. comm.).

Although there is much evidence of thrusting on the Zambian Copperbelt, and it is the main style of deformation in the exterior of the Lufilian Arc (in Zaire), folding rather than thrusting is considered the primary mode of deformation on the Zambian Copperbelt.

The remarkable linear alignment of the ore deposits (Figure 2.2) was discussed by Brock (1961), in the context of vertical tectonics. No structural feature is associated with the lineament, except for a shear zone, found where the lineament crosses the Basement, well to the south-east of the Copperbelt. Brock (1961) considered the lineament to be a fundamental fracture affecting the Basement, and this led him to interpret the Copperbelt as part of an ancient rift system. Raybould (1978a), expanding the rift hypothesis of Brock, suggested a relationship between Proterozoic stratiform copper mineralization and rift systems. However, the linear distribution of the deposits on the Zambian Copperbelt may

be explained in terms of their alignment along a Lower Roan shoreline (Fleischer et al., 1976), as defined by sedimentological evidence (Figure 2.2) without the need to resort to major regional tectonic control.

#### 2.2.4 The Age of the Lufilian Orogeny

The Lufilian orogeny is characterised by uraninites which yield U/Pb ages in the range  $656-456 \pm 15$  Ma (Cahen et al., 1961), while Rb/Sr and k/Ar analyses produce ages in the range  $575 \pm 17$  to  $430 \pm 3$  Ma (Snelling et al., 1984; Cahen and Snelling, 1971). The lower ages are considered by these authors to represent blocking temperatures, reflecting the cooling history ending the Lufilian orogeny. Metamorphic grade increases from lower greenschist to amphibolite facies in the south-west away from the Kafue Anticline (Fleischer et al., 1976), and appears to have had no appreciable effect on sulphide migration (McGregor, 1964).

#### 2.3 WHOLE ROCK Rb/Sr AGE DETERMINATION AT KONKOLA

Six whole rock samples from Borehole CP337, the location of which is shown in Figure 7.1, were chosen for analysis. The analyses were carried out at the British Geological Survey, London. Rb/Sr ratios were determined by XRF analysis using a Philips PW1450 automatic spectrometer. Strontium was separated by standard ion

exchange techniques, and the isotopic composition was measured using a V.G. Micromass 30 mass spectrometer. The results of the analysis are shown in Figure 2.4. The samples were chosen because whole rock carbonate isotopic analysis appeared to be unaffected by metamorphism (Chapter 6), and it was hoped that Rb/Sr isotope analysis might yield a primary depositional age.

The results indicate an age of  $529 \pm 29$  Ma, which almost certainly represents a Lufilian thermal re-equilibrium event. The scatter of points about the isochron (MSWD = 16.5) is greater than that expected from analytical errors (MSWD better than 2), and suggests that homogenization was not complete.

## 2.4 STRUCTURAL GEOLOGY OF THE KONKOLA MINE AREA

The regional geology of the mine area is shown in Figure 2.5. The major structures of the area are the result of a syntaxis of NW-SE and NE-SW trending anticlinal and synclinal structures. The South Orebody occurs on the south-west flank of the Kirila Bombwe anticline (part of the major Kafue anticline), while the North Orebody occupies the nose of the anticline, which plunges  $8^\circ$  to the north-west. The Konkola Orebody occupies part of the south-east flank of the Konkola Dome. The net result is the formation of a saddle-shaped structure between the north and the Konkola orebodies.



The structure of the South Orebody is complicated by a number of northerly plunging ( $30^{\circ}$ - $40^{\circ}$ ) parasitic drag folds and high angle thrusts which are thought by Preston (1975) and Raybould (1978b) to have resulted from the extreme development of drag folds. Possible bedding-parallel thrusts are associated with disharmonic folding in the Chambishi Dolomite member (M. Coward, pers. comm.) and probably belong to the same tectonic event.

Two parallel faults of approximately 300m throw occur in the mine area. These are the Luansobe or Phantom faults, and the Lubengele fault (Figure 2.5). The existence of the Lubengele fault is based on irregularities of contours for the base of the Ore-Shale (Clutten, 1974). From the Ore-Shale isopach pattern Naish (1973) concluded that, "it would seem likely that at the time of Ore-Shale deposition, there was no structural discontinuity in this area (Lubengele fault)".

The Luansobe or Phantom fault is one of the major structural features of the region. It affects the Orebody at Mufulira and extends as far as the Fitwola Syncline (Garlick, 1961; Raybould, 1978b). Schwellnus (1961) proposed that Luansobe-type faulting could be the result of pre-Roan tectonics. Ralston (1960) has shown that the fault has been reactivated a number of times.



Pre-Roan tectonics have certainly had a marked effect on Lower Roan sedimentation. Thickness contours for the Hangingwall Quartzite (up to 750m above the Basement Unconformity) reveal two trends which approximately parallel the Basement folding directions (Schwellnus, 1961; Drysdale, 1974), (Figure 2.6).

The occurrence in the Ore-Shale (more studied than other lithologies) of slump folding (Ralston, 1960), soft sediment boudinage and slide sheets (Naish, 1973) suggests rapid, possibly tectonically controlled subsidence.

The occurrence of five tectono-climatic events are reflected in the sedimentary record of the Mindola Clastic member of Mufulira and in the Chambishi-Nkana basin (Clemmey, 1974b). These events are defined by unconformities or rapid changes in sedimentary type (e.g. influx of sheet conglomerates) and can be recognised at Konkola (Figure 2.7). On a broader scale, Cahen (1974) interpreted sedimentary cycles (upward decrease in rudaceous and arenaceous sediments, increase in pelites and the introduction of a carbonate component) in the Katangan supergroup to reflect periods of regional uplift. Furthermore, Cahen (1974) was able to demonstrate that the cycles could be grossly correlated from the Zambian Copperbelt through the Shaba copper mines, to the Bushimay in the north-west of the Shaban province of Zaire.

There is thus much evidence, although a lot is indirect, for vertical tectonics during Lower Roan times.

## 2.5 PLATE TECTONIC SETTING OF THE COPPERBELT DEPOSITORY

There is ample evidence to suggest that there was no large scale movement between stable cratons up to and including Lufilian deformation times (approximately 550 Ma). Firstly, palaeomagnetic data closely constrains intercratonic movement (Briden, 1976; Piper, 1976; McWilliams and Kröner, 1981; and Piper, 1982). Secondly, there is stratigraphic continuity across the mobile zones (Shackleton, 1976; Kröner, 1976). On a larger scale, Proterozoic sediments from western and central Africa and South America have been correlated radiochronologically and palaeontologically (Bonhomme and Bertrand-Sarfati, 1982).

Shackleton (1976) proposed that many of the regional structures (shown in Figure 2.1) owe their origin to vertical tectonics, but did not rule out the case for plate tectonics. Certainly there must have been large vertical movements. Barr (1974) reports high pressure metamorphism (7-11 kb) associated with granites of  $945 \pm 30$  Ma age from the Rufunsa area of southern Zambia.

Kröner (1977), reviewing the Precambrian mobile belts

of south and east Africa, suggested that the driving forces required for stretching and rupturing of the crust became stronger with time. During the Precambrian (Irumide and Kibaride Belts of Figure 2.1) these forces failed to separate the crust, and instead produced ensialic belts. Pan-African times (definition discussed by Cahen and Snelling, 1984, p. 440) were still dominated by ensialic belts (Zambezi) but can display incipient rupture (Damaran). Rocks of ophiolite affinities have been described by Hartnady (1978) and Barnes et al. (1980) for the Damaran Belt, but no ophiolite rocks of Pan-African age have been recorded from southern Zambia (Coward and Daly, 1984).

McWilliams and Kröner (1981) proposed a model for the Damaran Belt, based on geochronological, palaeomagnetic and sedimentological data. The model allowed for crustal thinning and geosyncline formation, with the production of mafic volcanics, but they found no evidence for subduction of oceanic crust.

More recently Unrug (1983) has suggested that a spreading ridge was active in the Damaran Belt, and to a lesser degree in the Lufilian-Zambezi region, which was separated from the Damaran Belt by a transform fault, (Figure 2.8a). Closure of the Congo-Botswana Zimbabwe cratons, resulted in the cratons colliding first in the Zambezi region (Figure 2.8b). This collision partially



blocked the system and resulted in transcurrent fault formation (Figure 2.8c and 2.8d). The Lufilian Arc is thought (Unrug, 1983) to result from clockwise rotation of a 'Lufilian' fault-bounded microplate.

This model is considered overly complex, and is inconsistent with much of the evidence which implies that no spreading has taken place between the cratons. The evidence for transform fault displacement between the Damaran and Zambezi Belts is conjectural, and to quote Unrug (1983), the fault's existence is "partly directly observable and partly deduced". The existence of a 'Lufilian' microplate is highly speculative. Neither does the model explain the geometry of the Damaran or Zambezi Belts.

A simpler, more comprehensive, and therefore preferable explanation for the regional tectonic pattern is NE-ENE movement between the Congo and the Botswana-Zimbabwe cratons (Coward and Daly, 1984), (see overlay on Figure 2.1). This model explains the formation and geometry of the Damaran and Zambezi Belts. It also provides the source of the north-east compression suggested by Garlick (1961) who explains the formation of the Lufilian Arc by the north-eastward pushing of Katangan sediments between the Bangweula and Kibaran massifs.



## 2.6 CONCLUSIONS AND SUMMARY

The size and shape of Roan depositional basins was controlled by the syntaxis of Basement deformation. At Konkola, basin subsidence up until slightly after Ore-Shale times (1055 Ma), was tectonically influenced.

Three phases of Pan-African tectono-thermal events can be recognised on the Zambian Copperbelt. The Lomanian orogeny (950 Ma) which produced recumbent folding at Chingola and Luanshya; the Lusakan folding event (840 Ma) which has only been recorded on the Copperbelt by a phase of pegmatite formation, and the Lufilian orogeny (656-456 $\pm$ 15 Ma) which resulted in regional deformation, and at Konkola produced drag folds and associated thrusting, resulting in the duplication of the Ore-Shale at the South Orebody. Bedding-parallel thrusting of the Chambishi Dolomites Member is ascribed to the Lufilian, but may be earlier (possibly Lomanian), since the thrust plane is itself folded. A regional joint and minor normal fault pattern were developed during the Lufilian orogeny. Associated metamorphism continued after deformation.

Rubidium/Strontium dating of Konkola samples yields an age of 529 $\pm$ 20 Ma, and almost certainly marks a thermal re-equilibration event. Scatter of the data points about the isochron suggest that homogenization was not complete.

Finally, the regional Pan-African structural trends can be explained in their regional context. The deformation model which is simplest, and best fits the data, suggests a north-eastward relative movement between the Congo and the Botswana-Zimbabwe cratons. As well as explaining the formation and geometry of the Damaran and Zambezi Belts, the model (Coward and Daly, 1984) also provides for the north-easterly compression suggested by Garlick (1961). This produced the Lufilian Arc, by compressing the Katangan sediments between the Bangweulu and Kibaran massifs, and resulted in the Lufilian folding and bedding decoupling seen on the various mine properties.

## CHAPTER 3

### SEDIMENTARY AND FACIES INTERPRETATION OF THE MINDOLA CLASTICS FORMATION AND THE COPPERBELT OREBODY MEMBER

#### 3.1 INTRODUCTION

As previously explained in Chapter 1, logistic difficulties prevented the construction of detailed sedimentological logs, because the samples available for study were concentrated at, and in the immediate vicinity of the Copperbelt Orebody Member. The sedimentary descriptions and consequent facies interpretation rely on the few available relevant internal company reports, and the personal observations of the author made during a period of employment at Konkola Division.

The above problem is compounded by the fact that observations are restricted to underground exposure (surface exposure on the Copperbelt is minimal), which places severe constraints on access. Also the geometry of underground workings is such that rock exposure to the footwall of the Copperbelt Orebody Member can be extremely poor, and severely confined aurally.

After a brief description of the sedimentology, an attempt is made to interpret the facies and palaeoenvironment of individual lithological Units.



### 3.2 SEDIMENTOLOGY OF THE BANCROFT QUARTZITE MEMBER

The sediments of the Bancroft Quartzite Member is divided into five Units (see Table 2.1). The lower three are predominantly conglomeratic and usually poorly sorted. The remaining units although containing conglomerate horizons, are in general finer grained, and are usually better sorted.

#### 3.2.1 Boulder Conglomerate (approximate thickness 100-300m)

The Basement Complex is unconformably overlain by the Boulder Conglomerate. This is a poorly sorted conglomerate which lacks any planar fabric. The clasts consist of moderately rounded Basement schist, gneiss and quartzite boulders up to 50 cms in diameter in a sandy quartzitic matrix. The Boulder Conglomerate is poorly exposed in underground workings but grades upwards into the Pebble Conglomerate. A diagrammatic log of the Mindola Clastics and Lower Kitwe Formations is shown in Figure 3.1.

#### 3.2.2 Pebble Conglomerate (approximate thickness 30-40m)

The Pebble Conglomerate is more quartzitic in nature than the Boulder Conglomerate. Clasts range in size from 1-10 cms, are generally well-rounded, of Basement origin,



and often have sheared chlorite rich margins. The matrix is composed of dark grey quartzite with chlorite and some mica. Occasionally lenses of calcite and purple anhydrite cement occur. Towards the top of this unit fine grained dark grey quartzite predominates, but there are repeated lenses of microconglomerate up to 30 cms thick. Planar bedding is common, and occasionally graded bedding and cross bedding is observed.

### 3.2.3 Lower Porous Conglomerate (thickness 30m)

The Lower Porous Conglomerate, as the name implies, is extremely porous and vuggy. It is very similar in appearance to the Boulder Conglomerate but has a remarkably uniform thickness, however only its down dip extension at the same strike positions are exposed underground. The Lower Porous Conglomerate consists of poorly sorted coarse sub-angular to rounded clasts up to 50 cms diameter of quartzite and Basement rocks. Clasts are poorly cemented by quartz which was probably liberated during compaction and concomitant pressure solution of the mutually supporting clasts. Secondary clay and vuggy quartz line intergranular pores.

### 3.2.4 Footwall Quartzite (thickness 300-400m)

The basal 10 metres of the Footwall Quartzite is highly fractured and together with the Lower Porous

Conglomerate forms a major water hazard in the mine workings. The fracturing is certainly the result of the volume reduction in the conglomerate due to burial compaction and subsequent collapse of the base of the overlying quartzite.

The Footwall Quartzite is dark grey and well-bedded, often with streaks of hematite along bedding planes. Cross-bedding is very common, and indicate a current direction from the north-east (Fleischer et al., 1976). Occasional granule bands up to 2m, but more commonly 30 cms occur. These consist of rounded quartz and orthoclase pebbles, and generally show graded bedding.

Between 20 to 50 metres from the top of this unit, occurs a series of boulder channels striking south-east (Schwellnus, 1961b). The boulders are well-rounded and are of quartzitic and granitic material in an abundant matrix of quartz, feldspar and hornblende. The channels are approximately 5 metres wide (poor exposure makes determination difficult), have erosional bases and sharp almost vertical sides, and represent a localised depositional disconformity.

### 3.2.5 Argillaceous Sandstone (thickness 40m)

The Argillaceous Sandstone comprises a series of alternating dark grey argillite and medium grained

occasionally gritty sandstone. Each bed can be up to 30 cms thick, but they are usually less. The sandstone is usually structureless, although flaser bedding is seen towards the top of the unit, where sandstone dominates over argillite. The upper contact is erosional, and conglomerate filled scour channels have been reported by Naish (1973).

### 3.3 FACIES INTERPRETATION OF THE BANCROFT QUARTZITE MEMBER

The poor sorting, high matrix content, clast size, and lack of planar bedding in the Boulder Conglomerate indicate deposition by a debris flow mechanism of high viscosity, and are characteristic of the proximal part of alluvial fan deposits (Bluck, 1964, 1967; Collinson, 1978a). Their occurrence suggests periodic rainfall and sediment discharge, features common in arid to semi-arid climates (Schumm, 1977).

The Pebble Conglomerate although similar to the Boulder Conglomerate is considerably more matrix rich. The occurrence of mica suggests that the matrix was more clay rich than the Boulder Conglomerate, prior to metamorphism. There are several important differences between the Boulder Conglomerate and the Pebble Conglomerate. The latter is more bedded in nature, and displays cross bedding and graded bedding, indicative of a



more persistent water lain environment. The decrease in clast size (50 cms to 1-10 cms) and increase in matrix implies a lower energy more distal facies of deposition than the Boulder Conglomerate. The Pebble Conglomerate is similar to the Boulder Conglomerate of Bluck (1967) and is interpreted to be of stream flood origin. The presence of anhydrite suggests a low latitude semi arid environment, but the anhydrite may be of secondary origin.

The characteristic features of the Lower Porous Conglomerate (primarily its clast size of up to 50 cms diameter) reflect a return to higher energy depositional conditions. Whether this period of rejuvenated conglomerate growth was caused by climatic change or tectonic control cannot be determined. The known down dip extent of the Lower Porous Conglomerate is in the order of 700m at the South Orebody, which gives an idea of the scale of fan development. Lateral variations of this unit are not exposed due to the geometry of underground workings. However, it is not unreasonable to expect the Lower Porous Conglomerate proximal fan deposit to grade laterally and down dip into a more texturally mature distal fan equivalent.

The Footwall Quartzite poses a problem of interpretation, primarily because of its thickness which is in excess of 400 metres. Lithostratigraphically equivalent units have been considered to be aeolian at



Nkana (Clemmey, 1976), and Mufulira (Garlick, 1967, 1972, 1981), although Van Eden (1974) considered the Mufulira quartzites to be marine. Fliescher et al. (1976) considered the Footwall Quartzite at Konkola to be of marine origin, but point to the occurrence of a 2m aeolian unit, and the presence of thick aeolian deposits at Kafue some 6km to the south. Garrard (1972) describing the Chingola mine area (Chingola is some 10km south of No. 1 Shaft), notes the general trend from aeolian quartzites in the south to shallow water arkoses in the north. Lack of detailed sedimentological logs at Konkola make interpretation of depositional facies almost impossible. The transition from an alluvial to a marine facies is considered unlikely though not impossible. The primary objection to a purely aeolian origin is the very common occurrence of microconglomerate horizons consisting of well-rounded clasts displaying graded bedding, a feature not found in aeolian sandstones (Bagnold, 1941; Collinson, 1978b), and probably reflecting aqueous deposition.

The Footwall Quartzite is thought to represent predominantly aeolian deposition but with frequency lacustrine/marine incursions. The mixing of marine water and water from evaporation environment (aeolian) is borne out by carbon and oxygen isotope results of calcite cement from the Footwall Quartzite (Chapter 6). The boulder channels which cut through the Footwall Quartzite would reflect a temporary return to fluvial conditions, with the

incursion of stream incised channels. The thickness of the Footwall Quartzite is the result of the combined effect of basin subsidence and possible basin margin faulting. The Argillaceous Sandstone which marks the top of the Bancroft Quartzite Member, requires an environment capable of the regular separation of fine and coarse grained sediment. The evidence suggests that deposition took place possibly adjacent to a shallow tidal environment. Similar deposits to the Footwall Quartzite and Argillaceous Sandstone are described by Steel (1974, 1976), Link and Osborne (1978) and Ryder et al. (1976). A schematic diagram of the depositional environment of units of the Bancroft Clastics Member is shown in Figure 3.2.

### 3.4 SEDIMENTOLOGY OF THE KAFUE ARENITES MEMBER

The Kafue Arenites Member is divided into three coarse grained clastic units which are relatively well sorted. The overall rock colour changes from grey in the Bancroft Quartzite Member to red in the Kafue Arenites Member. The conglomerate clasts also vary from schists, gneisses and quartzites to a predominantly granitic/feldspar composition.

#### 3.4.1 Porous Conglomerate (thickness 10-20m)

Schwellnus (1961b) reports the presence of round to sub-angular boulders of quartzite, quartz, feldspar,



aplite and porphyry near the base of the Porous Conglomerate. This grades into a pebble conglomerate with a matrix of medium grained arkosic sand with traces of carbonate. Clasts vary in size from occasional boulders of 0.6m diameter to pebbles of between 2 to 7 centimetres. Naish (1972) describes the occurrence of a thin argillite horizon towards the middle of the Porous Conglomerate, which is immediately overlain by a medium to coarse grained feldspar sandstone which grades in turn into conglomerate. The argillite is not commonly seen, and its occurrence is probably patchy.

#### 3.4.2 Footwall Sandstone (thickness 5 - 20m)

The base of the Footwall Sandstone is locally marked by the development of a thin argillite horizon, but is more usually gradational with the Porous Conglomerate. The sandstone is medium to coarse grained, grey to reddish brown in colour, with thin irregular horizons of argillite. Thin interbedded lenses of conglomerate consisting of rounded pebbles of milky quartz and feldspar (mainly microcline) also occur, and often show a fining upwards of clast size. Specular hematite is relatively common and occurs as thin layers parallel to bedding (see Plate 3.1a). Cross-bedding is common, and indicates a dominant flow direction from the north-east (Fliescher et al., 1976). Leached cavities aligned parallel to bedding are relatively common, and are probably after carbonate.

The upper contact of the Footwall Sandstone may be gradational with the Footwall Conglomerate, but towards the south of the South Orebody is disconformable with the Ore Shale.

#### 3.4.3 Footwall Conglomerate (thickness 0 - 3.5m)

The Footwall Conglomerate is interbedded with lenses of arkosic sandstone, and rare argillite bands. The pebbles are sub-rounded and well-sorted, varying in diameter up to 8 cms with rare boulders up to 0.7m. The pebbles consist of rounded quartz, aplite and almost euhedral microcline feldspar. The matrix is generally feldspathic sand with rare biotite. Planar bedding is rare but graded bedding and cross-bedding are common. The cross-bedding frequently shows truncated tops (see Plate 3.1b) and indicates a current direction radiating away from the Kirila Bombwe Massif.

#### 3.5 FACIES INTERPRETATION OF THE KAFUE ARENITES MEMBER

The feldspathic nature of the Kafue Arenites Member compared with the Bancroft Quartzite Member led Schwellnus (1961b) to suggest that the base of the Porous Conglomerate represented an intraformational unconformity. Certainly the base of the Porous Conglomerate is erosive, as has been borne out by the occurrence of conglomerate filled scour channels reported



by Naish, 1973.

Fleischer et al. (1976) point to the similarity of the Porous Conglomerate to the Lower Conglomerate at Nkana-Chambishi. Clemmey (1976) considers the Lower Conglomerate to be the result of intraformational pedimentation, and the subsequent deposition of a flat topped lag conglomerate, the event itself marking a change in climate from semi-arid to a more humid environment. At Konkola, Schwellnus (1961b) and Mason (1968) have shown that the Porous Conglomerate radiates outwards as a series of fingers, and decreases in thickness away from the Kirila Bombwe Massif. The Footwall Conglomerate also appears to be wedge shaped (Naish, 1973), and essentially mirrors the thickness variation of the Porous Conglomerate. The gradational contacts between the units comprising the Kafue Arenites Member, and their lateral variation implies a similar mode of origin. The thickness variation suggests an overall coalescence of fan shapes, however the Kafue Arenites Member deposits are different than the fan deposits previously described in Section 3.2. Besides being more variable laterally and vertically, the Kafue Arenite Member deposits show a decrease in the occurrence of large (>5cms) clasts, and a marked increase in the volume of cross-bedded pebbly sandstone. Local scouring and graded bedding are more common, and rare interbedded argillite layers and mud drapes occur. All these features are common in braided

stream/river channel deposits of distal fan environments (Bluck, 1967), and are also typical of fan growth in humid climates (McGowan and Groat, 1971; Nilsen, 1982) which may lend credence to the climatic change proposed by Clemmey (1976).

### 3.6 SEDIMENTOLOGY OF THE COPPERBELT OREBODY MEMBER

The Copperbelt Orebody Member (locally termed the Ore-Shale and for brevity referred to as such in this thesis), rests unconformably on the Footwall Conglomerate, and Footwall Sandstones. Towards the 'Barren Gap', which separates the North and South Orebodies, a series of erosional channels up to 10m wide occur. The channels have a northeast-southwest orientation and are composed of angular to sub-round fragments of Footwall Conglomerate and 'barren' Ore-Shale in an arkosic matrix. The conglomerate grades upwards into a poorly cemented arkosic grit, (see Plate 3.2a). Bedding, where present, is parallel to the Ore-Shale, and occasionally includes truncated corss-bedding, features which rule out a collapse breccia origin for the channels. Mason (1968) reports that the uppermost surface of the Footwall Conglomerate/Footwall Sandstone frequently shows erosional features, notably truncated cross-bedding. The Ore-Shale has been subdivided into five units (Schwellnus, 1961).



Unit A (0.6 - 1m) consists of a finely interbedded grey laminated siltstone, with pink to brown carbonate (usually dolomite). It is often rich in chalcocite, which occurs as streaks and laminae (2 - 3mm) parallel to bedding. Ralston (1961) and Schwellnus (1961b) both record slump folding in this unit. Algal mats are reported from unit A of the Konkola Dome Orebody (Naish, 1972).

Unit B (1.4 - 2m) is a grey to yellow brown relatively massive sandy siltstone, which becomes more markedly laminated towards its top. Rare moulds after gypsum occur (see Plate 3.2b), otherwise the Unit is devoid of sedimentary structures. Mineralization generally occurs as uniformly disseminated fine grained sulphide.

Unit C (0.9 - 2m). This is a grey finely laminated siltstone intercalated with regular calcareous horizons of varying thickness up to 4 cms. Individual laminae are remarkably persistent and can be traced for hundreds of metres. Wave ripple marks (symmetrical with bifurcating crests) and load casts are common. Desiccation cracks and carbonate lenticles parallel to bedding also occur (Plate 3.3a). Sulphide mineralization takes the form of fine disseminations, lenticles (see Plate 3.3b) and sulphidite layers as defined by Garlick (1964), (see Plate 3.4a).



Unit D (1 - 1.8m) is a dark grey finely laminated siltstone with irregular calcareous arenite horizons, lenses of carbonate parallel to bedding occur. Ripple marks, load casts and sulphidite layers occur, but are less common than in unit C. Mineralization takes the same form as in unit C, but is more erratic in distribution, and the occurrence of sulphide lenses parallel to bedding more common (Fleischer et al., 1976). In the upper levels of the mine the top of unit D was marked by a well laminated, light grey siltstone/fine grained sandstone (Schwellnus, 1961b).

Unit E (0.6 - 1.5m) is a dark grey micaceous siltstone intercalated with reddish brown feldspathic sandstone, which become more numerous towards the top, where flaser bedding occurs. Mineralization in this unit is highly erratic and occurs as sulphide disseminations which are coarser in the arenite horizons. Unit D grades into the Hangingwall Quartzite, the top of the unit is considered as the base of the first thick (30 cms) arenite horizon.

### 3.7 FACIES INTERPRETATION OF THE COPPERBELT OREBODY MEMBER

The unconformable and sometimes erosive contact of the Mindola Clastics/Kitwe Formations contact represents a major non-sequence. The Orebody units are each useful

environmental indicators, and are summarised in Table 3.1.

Although algal mats can form at 10m depths in the subtidal environment, their preservation is favoured by an intertidal environment. Unit A is therefore interpreted as an intertidal carbonate mud (with an algal mat component). Slump folding indicates a moderate palaeoslope, but the folding may be of dewatering origin. Unit A reaches its maximum thickness in the region of the Barren Gap, and erosion at the Ore-Shale/Footwall Conglomerate implies that this area was then a palaeohigh. Continued transgression resulted in the deposition of unit B sediments. The unit B fine grained sandstone/siltstone represents a low energy environment (lower phase plane beds present), while the siltstone at the top of the unit marks a return to shallower higher energy (upper phase plane beds present) environment. The occurrence of gypsum moulds confirms the semi-arid climate.

The ripple marks and desiccation cracks of unit C are indicative of a regression and a return to a shallow water environment with occasional subaerial exposure. Carbonate, after anhydrite (see Chapter 4) develops an almost 'chicken wire' texture, (Plate 3.4b) suggesting a tidal flat to supratidal environment (Kinsman, 1966; Shearman and Fuller, 1969). The continuity and regularity of the interbedded finely laminated siltstone and

carbonate imply a stable 'low' energy environment. Fluctuations in water level, perhaps due to periodic flooding, would explain the alternating exposed and sub-aqueous sedimentary features, and probably reflect localised ponding.

Unit D is very similar to unit C but lacks the regularity of carbonate horizons, carbonate also becomes less common towards the top of the unit. Desiccation cracks are absent. An overall slightly deeper sub-aqueous environment of deposition is envisaged, reflecting the commencement of a transgressive phase towards the top of the unit.

An increase in energy of environment for unit E is noted by the disappearance of carbonate and the appearance of arkosic sandstone lenses. Lenticular and flaser bedding occur towards the top of the unit and indicate a transgression, to a shallow marine environment.

Units A to the top of unit B therefore reflect a transgressive event, while unit C to the top of unit D represent a regressive event. The top of unit D and unit E mark the return to deeper water conditions.



### 3.8 SEDIMENTOLOGY AND FACIES INTERPRETATION OF THE NCHANGA QUARTZITE MEMBER (30 - 150m)

The Rokana Evaporite Member (Table 2.1) is not developed at Konkola. Nchanga Quartzite sedimentation marks a change from silt to sand dominated deposition. It consists of massive tabular cross-bedded white quartzite and arkose with interbedded siltstone and argillite. A feldspathic quartzite, occasionally conglomerate occurs towards the top of this unit (Mulgrew, 1968). Desiccation cracks and occasional scour and fill channels are recorded (Naish, 1972). Minor copper mineralization (chalcopyrite) is sporadically developed. Major orebodies are found at the same horizon at Nchanga (Binda and Mulgrew, 1974).

The quartzite is well-sorted, the thin argillite capping on surfaces showing sub-aerial exposure confirm that there was little fine grained material in suspension. Flow directions suggest a north-easterly source of the sediments (Cohen, 1939). The sedimentary features particularly the tabular cross-bedding suggest shallow marine to tidal flat deposition. A similar conclusion was reached after a detailed study of the Nchanga Quartzite at Chingola (Southworth, 1980).

## CHAPTER 4

# DIAGENESIS OF THE COPPERBELT OREBODY MEMBER AND THE FOOTWALL CONGLOMERATE AND FOOTWALL SANDSTONE UNITS

### 4.1 INTRODUCTION

This chapter describes the diagenetic features of the Copperbelt Orebody Member, and the rocks in its immediate footwall i.e. the Footwall Conglomerate and Footwall Sandstone. The chapter includes a detailed presentation of the diagenetic features of these lithologies, and a brief examination of post-diagenetic effects. Paragenetic sequences of diagenetic events are proposed, and the chemistry of the diagenetic fluids is discussed.

### 4.2 POST DIAGENETIC FEATURES

Rocks of the Lower Roan have been subjected to metamorphism and tectonic deformation (see Chapter 2). To clarify discussion the effects of these events are discussed before examining the role of diagenesis in the sediments.

Deformation has resulted in the development of a faint cleavage, which is not well-developed throughout the mine area, but when present is best developed in unit B of the Ore-Shale, (see Plate 4.1A). Tectonic deformation and/or burial compaction has caused fracturing of detrital

quartz and feldspar. Such features are much more common in the Footwall rocks than the Ore-Shale. The Ore-Shale has responded to deformation by buckling and folding rather than fracturing as is the case in the more competent Footwall rocks.

Metamorphism of lower greenschist facies is reflected in the growth of muscovite, chlorite and epidote, and significantly has resulted in the destruction of diagenetic clay minerals. Metamorphism has also resulted in the recrystallization of some sulphides, but has not destroyed original zoning (Darnley and Killyworth, 1962; Brown and Bartholomé, 1972).

#### 4.3 DIAGENETIC FEATURES OF THE FOOTWALL CONGLOMERATE AND THE FOOTWALL SANDSTONE

The Footwall Conglomerate and Footwall Sandstone are discussed together since they are intimately linked sedimentologically, and display very similar diagenetic features. For the sake of brevity both of these lithologies will be referred to as the footwall rocks, and the Copperbelt Orebody Member will be referred to by its local name of the Ore-Shale. A number of diagenetic features are identified in the footwall rocks including, mechanical infiltration of clay, dissolution of unstable silicates, replacement of detrital minerals by clays and the formation of a suite of authigenic minerals. Many of



these features are also found in the Copperbelt Orebody Member. Each of the diagenetic features will be briefly discussed.

#### 4.3.1 Mechanical Infiltration of Clays

Clay coatings parallel to grain boundaries occur in the footwall rocks and to a much lesser degree in units C and D of the Copperbelt Orebody Member. The clay coatings themselves are often incomplete and rarely developed as well as described by Walker et al. (1978). This is probably due to the footwall rocks being flushed with marine waters during the transgression which marked the onset of Copperbelt Orebody Member sedimentation. Alternatively the clays may be of detrital origin. Metamorphism prevents the determination of the original clay phase. The clay 'skins' are diagenetically early, occurring before the authigenic overgrowth of haematite, feldspar or quartz (see Plate 4.2).

#### 4.3.2 Dissolution and Replacement Features

Dissolution of chemically unstable ferromagnesian minerals such as epidote and hornblende is a common diagenetic process in continental red beds. The footwall rocks are characterised by a lack of such minerals. Walker (1967) and Walker et al. (1978) have outlined the age dependent nature of removal of ferromagnesian minerals

by processes of dissolution. It may be that iron released during such processes is responsible for the red colouration of such sediments (Hubert and Reed, 1978). Dissolution voids are a commonly occurring feature of the footwall rocks, and sometimes show unaltered authigenic rims (see Plate 4.3A).

The replacement of feldspar, particularly plagioclase, by clays is very common. Various stages of this breakdown can be observed, from grain edge replacement to the production of clay ball pseudomorphs (see Plate 4.3B).

#### 4.3.3 Authigenic Minerals

Dissolution and replacement of detrital minerals in situ results in the release of a variety of elements into interstitial waters. The subsequent movement and precipitation of these elements under changing diagenetic conditions results in the formation of authigenic minerals and overgrowths, as discussed below.

##### 4.3.3. (a) Accessory Minerals

Haematite coating of detrital quartz and feldspar grains has already been discussed (Plate 4.3A). Fine dusty, generally incomplete, haematite coatings of grains are ubiquitous in the footwall rocks. The coarser

haematite coatings are confined to distinct areas, and are not necessarily associated with detrital haematite (Plate 3.1A).

Zoned overgrowths of zircon, rutile and tourmaline occur in the footwall rocks, but are much more common in the Ore-Shale, as borne out by petrographic observations and geochemical data (see Chapter 7). Frequently, the overgrowths are euhedral on rounded detrital cores (see Plates 4.4A and 4.4B). Although not common, clusters of authigenic rutile needles are found as pore-linings in the footwall rocks. The rutile clusters nucleated on quartz grain boundaries prior to authigenic quartz formation (see Plate 4.1B).

Electron microprobe analysis of zircon samples reveals that they contain significant amounts of thorium and uranium, while rutile contains niobium, zirconium, uranium and thorium (Table 7.3). Authigenic rutile seems to be slightly enriched in zirconium, suggesting it formed simultaneously with authigenic zircon, although further analyses would be necessary to confirm this.

#### 4.3.3 (b) Dolomite

Dolomite occurs in the footwall rocks in two distinct forms. The first of these, occurs as euhedral rhombs, nucleated on grain boundaries, see Plate 4.4C. These



euohedral dolomites can be seen to be replaced by malachite. Electron microprobe data (Table 4.1) reveal that these dolomites are exceptionally rich in cobalt, and also contain significant amounts of iron and manganese. Many of the dolomites are also slightly siliceous. The euohedral dolomites are non-luminescent, although their iron and manganese compositions plot within the carbonate luminescence field defined by Fairchild (1983). Perhaps the cobalt content of the dolomites suppresses their potential luminescence. The cathodoluminescence technique employed is described in Appendix 1.

The second type of dolomite in the footwall rocks is poorly crystalline (xenotropic), and is volumetrically insignificant compared with the euohedral dolomite. This dolomite luminesces bright yellow-orange, and fills post-authigenic quartz and feldspar pore space (see Plate 4.4D). It is only patchily developed, and was found in only a small number of the samples examined, where it replaces detrital silicate grains.

No petrographic relationship could be determined between the two dolomites, although, due to its euohedral form and its pre-quartz and feldspar overgrowth age, the euohedral dolomite is considered to be paragenetically earlier than the sparry pore-filling dolomite.

#### 4.3.3 (c) Quartz

Although authigenic quartz overgrowths occur in the footwall rocks, they are much more common in the Ore-Shale. Quartz occurs in two forms. The first form is diagenetically earlier than the second and consists of optically continuous overgrowths on detrital quartz grains. Often there is an intervening clay skin (now muscovite) between the detrital grain and the cleaner overgrowth, indicating that the quartz overgrowth is paragenetically later than clay skin formation. Chrysocolla replaces quartz along fractures and grain boundaries (Plate 4.4C), but it not common.

The authigenic overgrowths are rarely euhedral, unlike those described by Waugh (1970). This lack of crystal form may be an original fabric, or the result of late diagenetic pressure solution, or metamorphism, although the latter would tend to produce an idioblastic texture.

Diagenetically later pore-fill quartz cement occurs in significant amounts, and accounts for approximately a quarter of all the quartz in the footwall rocks.

#### 4.3.3 (d) Feldspars

Potassium feldspars are much more common than

plagioclase feldspars in the footwall rocks, which probably reflects the former's greater stability and resistance to dissolution (Goldich, 1938; Walker et al., 1978). The feldspars display replacement by sericite (Plate 4.3B). Replacement of feldspar overgrowths and detrital grains by sparry dolomite also occurs.

Two types of authigenic feldspar exist, microcline and plagioclase, both of which form optically continuous and discontinuous overgrowths (see Plates 4.5A and 4.1C and 4.1D). Optically continuous overgrowths are the most commonly occurring form, and appear to be paragenetically earlier than optically discontinuous overgrowths. Kastner and Siever (1979) consider optical discontinuity to reflect differences in the degree of Al/Si disorder between the feldspar detrital core and its overgrowth. Overgrowths rarely show well developed crystal shapes as described by Waugh (1978), but do tend to form euhedral outlines as can be seen (see Plate 4.1E).

#### 4.3.3 (e) Sulphides

Chalcocite is the only major copper sulphide to occur in the footwall rocks, although traces of bornite and chalcopyrite also occur (Sweeney, 1979). The copper sulphides occupy pore spaces and replace detrital grains. In Plate 4.6A chalcocite grains exhibit grain size and morphological variation identical to those of the



host detrital silicates. Were these sulphides of detrital origin then they would, because of their greater density, be expected to be associated with larger grains of silicate. The chalcocite grains seen in Plate 4.6A were not therefore deposited in hydrodynamic equilibrium with the matrix silicates and are not of detrital origin. In this instance the sulphides are either replacing original detrital grains or, since no replacement textures are evident, the sulphides may simply be occupying dissolution casts, possibly after plagioclase feldspar.

Of more interest in economic terms is the occurrence of carrollite ( $\text{Cu Co}_2 \text{S}_4$ ) in the footwall rocks. Plate 4.6B shows a subhedral crystal of carrollite, typical of those found in the footwall rocks of the economically important 200 - 800 mS area of No. 1 Shaft. The numerous silicate inclusions and general appearance suggest that the carrollite grew simply by infilling pore space prior to compaction. Carrollite grains in the Ore-Shale frequently display compaction-induced, crystallographically aligned fractures (Plate 4.6C) not found in the more competent footwall rocks, and suggests that carrollite formation in the Ore-Shale was earlier than Ore-Shale compaction. Feldspar inclusions in the carrollite crystals have authigenic overgrowths (Plate 4.6D), and indicate that carrollite formation was paragenetically later.

Compositional data for carrollite (Table 4.2), reveal that the Footwall samples are considerably enriched in copper with respect to the Ore-Shale samples. Experimental studies (Craig et al., 1979) have shown that the copper content of carrollite is dependent on  $aS_2$ . The data therefore suggest that  $aS_2$  was higher in the Footwall than in the Ore-Shale. Although  $aS_2$  and  $aSO_4$  may not be related, the data do suggest that there was sufficient sulphur in the Footwall to fix metals as sulphides, and that the Footwall sulphides were not simply a result of Ore-Shale dewatering. The uniformity of the compositional data for Footwall carrollites may be related to the uniformity of porosity in the Footwall, as suggested by Annels et al. (1983) for the Footwall carrollites at Chingola.

Chalcopyrite, and more rarely bornite, are found to partially rim and replace carrollite, and are considered as paragenetically later.

#### 4.4 PARAGENETIC SEQUENCE OF DIAGENETIC EVENTS IN THE FOOTWALL CONGLOMERATE AND FOOTWALL SANDSTONE

The first diagenetic event was the infiltration of clay which coated detrital grains prior to all authigenic overgrowths, with the possible exception of the heavy minerals, see Figure 4.1. Zircon and rutile overgrowths probably formed simultaneously as indicated by the



zirconium content of the rutile overgrowth. Rutile may be the end product of ilmenite breakdown, in which case the iron released could have contributed to the formation of haematite grain coatings. Detrital iron may also have been a source of iron for such coatings. Haematite coating of detrital grains occurred after infiltration of clay and before dissolution of plagioclase feldspar and ferromagnesian minerals. This was followed by authigenic overgrowth of feldspar and quartz on detrital grains of those minerals. All of these features are typical of diagenetic events in desert environments and have been described by Walker (1976) and Walker et al. (1978).

The next sequence of diagenetic events was the formation of carrollite crystals and non-luminescent cobalt-rich rhombs of dolomite, both of which occur after quartz and feldspar overgrowths. Copper sulphide growth post-dates that of carrollite. This sequence of events was followed by a period of luminescent dolomite and malachite precipitation. The luminescent dolomite is not common and no paragenetic relationship between it and malachite could be determined, indeed it only seems to occur in areas where malachite is absent. Malachite replaced rhombahedral dolomite which it post-dates. The quantity of malachite occurring in some areas (up to 10% by volume) suggests that, at the time of its formation, porosity was still high. The abundance of carbonate minerals and associated sulphides indicates that this



sequence reflects a change in environment and porewater chemistry from the preceding events, and probably represents the influence of the marine transgression which marks the commencement of Ore-Shale deposition.

A diagenetically late, pervasive, quantitatively important quartz cement resulted in a marked decrease in porosity. This silicification event may explain the occurrence of silica in malachite and dolomite recorded during microprobe analysis (Table 4.1). The release of copper, by replacement of malachite during this reaction, probably explains the formation of chrysocolla which occurs along quartz grain boundaries and fractures. Feldspar grains are also affected by late diagenetic alteration and frequently display breakdown to kaolinite (see Plate 4.6E). Present day kaolinisation of feldspar occurs in areas of high minewater flow. In these instances, the replacement is locally extensive and generally complete, whereas diagenetic alteration is sporadic and generally poorly developed.

#### 4.5 DIAGENETIC FEATURES OF THE COPPERBELT OREBODY MEMBER

Discussion in this section is confined to the formation of authigenic minerals and replacement features. Dewatering phenomena are briefly commented on in conjunction with fluid inclusion chemistry in Chapter

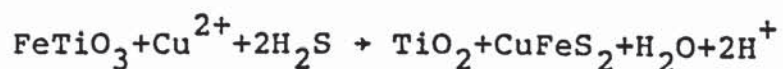
7. Features such as soft sediment deformation occur, (Plate 4.6F) but have not been examined in detail.

#### 4.5.1 Authigenic Minerals

Authigenic feldspar and quartz are well developed in the Ore-Shale. The development of sulphide minerals is considered an integral part of the diagenetic processes active in the host sediments, and is thus described in this section. Authigenic clay minerals would obviously have been formed, but subsequent metamorphism has destroyed the original phases, so the clay minerals will not be discussed here.

#### 4.5.1 (a) Accessory Minerals

Zircon and tourmaline both form overgrowths very similar in form to those of the footwall rocks. Rutile is common, often occurring as pseudomorphs after ilmenite (see Plates 4.6G and 4.6H). The lack of iron oxides implies that iron released during this reaction was used in the formation of the abundant local sulphide. Reactions of this nature are known to occur in reducing environments (Carroll, 1960 and Dimanche and Bartholomé, 1976), and can result in the formation of copper/iron sulphides:-



The reaction itself simply initiates crystal growth (possibly via a pyrite precursor), which continues at the expense of other materials. The amount of titanium dioxide present is therefore not necessarily directly related to the amount of sulphide finally produced (Dimanche and Bartholomé, 1976). However, at Konkola a close association between titanium dioxide and copper sulphides has been recognised, and is also reflected in the positive correlation between the elements titanium and copper (Appendix 7, Table A7.17). This relationship between titanium dioxide and copper sulphides has been recorded from a number of deposits (Bartholomé, 1974; Garrard, 1972 and Brown, 1971, 1978 and 1981), and is a potentially important process in localising sulphide minerals. It may also explain the concentration of sulphides accompanied by abundant detrital heavy minerals along foresets, troughs in ripple bedding, etc., and erroneously invoked to suggest a detrital origin for both (Garlick and Fleischer, 1972).

#### 4.5.1 (b) Dolomite

Dolomite occurs as thin beds and lenticles. The lenticles have been studied in detail since they provide important examples of relatively closed microenvironments, and are closely associated with sulphide mineralization.

The lenticles vary in size from 2 mm to 6 cms (see



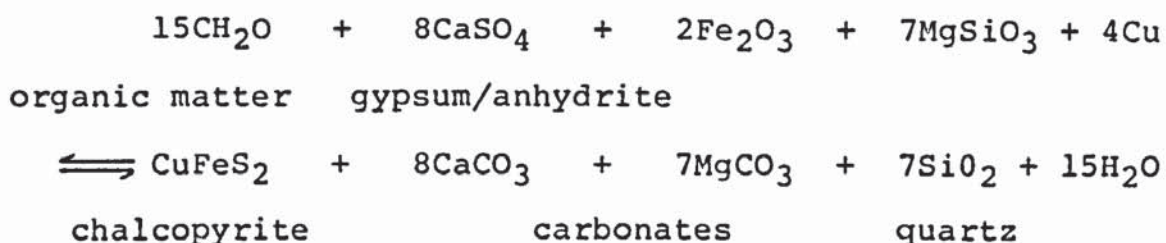
Plate 4.5B), and are best developed in units C and D of the Ore-Shale. They are composed of dolomite, sulphide, quartz and feldspar. The percentages of quartz and feldspar in a lenticle varies from 5 to 10% by volume, with the percentage sulphide in the remaining volume varying from a few percent to 100%. The dolomite contains traces of relict anhydrite, confirmed by electron microprobe analysis, and is considered to have formed as pseudomorphs after anhydrite. No unreplaced lenticular anhydrite was found at Konkola, although Annels (1974) was able to record all stages of the replacement in the Nkana Basin. The end products of the replacement, as described by Annels (1974), are identical to those found at Konkola. The quartz, feldspar and sulphide associated with the carbonate lenticles are discussed below.

Dolomites in the lenticles show a difference in form from core to rim, and also differences in isotopic and chemical composition (discussed in Chapter 6). Dolomite beds are intermediate in composition between the rim and core dolomites. The rim dolomites occur as elongate crystals approximately perpendicular to the lenticle edge, whereas the lenticle core dolomites occur as a sparry crystal mosaic (Plate 4.5C). Some lenticles consisting of only sparry dolomite do occur; these are usually barren of sulphide. As seen in Plate 4.5B, replacement takes place from the lenticle edge inwards; thus, where sulphide replacement is partial it is generally, although not

exclusively, associated with elongate crystals of rim dolomite.

The replacement of sulphate by carbonate and the concomitant formation of sulphide is potentially an important mineralising process (Annels, 1974, 1979; Hall, 1982; Brown and Chartrand, 1983) and merits further comment. Annels (1974) noted that lenticle anhydrite at Nkana North Limb is absent from areas of high grade ore, which is instead characterised by carbonate lenticles. A similar antipathetic relationship was demonstrated between the tenor of copper mineralization and non-lenticular anhydrite for the Mufulira orebodies (Annels, 1979).

At Konkola, the close relationship between the occurrence of sulphide and lenticular dolomite (after anhydrite) has already been mentioned. Whole rock analyses indicate a very strong positive correlation between the concentrations of sulphide copper and carbonate carbon (see Figure 4.2) and implies a close generic link, such as a common origin of carbonate and sulphide as a consequence of bacterial sulphate reduction. A generalised formula for this reaction is shown below (modified after Berner and Raiswell (1983), all untabled elements are by stoichiometric necessity).



The method of carbonate determination is explained in Appendix 2.

#### 4.5.1 (c) Quartz

Three types of authigenic quartz occur. These are:

- (i) overgrowths on detrital grains;
- (ii) authigenic crystals (a natural progression from type (i));
- (iii) a late diagenetic pore fill cement, very similar to and probably coeval with that occurring in the footwall rocks.

Authigenic crystals were formed on the perimeter of lenticle sidewalls and at the argillaceous edge of dolomite beds. These crystals were studied using the Scanning Electron Microscope, the dolomite matrix having been dissolved in warm 10% hydrochloric acid. The pitted nature of the grains examined (Plate 4.7A) is thought to represent coprecipitation of quartz with carbonate, indicating a pH of at least 7.4 (Blatt et al., 1972). The Ore-Shale dolomite is ferroan (Table 6.5), implying a reducing diagenetic environment.



The replacement of anhydrite and formation of quartz is pre-sediment compaction, as can be seen in Plate 3.3, where bedding traces wrap themselves around lenticles. Further, as the amount of quartz present in the carbonate lenticle decreases, the degree of lenticle elongation parallel to bedding increases, a feature also noted by Annels (1974). This indicates that the quartz growth took place before lithification, and probably during early diagenesis since many of the lenticles show almost no deformation.

A paragenetically late quartz pore cement similar to that in the footwall rocks is found and as in the footwall rocks, it replaces malachite.

#### 4.5.1 (d) Feldspars

Potassium and plagioclase feldspar both occur as optically-continuous and discontinuous overgrowths on detrital feldspar grains, and as euhedral crystals nucleated on carbonate lenticle sidewalls and along the argillaceous border of carbonate beds.

Some of the potassium feldspar overgrowths have a tendency to develop rhombic crystal forms as described by Waugh (1978) and Ali and Turner (1982), and indicate that porosity was relatively high during growth (see Plate

4.7B). Overgrowths are recognised by slight optical discontinuity with the host grain, or by the generally fresh appearance of the overgrowth and its tendency (often weak) towards crystalline form compared with the often cloudy and subrounded detrital host.

Overgrowths can also be of different composition to the host grain. Plate 4.7C shows an albite overgrowth nucleated on a microcline grain, although there is an intervening growth of muscovite, the compositions of the feldspars were obtained by electron probe micro analysis (Table 4.3, grain number 3). Spot analyses were performed on several authigenic overgrowths and their detrital cores. Several systematic variations in composition were noticed between overgrowths and host grains. The overgrowths show a decrease in sodium and barium content, and are nearer end-member composition than the detrital cores. Significantly, the copper content of the overgrowths is much higher than that of the detrital cores, although often both host and overgrowth are barren. Copper was therefore present in the pore solutions during the formation of authigenic feldspar. Diffusion of copper into the feldspars during metamorphism cannot explain the distribution of copper observed.

Cathodoluminescence studies established that authigenic feldspars can be readily distinguished from detrital cores by their differing luminescence colour.

Authigenic feldspar is generally considered to be non-luminescent (Kaster, 1971; Kaster and Siever, 1979) although in a review of typical mineral luminescence colours by Nickel (1978), it was found that although authigenic feldspars are commonly non-luminescent they can show brown, olive green or yellow green luminescence.

Long exposure times (20 - 30 minutes on 1000 ASA film) result in photographs of authigenic overgrowths showing a khaki-brown luminescence colour, while host grains frequently luminesce blue. Stablein and Dapples (1977) have suggested that blue luminescence is induced by the presence of barium in the feldspar, and probe data already presented suggest that this may indeed be the cause. However, Smith and Stenstrom (1965) point out that high temperature feldspars typically luminesce blue, and the detrital cores may simply luminesce blue because of their igneous provenance, as suggested from sedimentological evidence (Chapter 3).

Some of the feldspars in the Ore-Shale have crystallographically aligned patches of khaki-brown luminescence (authigenic feldspar colour) material in detrital cores (see Plate 4.8). This feature probably reflects partial dissolution of the core prior to infill and rimming by authigenic feldspar. Such dissolution features are much more common in the footwall rocks.



The volume reduction accompanying the replacement of anhydrite by carbonate would result in adequate space to allow the growth of euhedral crystals, which now line the perimeter of carbonate lenticles and beds. Because of their size (20 microns) the crystals are best studied using the Scanning Electron Microscope, with compositions being confirmed by on-line energy dispersive analysis. The carbonate matrix was removed by dissolution in warm 10% Hydrochloric acid. Microcline crystals (Plate 4.7D) were invariably found lining lenticles devoid of sulphide, whereas albite crystals are most frequently associated with chalcopyrite (see Plate 4.7E). Although only approximately fifteen samples were studied, the relationships observed suggest that microcline crystals grew before the main influx of copper in porewater, although the probe data indicate that some copper was in solution during microcline overgrowth formation.

Annels (1974) drew similar conclusions from his study of lenticular carbonate pseudomorphs from a marginally economic deposit in the Nkana basin. Based on petrographic studies, Annels demonstrated that when paragenetically early pyrite was the only sulphide present, microcline was the only feldspar found. Similarly when chalcopyrite was present, albite was the only feldspar to occur.

In conclusion, it would seem that authigenic

microcline formed before albite, and that this change mirrored a change from the formation of iron-rich to copper-rich sulphides.

#### 4.5.1 (e) Sulphides

Although economic mineralization is invariably confined to the Ore-Shale, significant amounts of copper sulphides are occasionally found in the Hangingwall rocks, and in the footwall rocks. Within the Ore-Shale, units C and D are the most sulphide-rich. The sulphides occur as fine disseminations and lenses aligned parallel to bedding. Sulphide minerals are closely associated with carbonate (pseudomorphs after anhydrite, Figure 4.2), and with leucoxene as discussed in Section 4.5.1 (a).

A general paragenetic sequence of Copperbelt primary sulphide mineralization is well established in general (Bateman, 1930) and for individual deposits (Konkola - Raybould, 1978; Chingola - Garrard, 1972; Baluba - Simmonds, 1980; Chambishi-Nkana - Rugman, 1977), and is summarised below.

pyrite - carrollite - chalcopyrite - bornite - chalcocite

At Konkola, pyrite is uncommon. Plate 4.7F shows a rare crystal of pyrite replaced by chalcopyrite and totally enclosed in a large 3 mm grain of carrollite. The



replacement of pyrite by chalcopyrite demonstrates that there was a copper mineralizing event before the main cobalt phase. The euhedral outline of the original pyrite is clearly defined. Had the chalcopyrite been the result of reaction between the carrollite and pyrite the original euhedral outline would certainly be lost. In Figure 4.3, the compositional variation of the mineral phases can be seen, and the pyrite clearly exhibits zonation with respect to cobalt. Pyrite grains on the Copperbelt are frequently zoned with an outer rim of cobalt (Darnley and Killingworth, 1962; Brown and Bartholomé, 1972), suggesting that the cobalt level in interstitial waters was high when pyrite growth came to an end.

The only cobalt sulphide of importance at Konkola is carrollite. The paragenetic position of carrollite is clearly seen in Plates 4.7G and 4.9A. In Plates 4.9A,B,C and D, two ages of carrollite can be observed. The grain core consists of carrollite with numerous silicate inclusions. Between the core and the outer, cleaner-looking carrollite lie stringers and patches of chalcopyrite, implying an intermediate period of copper mineralization. The rim carrollites are also compositionally different (Sample 638/6 in Table 4.2), with respect to the core carrollite; the rim carrollites are enriched in copper and depleted in cobalt and iron. These compositional differences are in agreement with the paragenetic position of carrollite formation being between



that of pyrite and chalcopyrite growth.

In Plate 4.7G, crystallographically aligned fractures in carrollite are infilled with chalcopyrite. The outer rim of chalcopyrite is in turn replaced by bornite. The fractures in carrollite are thought to be induced by burial, and are markedly different from tectonic fracturing (see Plate 4.7H). Tectonically-induced fracturing has resulted in a mosaic of carrollite islands which could be rebuilt to form the original grain. Throughout the Ore-Shale, chalcopyrite and bornite phases are both found to contain in the region of 1% arsenic. Chalcocite is found replacing and rimming both chalcopyrite and bornite, and is considered to be paragenetically later.

Although the generalised paragenetic sequence already presented is essentially valid, some minor modifications are necessary because of the early pre-cobaltian copper mineralising phase identified. A revised paragenetic sequence is shown below:

pyrite	-	chalcopyrite	-	carrollite
(last stages cobaltian)		(minor phase)		(two ages with intervening chalcopyrite)
chalcopyrite	-	bornite	-	chalcocite
(contain arsenic)				

The occurrence of minor mineral phases, and of breaks in mineralization, compound the complexity of chemical variation in porewaters. None-the-less, the paragenetic sequence reflects a change in composition of interstitial pore fluid from essentially iron-rich to cobalt enhanced iron-poor, and a final phase of iron/copper enrichment with copper being increasingly important.

#### 4.6 PARAGENETIC SEQUENCE OF DIAGENETIC EVENTS IN THE COPPERBELT OREBODY MEMBER

The paragenetic sequence recognised is summarised in Figure 4.4. Dissolution of detrital feldspar grains along crystallographically controlled directions was a very early diagenetic event, and may have taken place during or even before transportation to the depositional site. Overgrowths of tourmaline and zircon occur prior to quartz formation. The breakdown of ilmenite minerals under reducing conditions to titanium dioxide and pyrite resulted in the first sulphide formed. These pyrites, with their cobalt-rich rims, indicate the onset of a cobalt mineralizing phase, but not before a minor amount of copper sulphide was formed. Quartz overgrowth commenced before major amounts of sulphide were developed.

The replacement of porewater and lenticular anhydrite by silicates and carbonate with the concomitant production of sulphide marked the onset of a major sequence of

diagenetic events. The occurrence of feldspar overgrowths with their anomalous copper content demonstrates the presence of this element in porewater during overgrowth formation. Microcline growth proceeded that of albite. The co-existence of carbonate and quartz gives a tight control on pH conditions during anhydrite replacement, i.e. pH was greater than 7.4. The close chemical affinity of copper and cobalt sulphide with carbonate carbon indicates that anhydrite replacement and sulphide formation are closely linked.

The pseudomorphing of anhydrite occurred before sediment compaction since:

- (a) bedding traces are deformed around lenticles;
- (b) the amount of quartz present in a lenticle is reflected in its degree of compactional deformation (i.e. an increased percentage of quartz reduces the effect of compaction);
- (c) Carrollite grains frequently display crystallographically controlled, probably compaction-induced fracturing.

Within the anhydrite replacing event a sequence of sulphide mineral formation from carrollite to chalcocite





is identified.

Rarely, malachite is found replacing carbonate beds and nodules (Plate 4.9E), and is itself partly replaced by fine-grained quartz, identified only during microprobe analysis. This malachite is not associated with sulphides, and is not of obvious secondary origin. Secondary malachite does occur and was of importance in upper levels of the mine workings, where a sequence of secondary sulphide enrichment and associated malachite formation is recorded (Schwellnus, 1961).

#### 4.7 SUMMARY AND CONCLUSIONS

Sedimentation patterns suggest that the footwall rocks and the Copperbelt Orebody Member have a similar provenance, but have passed through differing diagenetic environments, see Figure 4.5.

The footwall rocks have undergone a period of semi-arid, oxic, meteoric water-controlled diagenesis similar to that described by Walker et al. (1978). This stage of diagenesis resulted in clay infiltration, dissolution and replacement which released into interstitial solutions the necessary Al, K, Mg, Na, Ca and Si to form a series of authigenic minerals. The production of haematite, quartz and feldspar overgrowths proceeded the main sulphide forming event, but quartz continued to precipitate for a

short time afterwards. During this period the footwall rocks were transgressed by marine waters, thus changing the pore fluid chemistry, and a period of sulphate reduction ensued. From this time onwards, diagenetic events in the footwall rocks were similar to those in the Copperbelt Orebody Member, the main differences being the result of the differing porosities and organic carbon composition of the two rock groups.

Prior to entering a reducing environment, the Copperbelt Orebody Member detrital components would have been modified. Feldspars show signs of dissolution, and there is a lack of ferromagnesian minerals implying their dissolution; also the detrital clay mineral component would be modified, particularly when it came in contact with marine water. The elements necessary for authigenic mineral formation could have a number of sources including dissolution and replacement reactions at the site of deposition; alternatively, the elements may have been contained in solutions (marine or porewater) migrating from the sedimentary basin or from a landward source.

Authigenic overgrowth of some quartz and possibly feldspar occurred before the main sulphide-forming event.

The replacement of sulphate by a combination of carbonate, sulphide or silicate minerals is well documented (Shearman and Fuller, 1969; Folk and Pittman,



1971; Annels, 1974; Harwood, 1980; Hall, 1982; Brown and Chartrand, 1983), and is undoubtedly linked with the formation of the bulk of Copperbelt Orebody Member sulphide. At Konkola the reaction took place during early diagenesis, and was complete before sediment compaction. Isotopic data (Chapter 6) establish that the pseudomorphing of anhydrite was a consequence of bacterial reduction.

Sedimentological evidence indicates that the Copperbelt Orebody Member porewater would have been a mixture of marine and groundwaters, with a probable meteoric component, which suggests a variation in mean pH of between 6.5 - 8.5 (Baas-Becking et al., 1960). The co-existence of quartz and carbonate found in the replaced lenticles implies a pH of at least 7.4 (Blatt et al., 1972). Birnbaum and Wireman (1984) have demonstrated that the growth of bacteria during sulphate reduction results in pH values being pushed towards neutrality. All the evidence suggests that pH conditions during sulphate replacement were slightly alkaline.

In Figure 4.6 the stability fields for waters pertinent to Copperbelt Orebody Member and footwall rock diagenesis are superimposed on the stability fields in the system Cu-Fe-S-O-H. During the initial period of footwall rock diagenesis, meteoric and groundwaters would have been active, and haematite an important authigenic mineral (as



shown in Figure 4.6). The marine transgression which marked the commencement of the Copperbelt Orebody Member would have resulted in the footwall rock porewater becoming more alkaline and reducing. Some of the haematite coatings are preserved by silicate overgrowths.

The growth of sulphides was marked by an early cobalt-rich phase. During bacterial sulphate reduction, the pH conditions were stable and near neutral. Porewater would probably have been intermediate in composition between that found in marginal marine sediments and in evaporites. The field defined in Figure 4.6 by the porewater stability zone and the established pH conditions, marks an area of complex sulphide stability, even ignoring the unknown effect that cobalt in solution may have had. The sulphide mineral paragenesis previously described can be formed within this field by small changes in either pH or Eh, and this may explain the overlapping zoning and other complexities superimposed on the general paragenetic sequence.

The change from potassium to plagioclase feldspar growth probably simply reflects the decreasing availability of potassium in the porewater, which because of the co-precipitated quartz must have remained highly silicaeous throughout feldspar formation. Precipitation of silica would have been enhanced by the lowering of pH during sulphate reduction.

Subsequent burial of the sediments must have resulted in a number of mineralogical changes (discussed in Chapter 8), which included pressure solution of grains and kaolinisation, both of which could be the source of silica for the late diagenetic silicification event previously described.

An understanding of the paleoenvironments of the sediments is important in interpreting the diagenetic environments through which they have passed. The sulphide minerals are considered an integral part of the host sediments and have a similar and closely linked diagenetic history.

## CHAPTER 5

### REVIEW OF ISOTOPE VARIATION IN GEOLOGICAL SYSTEMS

#### 5.1 INTRODUCTION

Our knowledge and understanding of stable isotope geology has advanced greatly in recent years, and this has led to new interpretations of the data from many of the early isotope studies. It is therefore considered necessary to include this chapter, in which the principles of isotope fractionation are briefly reviewed. Also recent ideas are presented on how the isotopic signatures of sulphur, carbon and oxygen in different mineral species can be interpreted in terms of their environments of formation.

#### 5.2 FRACTIONATION PROCESSES

Isotopes of an element have the same number and configuration of electrons, but have different atomic masses. Urey (1947) has shown that the strength of a chemical bond between atoms of two elements varies slightly with the masses of the isotopes involved, a light isotope forming a weaker bond than a heavier one. Because of this, although the isotopic ratios of naturally occurring pure elements are approximately constant, during chemical reactions, the ratios of the isotopes will change slightly. Such a process is known as fractionation. In



geological systems two types of isotopic fractionation are important; they are equilibrium and kinetic fractionation.

Equilibrium fractionation involves the partitioning of the trace isotope of an element relative to the major. The degree of fractionation of the isotopes of an element between two minerals at a fixed temperature is a function of the bond strength, with the lighter isotope being preferentially located in the more weakly bonded site. Thus, at a given temperature, the sulphur in chalcopyrite would be enriched in  $^{34}\text{S}$  compared with galena, the M-S bond being stronger in the former. However, the degree of fractionation is generally also an inverse function of temperature, the effect being greater at lower temperatures. Thus equilibrium fractionation provides the basis of isotope thermometry.

Kinetic fractionation is caused by the relatively faster rate of reaction of the lighter isotope in a system. Kinetic fractionation is most readily observed in the stable isotopes of carbon and sulphur (Coleman, 1977). During kinetic fractionation the initial products formed in a chemical reaction will be enriched in the lighter isotope. If the reaction is allowed to go to completion there will be no difference between the isotope ratios of the reactants and the final products. If, on the other hand, an aliquot of isotopically light product is removed, (i.e. does not take part in subsequent

reactions) the remaining reservoir of reacting material will be correspondingly isotopically relatively heavy. Subsequent aliquots of product, although isotopically lighter than the remaining reservoir will themselves be isotopically heavier than preceding aliquots of product. Thus a large spread of isotopic values will be observed. This process is known as the reservoir effect (see Figure 5.1).

### 5.3 SULPHUR ISOTOPE FRACTIONATION

Although sulphur has four isotopes, in practice only the ratio of the heaviest ( $^{34}\text{S}$ ) to the most abundant ( $^{32}\text{S}$ ) is usually determined.

#### 5.3.1 Equilibrium Fractionation

In equilibrium fractionation not only is temperature important, but it has been shown that the chemistry of the ore-forming fluid, particularly its pH and the fugacities of oxygen and sulphur have a marked effect on the degree of fractionation (Sakai, 1968; Ohmoto; 1972, 1974).

At a fixed temperature and low  $f\text{O}_2$  (so that sulphate is unimportant), a decrease in pH favours the formation of  $\text{H}_2\text{S}(\text{aq})$  and HS species, both of which prefer  $^{34}\text{S}$ . Thus a mineral formed at low pH would be enriched in  $^{32}\text{S}$ , relative to the same mineral formed from the same fluid at

a higher pH (see Figure 5.2).

At a fixed temperature and pH, an increase in  $fO_2$  would favour the formation of  $SO_4^{2-}$  which would preferentially concentrate  $^{34}S$ . Thus, any sulphide formed would show an increase in  $^{32}S/^{34}S$  ratio with increase in oxygen fugacity.

An increase of one unit in  $\log fO_2$  or pH can cause an increase in  $\delta^{32}S$  by more than 20 per mil at 150°C (Ohmoto 1972), for a given mineral phase.

However, the degree of fractionation between two species is constant at a given temperature. Only the absolute values are affected by variations in ore solution chemistry. Thus an original source material can be fractionated to give a range of values, the spread of which will be a function of the physical conditions operative.

### 5.3.2 Kinetic Fractionation

Kinetic fractionation occurs when there is a unidirectional reaction which affects the sulphur bond. The lighter isotope then reacts faster, and this will result in a product containing isotopically lighter sulphur.



In geological systems the most important process involving kinetic fractionation of sulphur isotopes is the reduction of sulphate by dissimilatory (respiratory) bacteria. These anaerobic bacteria use oxygen from sulphate ions to oxidise organic matter and in so doing produce  $\text{CO}_2$  and  $\text{H}_2\text{S}$  which is depleted in  $^{34}\text{S}$  with respect to the original sulphate.

Harrison and Thode (1957) showed that the purely chemical reduction of sulphate results in  $^{32}\text{SO}_4^{2-}$  reacting more rapidly than  $^{34}\text{SO}_4^{2-}$ , which causes the  $\text{H}_2\text{S}$  produced to be enriched in  $^{32}\text{S}$  by 22 per mil compared to the sulphate. These results are in good agreement with those produced by artificial laboratory cultures (Kemp and Thode, 1968; Smejkal et al, 1971) which produced maximum fractionations of up to 25 per mil.

In present-day anaerobic environments, depletion in  $^{34}\text{S}$  of up to 50 per mil has been recorded (Kaplan et al, 1963; Kaplan and Rittenberg, 1964; Nakai and Jensen, 1964). Various mechanisms involving different reaction pathways have been suggested to explain the discrepancy between natural and experimental observations (Trudinger and Chambers, 1973; Rees, 1973; McCready et al. 1974), and are reviewed by Chambers and Trudinger (1979), and will not be re-iterated here.

In summary the largest fractions occur with slow rates of bacterial growth, limited food supply, low

temperature and an infinite reservoir of sulphate. The rates of bacterial reduction and isotope fractionation are independent of pH in the range 6.2 to 8.2 (Kemp and Thode, 1968).

### 5.3.3 Factors Affecting the Magnitude of Kinetic Fractionation

Two major factors affect the magnitude of fractionation produced by sulphate reducing bacteria. These are, the availability of suitable organic matter and the availability of sulphate.

#### (a) Supply of organic matter

Goldharber and Kaplan (1974) have shown a positive correlation between sedimentation rate and the rate of sulphate reduction. They further demonstrated that there exists an antipathetic relationship between the rate of sulphate reduction and the size of the kinetic isotope effect. Thus, high rates of sedimentation favour the preservation of organic matter required for bacterial metabolism, and result in  $^{34}\text{S}$  enrichment of the sulphides formed.

The relationships between organic matter supply, sedimentation rate and  $\delta^{34}\text{S}$  were further refined by Irwin (1979).

(b) Supply of sulphur

Sulphide formation during bacterial sulphate reduction can obviously only proceed when there is available organic matter. If sulphate supply greatly exceeds that of organic matter, then as  $^{32}\text{S}$  enriched sulphides are produced, the remaining sulphate reservoir shows no appreciable depletion in  $^{32}\text{S}$ . Therefore large isotope fractionations can be expected. Such behaviour is described as an open system (i.e. open system fractionation).

In a closed system there is a limited sulphate source, thus as  $^{32}\text{S}$ -enriched sulphide is formed, the sulphate reservoir is  $^{34}\text{S}$ -enriched. Subsequent aliquots will undergo the same degree of fractionation as before, but sulphate and sulphide will both become progressively  $^{34}\text{S}$  enriched as the reservoir diminishes. If the sulphate reduction goes to completion, the resultant sulphide will have an isotopic composition equal to that of the initial sulphide.

Using these two extremes as models of sulphate reduction, Schwarcz and Burnie (1973), were able to relate  $\delta^{34}\text{S}$  values and their distributions to depositional environments.

However, a word of warning was given by Coleman



(1977) who was able to show that by progressive oxidation of sulphide to sulphate, a range of sulphide values could be obtained, even though the starting product was magmatic sulphur, and the degree of fractionation was constant (30 per mil), see Figure 5.3. The total sulphur isotope value is always 0 per mil despite the proportion of oxidised sulphur. It is therefore possible for magmatically derived sulphur to display a spread of  $\delta^{34}\text{S}$  values similar to that derived from bacterially derived sulphide. Thus, it is important not to use isotope data in isolation. An interpretation of formation environment of sulphide must combine data from other relevant sources (e.g. geochemistry, petrology etc.).

#### 5.3.4 Factors Affecting the Isotopic Composition of Initial Sulphate

.... Having examined the factors affecting the degree of fractionation during bacterial reduction, it is necessary to review factors controlling the isotopic value of the initial sulphate.

Present-day sea-water sulphate has a remarkably consistent isotopic composition, +21.0 per mil with a spread of 0.4 per mil (Rees et al., 1978). The crystallization of sulphate at room temperature involves an enrichment in  $^{34}\text{S}$  of 1-2 per mil relative to dissolved sulphate (Thode and Monster, 1965; Claypool et al.,

1980). By measuring marine evaporites of differing geological ages, considerable time variations have been found (Holser and Kaplan, 1966; Holser, 1977; Claypool et al., 1980).

Sulphate is generally considered to be of marine origin. However, input of detrital sulphate from pre-existing evaporites, and/or sulphate produced by oxidised sulphides could substantially offset (towards lighter values) the isotopic composition of a basin sulphate reservoir. Such a source of contamination has been proposed by Holser (1979) for the Rotliegendes of N.W. Europe.

#### 5.4 CARBON FRACTIONATION

##### 5.4.1 Equilibrium Fractionation

The isotopic compositions of carbonate phases formed from solution is dependent on the temperature and chemistry of the fluid (Ohomoto, 1972). The affect of chemical changes on the carbon system is very similar to that just described for sulphur (see Section 5.2.1), and will not be discussed here.

#### 5.4.2 Kinetic Fractionation

Kinetic fractionation is important in controlling the isotopic composition of carbonates formed in the sedimentary environment, and in the production of organic matter during photosynthesis (reviewed in Fauré, 1977).

Porewater bicarbonate can show a large range of carbon isotope composition (Nissenbaum et al., 1972; Claypool et al., 1973). Carbon isotope fractionation between the carbonate species (bicarbonate and calcite) is small, between 1 per mil and 3 per mil in the temperature range 10°C to 60°C (Emrich et al., 1970), and reaches a maximum of 3.8 per mil at about 400°C (Robinson, 1975). The isotopic composition of porewater bicarbonate will thus be very similar to any resultant calcite produced.

Curtis (1977, 1978) and Irwin et al. (1977) have demonstrated the existence of a series of environmental zones within a sediment, which can be characterised by the carbon isotope compositions of diagenetically formed carbonates, (see Figure 5.4).

In zone I,  $\text{HCO}_3^{2-}$  is produced by bacterial oxidation of organic matter, which is consumed as an energy source. The depth of this zone is determined by the limit of downward diffusion of molecular oxygen. Free upward migration of bicarbonate would mean that the potential for



carbonate formation would be low.

Benmore (1983) has proposed that once molecular oxygen becomes limiting, there may exist a subzone where other oxidants may be consumed. Indeed, Froelich et al. (1979) recognised a suboxic zone where  $\text{Mn}^{2+}$ ,  $\text{NO}_2^-$  and  $\text{Fe}^{2+}$  were concentrated. This bacterial reduction zone (Benmore, 1983) may extend over a range of tens of centimetres in sediments of low organic content.

In zone II, sulphate is metabolised by bacteria. Presley and Kaplan (1968) have demonstrated that the bicarbonate formed during this reaction is unfractionated with respect to the organic matter source. Thus, the carbonate formed is isotopically light and approximates the range for organic matter. The extent of this zone is limited by the depth of downward sulphate diffusion, or the depletion of the organic matter reservoir.

Zone III is characterised by bacterial fermentation. The process is not yet well understood, but involves the production of methane. Claypool et al. (1973) have shown that such methane can average close to -75 per mil P.D.B., with the resultant bicarbonate formed being proportionally enriched in  $^{13}\text{C}$ . Isotopic values of bicarbonate in the region of +10 per mil to +15 per mil can be expected.

The processes active in zone IV are poorly documented. The thermal degradation process of decarboxylation is one possibility, and would result in the formation of isotopically light carbon dioxide.

Carbonates precipitated within each zone will therefore have characteristic carbon isotope values, and, to a lesser degree, differing carbonate mineralogies.

A number of factors could potentially blur these zones. Primary carbonate (0 per mil) may become unstable, and add carbon of intermediate composition to the porewater reservoir. Methane produced during fermentation may migrate upwards and become oxidised near the sediment/water interface and could produce very light bicarbonate. Methane may also react with sulphate (Davis and Kirkland, 1970) and produce very light carbonates. However the reaction rates are such that it is probably only significant at temperatures greater than 200°C (Dhannoun and Fyfe, 1972).

#### 5.4.3 Carbon Reservoirs

The major reservoirs of carbon are marine water and organic matter. The isotopic composition of marine water bicarbonate is fairly uniform at 0 per mil, with respect to  $\delta^{13}\text{C}_{\text{PDB}}$  (Craig, 1953; Keith and Weber, 1964; Viezer and Hoefs, 1976). Organic matter in sedimentary rocks has a

fairly restricted range of values, with a mean of -25 per mil w.r.t.  $\delta^{13}\text{C}_{\text{PDB}}$  (Eckelmann et al., 1962; Hudson, 1977). However, the isotopic ratio of carbon in marine phytoplankton is related to oceanic surface water temperatures and varies between -30 per mil at 2°C and -20 per mil at 15°C (Sackett et al., 1973).

Fresh water shows a variable  $^{13}\text{C}/^{12}\text{C}$  ratio, but is generally enriched in  $^{12}\text{C}$  relative to marine water. This is probably due to the contribution of isotopically light, soil derived  $\text{CO}_2$  (Keith and Weber, 1964).

#### 5.4.4 Variations in the Carbon Isotope Composition of Marine Water

Numerous authors (reviewed by Viezer and Hoefs, 1976) have shown that  $\delta^{13}\text{C}$  does not show secular variations, although certain periods (Permian and late Proterozoic) may have been characterised by heavy  $\delta^{13}\text{C}$ . Veizer et al. (1980) using a larger data set have shown that the  $\delta^{13}\text{C}$  of carbonates has fluctuated with time, over a 3 per mil range, between the Quaternary and the Late Proterozoic. They further demonstrated that these changes were independent of facies or post-depositional change and were of global cause. They suggested the  $\delta^{13}\text{C}$  changes reflected secular variations of seawater bicarbonate.



## 5.5 OXYGEN FRACTIONATION

### 5.5.1 Equilibrium Fractionation

Equilibrium fractionation of oxygen isotopes is far more important geologically than kinetic fractionation, and is particularly important where meteoric water is concerned. Isotopic fractionation during evaporation and condensation results in water vapour being depleted in  $^{18}\text{O}$  by approximately 10 per mil compared with the liquid water with which it was in equilibrium. Consequently, because of the reservoir effect, (Figure 5.1), rainwater is depleted in  $^{18}\text{O}$  at higher altitudes and latitudes (Dansgaard, 1964).

### 5.5.2 Temperature Determination

The oxygen isotope composition of any minerals formed in isotopic equilibrium from a liquid depends on the oxygen isotope composition of that liquid and the temperature of formation. Thus, if the fractionation factors for any two minerals formed in equilibrium from a liquid are known, since the isotopic composition of the fluid is common to both, their formation temperature can be determined.

The calcite-water isotopic temperature scale was determined by McCrea (1950) and modified by Craig

(1965). The relationship between fractionation and temperature is given by:-

$$t(^{\circ}\text{C}) = 16.9 - 4.21(\delta\text{c}-\delta\text{w}) + 0.14(\delta\text{c}-\delta\text{w})^2$$

where  $\delta\text{c}-\delta\text{w}$  = the difference between  $\delta^{18}\text{O}_{\text{PDB}}$  calcite and  $\delta^{18}\text{O}_{\text{PDB}}$  water.

A similar relationship for dolomite-water was determined by Irwin et al. (1977) and is shown below:-

$$t(^{\circ}\text{C}) = 31.9 - 5.5S(\delta\text{d}-\delta\text{w}) + 0.17(\delta\text{d}-\delta\text{w})^2$$

where  $\delta\text{d}-\delta\text{w}$  = the difference between  $\delta^{18}\text{O}_{\text{PDB}}$  dolomite and  $\delta^{18}\text{O}_{\text{PDB}}$  water.

The use of these equations relies on three assumptions:

- (1) The estimated value of  $\delta^{18}\text{O}$  water is correct,
- (2) Isotopic fractionation has occurred in equilibrium,
- (3) Neither the calcite nor dolomite isotopic composition has changed since its formation.

In using these equations to calculate temperatures, if preglacial ( $10^4$  yrs) seawater was involved in the carbonate formation, then a  $\delta^{18}\text{O}_{\text{PDB}}$  value of -1.2 per mil

for water should be used (Shackelton and Kennet, 1975). This is to correct for isotopically light water released into the oceans when the ice caps were melted.

### 5.5.3 Oxygen Reservoirs

Present-day seawater has a narrow range of oxygen isotopic composition, and is generally considered to have a value of 0 per mil (SMOW). Evaporation processes result in preferential depletion of the lighter isotope in the aqueous phase (Epstein and Mayeda, 1953). Consequently, saline waters are generally enriched in  $^{18}\text{O}$ , and a linear relationship can be shown to exist between salinity and  $\delta^{18}\text{O}$  (Fauré, 1977).

There is growing evidence (reviewed in Viezer and Hoefs, 1976) that secular trends in  $^{18}\text{O}/^{16}\text{O}$  ratios may reflect variations in the isotopic composition of seawater. The changes themselves can be large, and are discussed with respect to Precambrian values in Chapter 7.

The oxygen isotpic composition of groundwater can be shown to be similar to that of the recharge area (Gat, 1971), although it may be modified by evaporation and exchange with the country rock through which it has passed. In essence, groundwaters exhibit a similar range in isotopic compositions to meteoric waters (discussed above), with a shift towards more  $\delta^{18}\text{O}$  -enriched values.



Groundwaters will thus be distinct from marine seawater; the isotopic difference being a function of paleo-latitude and elevation of the recharge area, combined with the degree of post-aquifer recharge change.

Magmatic waters are considered to have an isotopic composition of +6 per mil to +8 per mil (SMOW) (Taylor, 1974).

#### 5.6 CONCLUSIONS

The absolute value and range of isotopic composition of an element in a mineral species is dependent on the isotopic composition of the source of that element, the mode of fractionation, temperature of deposition and, in the case of equilibrium fractionation, on the composition of the formation fluid. Thus, isotopic data must be interpreted in conjunction with other relevant geological information on the environment of formation and subsequent changes to any mineral phases examined.

## CHAPTER 6

### STABLE ISOTOPE RESULTS FROM THE KONKOLA BASIN

#### 6.1 INTRODUCTION

The first sulphur isotope work on the Copperbelt was published by Bateman and Jensen (1956). It comprised a total of ten analyses from the Zambian Copperbelt and Katanga. The data of Bateman and Jensen, were augmented by a further three analyses presented by Darnley in 1960. This work was intended to confirm either one of the rival syngenetic or epigenetic hydrothermal theories of origin proposed for the Copperbelt ores at that time. In both cases the authors concluded that the results were non-diagnostic, and suggested the need for further work.

In 1962, Jensen and Dechow reported the  $\delta^{34}\text{S}$  composition of 122 samples, 65 of which were from the Zambian Copperbelt. They showed a strong correlation between enrichment in  $^{32}\text{S}$  with ore grade and abundance of carbonaceous material for samples from the Mufulira Mine. Based on this evidence, the greater spread of  $\delta^{34}\text{S}$  values in the results compared to those from magmatic-hydrothermal deposits, and the similarity of  $\delta^{34}\text{S}$  with the copper deposits of Mt. Isa and White Pine, the authors concluded that the results were "much more suggestive of a biogenic origin for the sulphur of the Rhodesian Copperbelt than a magmatic hydrothermal origin".

In an extended study, Dechow and Jensen (1965) suggested that the  $\delta^{34}\text{S}$  results were not diagnostic of either a magmatic-hydrothermal, or biogenic origin of the sulphur. They further suggested that the data may show evidence of the role of metamorphism in the formation of the ore deposits and in re-adjusting the  $\delta^{34}\text{S}$  values. These conclusions are based on the apparent enrichment in  $^{34}\text{S}$  with increasing metamorphic grade, but did not take into account changes in sedimentary facies or lithology.

In 1973, Schwarcz and Burnie incorporated the data of Dechow and Jensen (1965) in their model of open and closed system fractionation. Using sedimentological evidence of paleo environments, and the degree of fractionation from source sulphate, they were able to demonstrate that the  $\delta^{34}\text{S}$  values and their distribution can be useful indicators of the environment of formation. They considered the Copperbelt isotope results to reflect closed system fractionation.

This chapter looks in detail at the isotopic relationships involving sulphides (mainly chalcopyrite) and calcite and dolomite. Malachite samples from the Ore Shale and the Footwall Rocks were also examined. The  $\delta^{18}\text{O}$  values of quartz and feldspar from veins which crosscut the Ore Shale were determined in an attempt to quantify metamorphic temperatures.



## 6.2 SULPHUR ISOTOPE RESULTS

In order to examine if there is any variation in  $\delta^{34}\text{S}$  values of the sulphide minerals in various host lithologies, borehole AP978 (Figure 7.1) was systematically sampled. This borehole was chosen because the sulphides are essentially mono-mineralic, being chalcopyrite with only trace amounts of carrollite ( $\text{CuCo}_2\text{S}_4$ ). The chalcopyrite occurred as finely-disseminated, and lenticular material.

### 6.2.1 Discussion of Sulphate Source and its Isotopic Composition

The link between the replacement of anhydrite and the consequent formation of carbonate and sulphide has been discussed in Chapter 4, Section 4.5.1(b). The lack of suitable amounts of anhydrite prevented the determination of  $\delta^{34}\text{S}$  values for Ore Shale seawater sulphate at Konkola. Nonetheless, a mean value can be estimated from values obtained elsewhere.

Viezer et al. (1980) report a mean Late Proterozoic sulphate value of +18.9 per mil  $\pm 0.9$  per mil. On the Copperbelt, at Chambishi a mean sulphate value of +17.8 per mil is recorded (M. Cunningham, pers comm.), and at Mufulira a mean value of +17 per mil (J. Surman, pers.

comm.) for barren sulphate. A mean value of  $\delta^{34}\text{S}$  of +18 per mil for seawater sulphate at the time of formation of the Ore Shale therefore seems likely.

#### 6.2.2 Ore-Shale Results

The methodology of sample preparation and analysis is discussed in Appendix 3.

The results of chalcopyrite and carrollite analyses for borehole AP978 are shown in Table 6.1 and Figure 6.1. The isotopic compositions of the sulphides fall within the range -7.0 per mil to +1.2 per mil, with a mean value of -2.8 per mil.

Lenticle and disseminated chalcopyrite isotope values show only a slight difference in  $\delta^{34}\text{S}$ , with the general trend towards disseminated chalcopyrite being isotopically lighter. However, the differences are probably within the limits of analytical error.

As a check on any isotopic zonation within individual lenticles, a chalcopyrite lenticle (sample AP978/10) was analysed. The lenticle was slightly elongate parallel to bedding, with its longest dimension being 1.7 cms. Chalcopyrite was taken from the core of the lenticle, and from a 2mm annulus around the perimeter. Care was taken to avoid contamination with disseminated chalcopyrite.

The lenticle core material was found to be depleted in  $^{34}\text{S}$  by 0.4 per mil, compared to the edge. Shearman (1982) has shown that anhydrite nodules grow displacively from the core outwards. The change in isotopic composition from lenticle core to edge, assuming a constant sulphate-sulphide fractionation factor, probably reflects an enrichment in  $^{34}\text{S}$  of primary sulphate during lenticle growth.

The data from AP978 and the Footwall rocks are combined in Figure 6.2 with the results obtained for Konkola from the study of Dechow and Jensen (1965). When plotted in stratigraphic order, the results from both studies display parallel trends. The isotopic displacement in the trends may be explained in terms of the different mineral species analysed (mainly chalcopyrite as opposed to bornite/chalcocite) and the different sample locations. The samples used in the Dechow and Jensen study were taken from approximately 420m updip and 320m along strike (to the North) from those of borehole AP978. The trends show a progressive depletion in  $^{34}\text{S}$  towards the top of unit B followed by an enrichment in  $^{34}\text{S}$  upwards towards the unit D/E contact, and subsequent depletion in  $^{34}\text{S}$  in unit E. A strong stratigraphic control is implied, and possibly reflects the influence of environmental conditions during Ore Shale deposition.



### 6.2.3 Discussion of Ore-Shale $\delta^{34}\text{S}$ Values

A metasomatic origin for the mineralization has been proposed by Darnley (1960) and Vaes (1962). However, it is thought unlikely that a metasomatic origin could explain the subtle yet consistent, rapid vertical change in sulphide isotopic compositions. Any variation in mineralising fluid composition should be mirrored in the isotopic composition of the precipitated sulphides. A lowering of pH at fixed temperature and  $f\text{O}_2$  should result in sulphides enriched in  $^{32}\text{S}$  (see Section 5.2.1). Thus fluids passing through unit A, which is carbonate-rich, should precipitate sulphides which are isotopically light relative to the more siliceous unit B. Similarly, unit D sulphides should be light relative to those in unit E. From Figure 6.2, the reverse is found to be the case. During metasomatism, the temperature difference across the orebody would be minimal. Thus, unless one resorts to large and rapid variations in  $f\text{O}_2$  to mask the potential change in pH, metasomatism is not able to explain the isotopic distribution observed.

A number of factors may be responsible for the variation of isotopic composition in the sedimentary environment. Variations in:

- (a) fractionation factor;
  - (b) supply of organic matter/sedimentation rate;
  - (c) isotopic composition of porewater sulphate,
- could all play a part (see Section 5.2).

(a) Fractionation Factor

The range and distribution of the isotope values (see Figure 6.1) suggest a closed system fractionation model (Schwarcz and Burnie, 1973) similar to that proposed by these authors for the Copperbelt data produced by Dechow and Jensen (1965). A fractionation factor ( $\delta^{34}\text{S}_{\text{sulphate}} - \delta^{34}\text{S}_{\text{mean sulphide}}$ ) of 20.8 per mil (18 per mil - (-2.8 per mil)) is also consistent with a closed fractionation model. Changes in the fractionation factor due to, for instance, differences in nutrient supply or type cannot be ruled out, but the distribution of isotope result (lack of marked skewness) make this unlikely.

(b) Supply of Organic Matter/Sedimentation Rate

Variation in the supply of organic matter and in the sedimentation rate have a similar effect (Irwin, 1978; see Section 5.2.3). Fast sedimentation rates result in greater preservation of organic matter, and general enrichment in  $^{34}\text{S}$ . Variations in these parameters cannot be ruled out when comparing unit A and unit B which is sedimentologically different. However, in terms of sedimentology, units C and D are almost indistinguishable; their sedimentation rates would therefore be very similar. The two units also have very similar organic carbon and carbonate carbon (most of it from oxidised



organic matter, see Section 6.3) compositions. Thus units C and D would be expected to have comparable sulphur isotope values. But it is over these units that the isotopic composition of the chalcopyrite samples displays its greatest variation (see Figure 6.2).

(c) Isotopic Composition of Porewater Sulphate

Units C and D were deposited during a regressive phase (see Chapter 3), and thus replenishment of the porewater sulphate reservoir would not be possible. Closed system fractionation of the porewater sulphate reservoir would result in progressively heavier sulphides forming, and seems the most likely cause of the isotope results obtained for units C and D. The transgressive events following deposition of unit D, would result in recharging of the porewater reservoir with isotopically relatively light sulphate. This would result in  $^{32}\text{S}$ -enriched sulphides forming in unit E, as is observed.

Using the linear section of Figure 6.2, the thickness of sediment accumulated during sulphate lenticle growth can be estimated. The observed lenticle zonation of 0.4 per mil (only one set of data), would represent a deposition of 0.2m of sediment. This assumes a uniform sulphate-sulphide fractionation, and would be equivalent to an accumulation of some 0.5m of unconsolidated sediment, from commencement to completion of lenticle



growth. At this depth, the sediment would have entered the zone of bacterial reduction (Curtis, 1977).

In summary the distribution of  $\delta^{34}\text{S}$  values is not compatible with a metasomatic origin for the sulphides. The  $\delta^{34}\text{S}$  distribution can be explained in terms of closed system fractionation of bacterially reduced sulphate. The controlling factors would have been the sedimentation rate, the supply of organic matter and the variation in porewater sulphate reservoir. These factors can be linked using sedimentology to transgressive and regressive events at the time of Ore Shale formation. The influence of transgressive/regressive events is reflected in the bimodal distribution of  $\delta^{34}\text{S}$  values, (see Figure 6.1).

#### 6.2.4 Footwall Results and Discussion

All of the samples with the exception of those prefixed KLB and Mbula are taken from crosscuts and boreholes in approximately the same area as borehole AP978. The  $\delta^{34}\text{S}$  values of Footwall samples show a range from +8 per mil to -8 per mil (see Table 6.2) which is much wider than that exhibited by the Copperbelt Orebody Member (Ore-Shale) samples. The samples get progressively isotopically heavier with increasing depth below the Copperbelt Orebody/Kafue Arenites Member contact.

The sulphur isotopic composition of the Footwall samples is probably best explained by closed system fractionation of porewater sulphate.

The onset of the transgressive event, which marks the formation of unit A, would result in the Footwall microconglomerate pore spaces being charged with sulphate-rich water. The initial sulphides formed would be relatively isotopically light. The depth of sulphate diffusion is approximately 6cms for mud (Hartmann and Nielson, 1969), but would presumably be greater in the Footwall, because of its higher porosity. Nonetheless, as the sulphate diffusion depth is exceeded, the porewater system is effectively a closed system. Deposition of unit A sediments would hasten this. Progressive depletion of sulphate would result in later formed sulphides being enriched in  $^{34}\text{S}$ . This, combined with marine sulphate-rich water mixing with any sulphate-poor porewater in the microconglomerate at depth, would result in  $^{34}\text{S}$  enrichment of sulphides with depth below the Copperbelt Orebody/Kafue Arenites Member contact.

#### 6.2.5 Conclusions

The sulphur isotope data are not compatible with a metasomatic origin for the sulphides. The data, in fact, can all be explained by closed system bacterial fractionation, with changes in the supply of organic matter (sedimentation rate) combined with the reservoir effect accounting for the variations observed.



The data also show that since isotopic features are observed which reflect conditions of initial formation, no overall re-equilibration of  $^{34}\text{S}/^{32}\text{S}$  ratios has taken place on the macro scale due to metamorphism. Further confirmation of this has been obtained by the study of eight co-existing chalcopyrite-bornite samples (Table 6.2), aimed at using temperature-dependent fractionation for geothermometry. The fractionation curve for chalcopyrite-bornite is very flat and liable to error (Wedepol, 1978). As recorded in Table 6.2, only three of these sample pairs gave temperatures in line with petrological evidence. The three sample pairs gave temperatures of 330°C, 325°C and 350°C, although there is no evidence that these were actually formed in isotopic equilibrium. The remaining samples gave excessively high temperatures. Thus, although localised re-equilibration may take place, overall re-equilibration evidently requires factors other than increased temperature, probably the presence of a fluid medium.

### 6.3 CARBONATE $\delta^{18}\text{O}$ AND $\delta^{13}\text{C}$ ISOTOPE RESULTS

Before presenting and discussing the isotope data, it is necessary to examine the effects that;(a) metamorphism, (b) the isotopic composition of Precambrian water and (c) dolomitization may have had on the original isotopic composition of the carbonates.



### 6.3.1 Discussion of Factors Affecting the Interpretation of Precambrian Carbonate Isotope Values

#### (a) Metamorphism

In the mine areas, the Copperbelt has been subjected to metamorphism from lower to upper greenschist facies. The grade of metamorphism increases in a south to southwest direction (Mendlesohn, 1961), Konkola being of lower greenschist facies.

Isotopically, the effect of regional metamorphism is to decrease the  $^{18}\text{O}/^{16}\text{O}$  ratios with increasing grade (Hoefs, 1980). Decarbonation reactions can be expected to deplete  $^{13}\text{C}$  values in calcite (Taylor and O'Neil, 1977). However, Hoefs (1980) points out that the degree of depletion in  $^{13}\text{C}$  will also be a function of the organic content of the rock, and more importantly, the effect, if any, of an external source of carbon.

That wholesale re-equilibration does not always take place has been clearly demonstrated by Anderson (1967). Perhaps the most detailed study of the lack of isotopic re-equilibrium during metamorphism is that in which Rye et al. (1976) made a comprehensive study of C and O isotopes in interlayered marble and schist subjected to metamorphism up to 700°C. The marble units varied in thickness from 6cms to 51m. In all instances it was

observed that below 540°C,  $^{18}\text{O}$  exchange was limited to the margin of marble/schist contact, and could be related to fluid flow along this plane, while the rest of the marble remained unaltered. The carbon isotope values of the marbles remained unaltered, and maintained their original marine values, even though they had been recrystallised.

Thus it would seem that the degree of isotopic re-equilibration during regional metamorphism is a function not only of temperature, but of the water/rock ratios, and the extensiveness of the permeation of the fluid. Recrystallization in a dry environment appears to have little effect.

In Ore deposits, Lambert et al. (1980, 1984) have shown that C and O isotope ratios of dolomites in the Kapunda and Copper Claim deposits (S.W. Australia) are unaffected by metamorphism up to 300°C. Ruxton (1981) working on copper deposits in Namibia (very similar to the Zambian Copperbelt), concluded that metamorphism of lower greenschist facies, had no effect on the carbonate C and O isotopic values.

At Konkola, metamorphism postdates deposition by approximately 500 my (see Chapter 2), therefore sediment compaction would be expected to be advanced, and porosity within the Ore Shale would be low. Recrystallisation has undoubtedly taken place in carbonate lenticles but crystal

morphology differences remain, and are discussed in Section 4.5.1. Although there was some fluid flow through the Ore Shale during metamorphism, it may not have played an important part in aiding isotopic re-equilibration, an observation borne out by the lack of sulphur isotope re-equilibration. Thus as far as metamorphism is concerned, it is probable that the carbonate isotopic compositions have remained unaffected.

(b) Isotopic Composition of Precambrian Water

Precambrian marine carbonate oxygen isotope values are isotopically light for a given depositional environment compared with more recent equivalent (Vieser and Hoefs, 1976; Becker and Clayton, 1976; Keith and Weber, 1964). This can be explained in one or more of three ways:

- (1) Oceanic water was at a higher temperature during the Precambrian;
- (2) The oceans at that time were isotopically lighter;
- (3) The carbonates have undergone more exchange with post-depositional water.

Knauth and Epstein (1976) have suggested that the isotopic composition of the oceans has remained essentially static through geological time. They argued that the relatively large changes involved are more easily explained in terms



of temperature fluctuations rather than mass exchanges due to glaciation, sedimentation or volcanic input. Perry and Tan (1972) explain the isotopically light Precambrian (3.2 by) water in terms of isotopic exchange between what was then a smaller ocean and crustal material. Light oceanic water (-10 per mil SMOW) was used by Friedman (1975) to explain isotope values obtained from apparently unaltered Ordovician marine carbonates. Using Chert samples which became closed to isotopic exchange at low temperatures, Becker and Clayton (1976) were able to show that oceanic  $^{18}\text{O}$  values 2.2 by ago were within the range -3.5 per mil to -11 per mil.

Changes in  $^{13}\text{C}/^{12}\text{C}$  have been reviewed in section 5.3.

Although isotopic exchange with post-depositional waters occurs, there are too many examples of preserved carbonate isotope values to consider this phenomenon to be pervasive.

Thus, for rocks of Ore-Shale age(=1000 my) one would expect  $^{13}\text{C}$  to be slightly lower (negligibly so), and  $\delta^{18}\text{O}$  to be (using an average value) 9 per mil lower.

(c) Dolomitization

The formation of dolomite and the effects which this formation has on stable isotope ratios remains a controversial subject. Experimental studies (Northrop and Clayton, 1966; O'Neil and Epstein, 1966) predict that dolomites (at 25°C) should be enriched in  $^{18}\text{O}$  by 5.0 to 7.0 per mil compared to co-existing calcite, and Sheppard et al (1970) have suggested an enrichment in  $^{13}\text{C}$  of 2.5 per mil. Viezer and Hoefs (1976) have shown that Proterozoic dolomites are, on average, 5 per mil enriched in  $^{18}\text{O}$  compared with coeval limestone, and are generally  $^{13}\text{C}$  enriched.

Other workers (Epstein et al., 1963; Friedman and Hall, 1963; Fritz et al., 1970) have shown that  $^{18}\text{O}$  differences are less than theory predicts. Degens et al. (1964) have explained this difference by suggesting that dolomitization proceeds under solid state conditions without isotopic exchange; any difference in co-existing calcite is a result of the ease with which calcite would re-equilibrate with post-formation waters relative to dolomite (Epstein et al., 1963). Hoefs (1980) suggested that dolomite is not in equilibrium with co-existing calcite, and that its  $\delta^{18}\text{O}$  value depends on that of the dolomitizing solutions, and thus its time of formation, which may be markedly different from that of the calcite.

Fritz and Smith (1970) demonstrated that dolomite which formed via a protodolomite precursor would have a smaller difference to calcite (3 to 4 per mil) than dolomite formed directly from water (5 to 7 per mil). This hypothesis was further refined by Katz and Mathews (1977). They imply that dolomitization occurs via a magnesian calcite, and that the reaction is not in equilibrium with the bulk solution, but is restricted to solution zones around the dissolving grain. Mathews and Katz (1977) confirm this and show that  $^{18}\text{O}$  correlates well with the  $\text{Mg}:(\text{Mg}+\text{Ca})$  ratios of the phases, and suggest that the reaction-zone model can explain the low dolomite-calcite oxygen isotope fractionations. The bulk of the evidence, however, supports the view that dolomitization enriches  $^{18}\text{O}$  by about 3-5 per mil and  $^{13}\text{C}$  by 2-3 per mil, although there is less evidence to support the  $^{13}\text{C}$  enrichment.

Thus it can be suggested that the overall effect of metamorphism, Precambrian water values and dolomitization would be to deplete  $^{18}\text{O}$  by approximately 6-8 per mil and, possibly, to enrich  $^{13}\text{C}$  by 2-3 per mil in the samples studied.

#### 6.3.2 Dolomite Results

Samples from (a) the Ore-Shale (consisting mainly of lenticle carbonates), (b) the Footwall (consisting mainly



of euhedral dolomite crystals) and (c) whole rock samples from borehole CP197 were analysed for their oxygen and carbon isotope values. The results from the Footwall and Ore-Shale are shown in Figure 6.3 and Table 6.3.

(a) Ore-Shale Samples

The bulk of the Ore-Shale samples analysed were taken from lenticle dolomites, the occurrence and form of which have been discussed in Chapter 4, Section 4.5.1(b). The Ore-Shale and Footwall samples are isotopically distinctly different. The Ore-Shale lenticles themselves show a marked zonation with respect to  $^{13}\text{C}$ . Samples from the lenticle cores have a mean  $\delta^{13}\text{C}$  value of -9.2 per mil, and those from the lenticle rim have an average  $\delta^{13}\text{C}$  value of -18.5 per mil, but with values down to -20.5 per mil. Samples from carbonate laminae have intermediate  $\delta^{13}\text{C}$  values. The Ore-Shale samples display little difference in  $^{18}\text{O}$  values, although there is a tendency for the core samples to be slightly depleted in  $^{18}\text{O}$  relative to the rim samples.

(b) Footwall Samples

Dolomite occurs in the Footwall as an interstitial cement, invariably as euhedral rhombs nucleated on clast boundaries (see Plate 4.3). Some pore-filling sparry dolomite does occur, but is much less abundant than the

euohedral dolomite.

The Footwall dolomite samples are  $^{13}\text{C}$ -enriched and  $^{18}\text{O}$ -depleted relative to the Ore-Shale samples.

Two samples from the Bancroft Quartzite Member were analysed. The calcite occurs as a coarse interstitial cement. Isotopically the samples are considerably enriched in  $^{13}\text{C}$  and depleted in  $^{18}\text{O}$  compared with all the other samples analysed.

(c) Whole Rock Samples

A total of 20 whole rock samples were analysed from borehole CP197, the location of which is shown in Figure 7.1. All the samples analysed appeared to be fresh and unweathered. The results are shown in Figures 6.4 and 6.5 and Table 6.4. Although no unit B was recorded in the borehole log, it is included in these figures, on the basis of hand sample identification.

The  $\delta^{13}\text{C}$  values display a progressive depletion in  $^{13}\text{C}$  from the Footwall (-5.55 per mil) through units A and B, with units C and D exhibiting similar values (approximately -17 per mil). From the top of unit D through unit E and into the Hangingwall (-13 per mil) the samples become more  $^{13}\text{C}$  enriched (see Figure 6.4).

The  $\delta^{18}\text{O}$  values (see Figure 6.5), show a progressive depletion in  $^{18}\text{O}$  from the Footwall (-22 per mil SMOW) through to unit A. The  $\delta^{18}\text{O}$  values in the remaining lithological units, although showing some variation, are similar, with values in the range 16.7 per mil to 15.5 per mil (SMOW).

### 6.3.3 Geochemistry of Dolomite Samples

The core and rim dolomites from lenticles within the Ore Shale differ not just in morphology, and isotopic composition but also chemically, see Table 6.5. The rim dolomites have lower sodium and strontium concentrations than the core samples. Electron microprobe analyses reveal that the rim dolomites have higher cobalt and manganese contents, but that both types of dolomite are calcium-rich.

The Footwall dolomites have higher strontium concentrations than the lenticle samples, and sodium values intermediate between the lenticle rim and core samples. Microprobe analysis of the dolomites revealed that several of the phases are cobalt-rich (see Table 4.1) with cobalt carbonate concentrations of up to 4.9%.

A strong positive correlation (+0.78,  $n=20$ ) between strontium concentration and  $\delta^{13}\text{C}$  value was found for borehole CP197 samples. The correlation between rubidium



and strontium was -0.63, and between rubidium and  $\delta^{13}\text{C}$  was -0.33. Strontium, besides occurring in carbonates, can also substitute for Ca in plagioclase feldspar. However, calcium feldspar is most common in units C/D where strontium is least abundant. It is therefore concluded that the bulk of the strontium occurs in carbonates, where it reflects the degree of marine influence (Clemmey, 1976).

#### 6.3.4 Discussion of Dolomite Isotope Data

The compositional data for Konkola mine waters is shown in Table 6.6, and precludes the formation of recent dolomite at Konkola (see Folk and Land, 1975). The isotopic composition of the water (-6.2 per mil SMOW) is not compatible with the formation of dolomite with the  $\delta^{18}\text{O}$  values of the data presented.

If the carbonates are accepted as being primary, which seems most probable from the textural evidence already discussed (Section 4.3.2), then the isotope results must be corrected for the factors discussed in Section 6.3.1. The data are presented in corrected form in Figure 6.6.

The Footwall samples  $\delta^{18}\text{O}$  values are clearly dominated by seawater-derived oxygen. The Ore-Shale  $\delta^{18}\text{O}$  values are remarkably consistent, and are about

7 per mil depleted in  $^{18}\text{O}$  relative to the Footwall samples. If we assume a similar oxygen (i.e. seawater) source for the Ore-Shale and Footwall samples, then using the equation derived by Irwin et al. (1977), a temperature differential can be derived for the formation of the Ore-Shale samples relative to the Footwall samples. Assuming  $\delta\text{d}-\delta\text{w} = 0$  per mil for the Footwall samples ( $T=31.9^\circ\text{C}$ ), then  $\delta\text{d}-\delta\text{w} = -7$  per mil for the Ore-Shale samples ( $T = 79^\circ\text{C}$  greater than that of the Footwall samples). This temperature differential of  $+79^\circ\text{C}$  is independent of any correction factors applied to the data, since it uses only the  $\delta^{18}\text{O}$  differences between the Footwall and Ore-Shale samples. If the initial assumption is correct ( $\delta\text{d}-\delta\text{w} = 0$  per mil for the Footwall samples), then the absolute temperature of Ore-Shale formation is  $31.9 + 79 = 110.9^\circ\text{C}$ , (which is far too high a temperature for bacterial sulphate reduction to occur).

An alternative hypothesis is that the Ore-Shale samples inherited their  $\delta^{18}\text{O}$  values from groundwater. As discussed in Chapter 5, groundwater is generally depleted in  $^{18}\text{O}$  compared to marine water. The degree of depletion in  $^{18}\text{O}$  is dependant on paleolatitude and elevation. The paleolatitude of the Copperbelt can be estimated at  $+20^\circ$  using the data of McWilliams and Kröner (1981). Although the isotopic composition of paleogroundwater can obviously not be determined, a depletion of 7 per mil relative to marine water is not considered excessive for Ore-Shale

times. Groundwaters can have remarkably uniform isotopic compositions. Vogel and Urk (1975) have demonstrated that the groundwater  $\delta^{18}\text{O}$  values for present-day semi-arid area samples from South Africa varies less than 0.5 per mil.

Thus in terms of  $\delta^{18}\text{O}$  values and their uniformity, the Ore-Shale samples are compatible with a groundwater origin, and the Footwall samples are compatible with a marine origin.

A number of factors combine to suggest that an important source of bicarbonate was bacterial consumption of organic matter during sulphate reduction. These include the textural evidence for carbonate production by replacement of anhydrite, the strong positive correlation between the percentage of carbonate carbon and the percentage of copper occurring as sulphide (Figure 4.2) and the sulphur isotope data.

Since oxidation of organic matter occurs without  $^{13}\text{C}$  fractionation, carbonates produced during bacterial sulphate reduction would be expected to have  $\delta^{13}\text{C}$  values typical of organic matter (approximately -25 per mil  $\pm 5$  per mil).

The lenticle rim dolomites with their associated sulphides have  $\delta^{13}\text{C}$  values (average -18.2 per mil) in accord with such an origin. Samples from the lenticle



core (formed after the rim) have a marked enrichment in  $^{13}\text{C}$  (mean  $-9.6$  permil), and the Footwall samples are even further  $^{13}\text{C}$  enriched (mean  $-6.2$  per mil), suggesting a contribution from isotopically heavy bicarbonate.

The progressive enrichment in  $^{13}\text{C}$  can be explained in a number of ways. The source of isotopically heavy bicarbonate could be due to fermentation processes active during burial or, alternatively a contribution from marine bicarbonate. The latter source is considered most likely since it is compatible with:

- (a) the Footwall  $\delta^{18}\text{O}$  values (being in the marine field, one would expect a large marine bicarbonate contribution);
- (b) the gross sedimentology (reflecting transgressive/regressive events) which provides the opportunity of mixing marine/fresh waters, a feature reflected in the sulphide  $\delta^{34}\text{S}$  variations;
- (c) the chemistry (Na and Sr composition) of the dolomites.

Marine waters are enriched in Na and Sr compared to groundwaters. The Na and Sr values obtained, and shown in Table 6.5 are consistent with a model of mixing-zone dolomite formation (Land, 1973; Sibley, 1980). Further, the increase (particularly in Sr) between rim, core and Footwall dolomite samples reflects the increased

importance of marine waters as predicted by the changes in  $^{13}\text{C}$  and  $^{18}\text{O}$  of the dolomites. This is particularly well shown by the whole rock analysis (see Figure 6.4). The  $\delta^{13}\text{C}$  values reflect the differing contribution from marine carbonate ( $\approx 0$  per mil) and carbonate produced by bacterial sulphate reduction ( $\approx -20$  per mil). Transgressive/regressive events as predicted by Naish (1973) on sedimentological grounds, should be reflected by a trend towards isotopically heavier carbonate (i.e. more marine values) in units B, A and in the Footwall and from the top of unit D through unit E. These predicted trends are observed, and are further confirmed by the strong correlation between strontium concentration and  $^{13}\text{C}$  enrichment of the whole rock samples. Similar, though less strongly correlated trends, are observed in the  $^{18}\text{O}$  variations.

In summary the carbonate results can be best explained in terms of a mixing model. The  $\delta^{18}\text{O}$  values are inherited from marine/fresh water components and the  $\delta^{13}\text{C}$  values reflect the differing contributions from marine/oxidation of organic matter sources. Finally, the isotopic composition of the carbonates mirrors paleo-environmental changes at the time of Ore-Shale deposition.

The two calcite samples taken from the Footwall Quartzite are plotted in Figure 6.6. The samples have marine carbon isotope values but are very depleted in



$^{18}\text{O}$ . If the original  $\delta^{18}\text{O}$  values were marine, the  $^{18}\text{O}$  depletion could be explained by their formation at a temperature of approximately  $70^{\circ}\text{C}$  (allowing for Precambrian water being depleted in  $^{18}\text{O}$  by 9 per mil). Alternatively, because the  $\delta^{18}\text{O}$  values are very similar to those of the Ore-Shale, and these have been interpreted as an indication of groundwater, it is possible that the original carbonate was marine and was later modified by groundwater. Because groundwaters contain little carbon as compared to oxygen, the carbon isotope composition of the samples would change much less than the oxygen isotope composition. Such an origin is in agreement with sedimentology which suggests that the quartzite represents the intermittent marine reworking of distal fan/aeolian material.

#### 6.3.5 Malachite Results

Only one of the malachite samples was clearly of secondary origin, the remaining samples were not associated with either faults or joints. The samples were taken from drill cores and freshly mined crosscuts in the 400 mS area between the 2200 and 2400 levels of the South Orebody. A sequence from the Footwall Conglomerate stratigraphically upwards into units A and B of the Ore-Shale was sampled.

In the Footwall, the malachite forms an interstitial



cement to the conglomerate clasts, and in the Ore-Shale it occurs as laminae and as lenticles very similar to those discussed above. On textural grounds, the formation of malachite took place after Footwall dolomite formation (replacement phenomena are common, see Plate 4.3), but before a major silicification event. The silicification event effectively sealed-off and partially replaced nodular malachite from unit A. The single sample of secondary malachite came from a leached vein, and was botryoidal in form.

The results of the isotopic analyses of the malachite samples are shown in Figure 6.7 and Table 6.7. The samples obtained from the Ore-Shale are  $^{13}\text{C}$  depleted and  $^{18}\text{O}$  enriched compared to the Footwall samples. In Figure 6.7 the samples are numbered in descending stratigraphic order, and show a systematic enrichment in  $^{13}\text{C}$  from unit B to the underlying Footwall conglomerate samples.

#### 6.3.6 Discussion of Malachite Isotope Data

The textural data already discussed suggests that much of the malachite studied may not be a result of recent oxidation of sulphide. Although Konkola is a wet mine, the Ore-Shale acts as an efficient aquaclude and would prevent mixing of Hangingwall and Footwall water, waters which are in any case isotopically identical (see Table 6.6). Fractionation data is not available for

malachite, but the range in  $\delta^{18}\text{O}$  and  $\delta^{13}\text{C}$  (6 per mil and 9 per mil respectively) of the malachite samples analysed cannot be explained by precipitation from present day mine waters unless these values are, in part, inherited from pre-existing carbonates, for which there is no textured evidence.

The stable isotope data suggest that the malachite formed in one of the following situations:- (a) a result of an early diagenetic mixing event between Footwall water and water evolved from the Ore-Shale during burial compaction, or (b) the change in  $\delta^{18}\text{O}$  may simply reflect the Footwall malachite samples having formed at a higher temperature, as a result of burial, than the Ore-Shale samples. In the latter case the change in  $\delta^{13}\text{C}$  values may represent an increased contribution of fermentation derived bicarbonate, as burial progressed. Fermentation-derived carbonate can have  $\delta^{13}\text{C}$  values of +15 per mil (Curtis, 1978) and is an active source of bicarbonate down to burial depths of approximately one kilometer.

Malachite is stable up to a temperature of 315°C (Dana, 1951), and although the effect of pressure is unknown, it is probable that diagenetically-formed malachite could survive metamorphism of lower greenschist facies.



Quartz and potassium feldspar from veins which crosscut the Orebody were analysed in an attempt to determine the temperature of metamorphism. All samples were examined in thin section and were checked for purity by XRD. The method of analysis was as described by Clayton and Mayeda (1963). All samples were analysed at least twice, and gave good gas yields on reaction. The  $\delta^{18}\text{O}$  results are shown in Table 6.8. The temperatures deduced are shown in Figure 6.8. The temperature curves used were those of Bottinga and Savoy (1973) for quartz-feldspar and O'Neil et al. (1969) for quartz-calcite.

On petrographic grounds, the quartz and feldspar are thought to have coprecipitated. Indeed, small microcline crystals are found in quartz fluid inclusions (see Plate 7.2). Morphologically, the calcite and sulphides formed after the silicates. None of the samples analysed showed signs of weathering.

From Figure 6.8 it is apparent that the quartz-feldspar, and to a lesser degree quartz-calcite pairs gave anomalously high temperatures. In view of the purity checks and the good gas yields on reaction, contamination to give  $^{18}\text{O}$  enriched quartz or  $^{18}\text{O}$  depleted feldspar or calcite seems unlikely. Fluid inclusions, which are common, are an obvious potential contaminant. However,



the fluid phase of inclusions would be vapourised during sample crushing, and would certainly be decrepitated and lost during thermal outgassing of the sample prior to reacting.

The data suggest that the calcite, dolomite and feldspar did not re-equilibriate during metamorphism, or that post-metamorphism changes have affected the mineral phases.

## 6.5 SUMMARY AND CONCLUSIONS

The sulphide and carbonate isotope data are compatible with their formation due to bacterial reduction of sulphate.

The changing  $\delta^{34}\text{S}$  values of the Ore-Shale (Copperbelt Orebody Member) sulphides can be explained by a combination of varying sedimentation rate and sulphate supply as predicted on sedimentological grounds. Lenticular and finely disseminated sulphide from the same horizon and locality have similar isotope values. Isotopic zonation of lenticular sulphide and the lack of isotopic re-equilibrium of co-existing different sulphide phases strongly suggest that metamorphism has not altered the sulphur isotope values even on the micro scale.

Footwall sulphide isotope values display progressive

enrichment in  $^{34}\text{S}$  with increasing depth below the Copperbelt Orebody/Kafue Arenite Member contact. This is interpreted as reflecting closed system fractionation, or possibly mixing at depth with sulphate poor groundwater.

The isotopic composition of dolomite phases from the Footwall rocks and the Copperbelt Orebody Member mirror the varying influence of ground and marine waters (affecting  $\delta^{18}\text{O}$  values); and bicarbonate produced during sulphate reduction and from marine waters which affect  $\delta^{13}\text{C}$  values. The variation in  $\delta^{18}\text{O}$  and  $\delta^{13}\text{C}$  of the different phases is also reflected in their Na and Sr content; higher Na and Sr values being associated with more marine dolomites. The morphological and chemical differences between the carbonate phases, combined with their differing isotopic composition imply that, although some recrystallization may have taken place, metamorphism has not obliterated earlier geochemical or isotopic variations.

The malachite samples show progressive enrichment in  $^{13}\text{C}$  and depletion in  $^{18}\text{O}$  below the Copperbelt Orebody/Kafue Arenite Member contact. The malachite is interpreted as forming from copper-rich porewater expelled from the Ore-Shale during burial. The progressively lighter  $\delta^{18}\text{O}$  values are thought to result as a consequence of increased burial temperature, and the  $\delta^{13}\text{C}$  enrichment to result from the increasingly important contribution of

heavy ( $^{13}\text{C}$  enriched) bicarbonate produced during fermentation. If this interpretation is correct, and it is in agreement with the paragenetic position of malachite determined in Chapter 4, then much (but not all) of the malachite in deeper mining levels ( 2200 feet) is late diagenetic in origin.

Data from silicate oxygen isotope thermometry of apparently co-existing quartz and feldspar yield temperatures inconsistent with petrographic observations, and again strongly suggest that metamorphism did not result in isotopic re-equilibration of the phases studied.



## CHAPTER 7

### COPPERBELT GEOCHEMISTRY WITH SPECIAL REFERENCE TO THE KONKOLA BASIN

#### 7.1 INTRODUCTION

Little systematic geochemical work has previously been carried out on Copperbelt mineralization and the associated host rocks. The geochemistry of the Copperbelt has been discussed by Darnley (1960), Mendelsohn (1961) and Fleischer et al. (1976). Simmonds (1980) cited an unpublished review by Dawson (1977) in which the following conclusions were reached:-

- (1) Potassium enrichment is widespread
- (2) Soda ( $\text{Na}_2\text{O}$ ) enrichment is associated with many copper orebodies, but is not so widespread as potash metasomatism.
- (3) Boron enrichment is locally associated with copper mineralization in some orebodies.
- (4) Accessory titanium minerals are often prominent within copper orebodies.
- (5) Cobalt-enriched copper ores are found only to the west of the Kafue Anticline and may have some general association with amphibolite sills.

The potassium and sodium enrichment has been interpreted

by Darnley (1960) and Vaes (1962) as of metasomatic origin, whereas Annels (1974, 1979) and Simmonds (1980) invoke a late-stage diagenetic/metasomatic explanation.

In terms of sediment provenance, Mendelsohn (1961) suggests that "the high potash nature of the Katanga rocks appeared to be adequately explained by the soda-poor, potash-rich nature of the Basement Complex. Walker et al. (1978) have demonstrated the relatively high resistance of potassium feldspar to breakdown during early diagenesis, and thereby the potential concentration of that element in the remaining sediment. The abundance of sodium and potassium bearing authigenic feldspar overgrowths is discussed in Chapter 4 and would also help to explain the anomalous concentration of these elements. Engel et al. (1974) point out that on a worldwide basis, potassium is abnormally high in late Proterozoic sediments.

The importance of boron enrichment is debateable (Visser, 1974; Karowski, 1978). Boron is known to be diagenetically enriched in some semiarid closed basin of the USA, Sheppard and Gurde (1973). Clemmey (1976) has shown that tourmaline overgrowths on detrital tourmaline and quartz have occurred during early diagenesis, and that on a microscopic scale these are, in fact, absent in areas of sulphide mineralization.

The first three observations of Dawson are thought to

have achieved an exaggerated importance in studies of Copperbelt mineralization, and are not thought to be diagnostic of metasomatism as previously thought (Vaes, 1962; Darnley, 1960).

Previous geochemical studies at Konkola are limited to those of Schwellnus (1961) and Fleischer et al. (1976). In the present investigation sixteen borehole intersections of the Ore-Shale and its immediate hangingwall and footwall were examined. Analysis was by X-ray fluorescence, samples being analysed for trace elements only. The reasons for this, and the methodology involved are given in Appendix 5. The results were then statistically analysed and an attempt made to link the geochemical data with petrographic observations and mineralogy, with particular reference to the major economic elements copper and cobalt. Finally, the chemistry of fluid inclusions from veins which crosscut the orebody were examined, to determine the mode of vein formation. Both solid and liquid/gas phases of the inclusions were analysed.

## 7.2 TRACE ELEMENT GEOCHEMISTRY

The location of the borehole cores analysed is shown in Figure 7.1. The results, along with lithological boundaries, are plotted in Figures A8.1 to A8.16 and are presented in Appendix 8. All results are quoted in parts



per million. The sample interval is approximately 0.5m true thickness.

R mode correlation matrices were made for all element pairs within individual boreholes, (Tables A7.1 - A7.16 are presented in Appendix 7) and for the combined data (Table A7.17) which are also tabulated in Appendix 7. There are variations in significantly correlated elements between individual boreholes, but meaningful trends also become apparent.

From Figures A8.1 to A8.16 copper can be seen to display the following features:-

- (a) There is generally a sharp cut-off in grade at both hangingwall and footwall of individual boreholes.
- (b) Peak concentration of copper occurs at a lower stratigraphic level in the North Orebody.
- (c) There is no economic ( $>1\%$  Cu) footwall mineralization at the North orebody.

Copper concentration peaks in unit C of the Ore-Shale, with an average grade of 3.25 wt%. Copper occurs mainly as chalcopyrite, bornite and chalcocite with minor covellite and malachite. Trace amounts of copper occur in authigenic feldspar overgrowth, see Table 4.3.

Three areas of anomalously high cobalt occur in the

mine area, and have been described by Raybould (1978c). At the North Orebody, cobalt (values 0.1%) occurs on both sides of the anticlinal axis, and at the South Orebody, high cobalt values occur immediately south of the Central Drag fold area, where values up to 0.5% cobalt occur. Isolated small high grade areas occur north of the drag fold.

Highest cobalt grades occur almost invariably in the middle and upper parts of the payable zone at both orebodies. Cobalt mineralization also occurs in the footwall of the South Orebody, but only in areas where there are high ( 0.2% Co) cobalt values in the Ore-Shale.

The main cobalt bearing mineral is carrollite although cobaltian dolomite and trace amounts of cobaltiferous pyrite also occur.

Electron-probe micro-analyses of carrollite (Table 4.2) show an upward increase of iron content, mimicking the increased iron content of the Ore-Shale from footwall to hangingwall. The nickel content of the carrollites varies from 0.15% in the Footwall to 0.47% in the Ore-Shale, and probably accounts for all the nickel recorded in the whole rock analysis (a mean of 30 ppm). Cobalt to nickel ratios of greater than unity are uncommon in the sedimentary environment (Davidson, 1962), and are considered by Simmonds (1980) to be indicative of an



igneous source. The cobalt to nickel ratio of Konkola samples (n=278) falls within the range 2:1 and 85:1 with an average of 31:1. The significance of this is discussed in the next chapter.

Zinc and lead are present in low concentrations varying from 10 to 100 ppm, and 0 to 190 ppm respectively. Sphalerite does occur but it is extremely rare. It was thought that zinc and to a lesser extent lead would occur in solid solution or as sulphide micrograins within chalcopyrite. The results of electron-probe micro-analysis of 29 chalcopyrite grains are presented in Table 7.1 All the chalcopyrite grains contain traces of lead but no zinc, and depart from stoichiometry in that they are copper poor and enriched in iron and sulphur. Samples of finely disseminated (shale hosted) and coarse grained (carbonate hosted) chalcopyrite was analysed. The coarse grained or lenticular chalcopyrite were relatively enriched in iron and sulphur compared with the finely disseminated material. Like chalcopyrite, the bornite grains analysed (Table 7.2) were enriched in iron and sulphur compared with their theoretical-assay percent, but showed no significant compositional differences between fine and coarse grained samples. The occurrence of sulphur-rich bornite, was investigated experimentally by Brett and Yund (1964), who concluded that such bornites were deposited below about 75°C. They also noted that sulphur-rich bornite, particularly when also iron rich,



exsolves chalcopryrite when heated. This was not observed in the Copperbelt samples, and if such exsolution does take place it presumably happens on the submicroscopic scale.

In the case of bornite samples, the analytical totals are low. This is probably due to a tarnish, which formed rapidly on all the bornite samples examined. In the majority of boreholes, zinc concentration peaks stratigraphically above that of lead.

From the EPMA results (Tables 7.1 and 7.2) arsenic is found to substitute for sulphur by up to 1% in chalcopryrite, and by up to 1.9% in bornite.

Iron concentrations vary from 1.56% Fe in the Footwall to 2.05% in the Hanging-wall and within the Ore-Shale vary from 2.2% to 2.5%. Much of the iron can be explained in terms of the iron content of the copper-iron sulphides, with micas, carbonate and epidote accounting for much of the remainder. In the Footwall, iron occurs as hematite with minor contributions from the copper-iron sulphides.

Manganese concentration peaks in unit A with an average of 950 ppm, and drops to an average of 350 ppm in unit E. Manganese occurs in carbonates and as oxides. Although manganese correlates well with cobalt, it is not

now present in amounts sufficient to account for the concentration of cobalt by the adsorption of  $\text{Co}^{2+}$  ions onto hydrous manganese dioxides within the sedimentary environment, as was suggested by Murray (1975) for the concentration of cobalt in Black Sea sediments. However, it may be that more cobalt can be adsorbed by manganese oxides than suggested by Murray. Alternatively, it is possible that manganese was preferentially removed during metamorphism or during diagenesis. Manganese oxides would certainly be more mobile during metamorphism than cobalt sulphides. Heggie and Lewis (1984) have demonstrated that during diagenesis, cobalt adsorbed on manganese oxides is released to porewater during manganese reduction, and diffuses upwards towards the more oxic sediment/water interface. Thus although manganese and cobalt are intimately linked, their present relative concentrations do not necessarily reflect their original relative concentrations. It is interesting to note that Simmonds (1980) recorded a similar sympathetic relationship between cobalt and manganese concentration at the Buluba orebodies. Thus, where deposits have been analysed in detail for cobalt and manganese, these elements are found to be closely associated. This suggests that cobalt was initially transported along with manganese.

Zircon (Table 7.3) probably accounts for all the zirconium of the whole rock analysis, and also for much of the uranium and thorium, and may explain the ytterbium

concentrations (Deer et al., 1977).

Rutile, which is common in mineralised horizons, contains up to 0.68 % niobium oxide as well as trace amounts of uranium and thorium (see Table 7.3). Rutile occurs as a replacement after ilmenite, and as detrital grains with thin authigenic overgrowths, resulting in the formation of euhedral crystal forms.

Titanium is very strongly correlated with copper concentration. There is a noticable increase in the detrital minerals zircon and particularly rutile (reflected in the elements zirconium and titanium) from the base to the top of the Ore-Shale. Concentrations in the Footwall average approximately half those in the Ore-Shale, with the former containing 140 ppm zirconium and 2500 ppm titanium.

Barium substitutes readily for potassium in feldspar (see Table 4.3) as to a lesser extent do rubidium and strontium. Annels (1979) has used whole rock barium contents to map out variations in the amount of detrital potassium feldspar at Mufilira. Barium concentrations are high in the Footwall (average 3300 ppm), reflecting the high potash feldspar content of the Footwall lithologies, as discussed in Chapter 4. In the Ore-Shale, values peak in unit B (2700 ppm) and decline upwards to a mean value of 1500 ppm in unit E, and 1100 ppm in the Hangingwall



lithologies. This probably represents an increased rate of sedimentation in the Hangingwall and unit E. This would result in less destruction of plagioclase feldspar, and thus a relative decrease in potassium feldspar; a feature born out by petrographic observations.

#### 7.2.1 Analysis of Trace Element Results

An attempt is now made to link the geochemical data with mineralogy and provenance, with particular reference to the major economic elements copper and cobalt.

Several of the elements are considered to be diagnostic of detrital minerals. The elements Ti, Fe, Nb, Zr, Y and Th are all strongly positively correlated and are represented by the detrital minerals zircon and rutile, or intimately associated with their alteration.

Annels (1979) has shown that a linear relationship exists between strontium and anhydrite concentrations in the Mufilira orebody. Clemmey (1976) has used the strontium content to indicate the degree of marine influence in the Orebody Member of Kitwe. The very strong positive correlation between manganese and strontium suggests a genetic link. It is therefore proposed to use strontium and manganese as indicators of the presence of marine water in the original sediment, see also Chapter 6.

Table 7.4 shows the elements which correlate at the 95% confidence limits, for the combined borehole samples. It should be remembered that this combines the data from sixteen individual boreholes, and that an attempt is being made to distinguish between what are essentially mixing phenomenon (i.e. elements derived from a landward and a basinward source).

The negative correlation between copper and many of the detrital index elements is at first perplexing, although there is a tendency for copper to be correlated with the detrital index elements in individual boreholes. The strong positive correlation of copper with Ba, Y and Th (elements released during diagenetic breakdown of feldspar and zircon) is suggestive of copper being fixed from solutions containing these elements during early diagenesis.

A link between cobalt and marine interstitial water has been made in Chapter 6. This is confirmed by the antipathy shown by cobalt and the detrital index elements, and its strong positive correlation with manganese.

Element dendograms have been produced for samples from each lithological unit in the Ore-Shale, and for samples from the immediate Hangingwall and Footwall, Figures 7.2 to 7.5. Particular attention is paid to the economically important elements copper and cobalt.

In the Footwall there is a very obvious division between cobalt associated with strontium and manganese, and copper, nickel, lead and zinc associated with the detrital index elements.

Units A, B and C show a similar division between copper and cobalt, but the link between copper and the detrital index elements is less well developed. This is probably a result of the reasons mentioned above.

In the upper Ore-Shale units, copper and cobalt are quantitatively less important. The distinct division between copper and cobalt is poorly developed.

Thus, although it probably cannot be considered determinant, the statistical analysis of the geochemical data suggests that copper and cobalt may have different sources, and that copper was in solution along with elements released during diagenetic breakdown.

### 7.3 VEIN OCCURRENCES

At Konkola, veins are found crosscutting most lithologies, but are more common in the Kafue Arenite and Copperbelt Orebody Members, and in the Boulder Conglomerate unit.



In the Boulder Conglomerate, veins up to 1m wide occur. They are composed of coarsely crystalline white quartz, microcline feldspar, carbonate and anhydrite with minor amounts of biotite and rutile.

Vein sheets cut the Kafue Arenite Member and continue through the Copperbelt Orebody Member (Ore-Shale). In the footwall of the Ore-Shale, the veins may be up to 1m in diameter but are more usually between 10 and 30 cms wide. The main components of the veins are quartz, microcline, biotite much hematite and minor carbonate and anhydrite.

In the Ore-Shale veins cut sharply across bedding, but more usually bifurcate and run sub-parallel to bedding. They are rarely more than 10 cms wide and contain the same minerals as in the Footwall except that hematite is absent and sulphides of copper and cobalt occur. Leached margins are developed to various degrees (usually poorly) in both the Ore-Shale and Footwall veins.

Initially, veins on the Copperbelt were considered to be intrusive in nature (Mendelsohn, 1961), and have been referred to as pegmatites (Cahen et al., 1970). After extensive studies, Garlick and Brummer (1951) and Garlick (1964) established that there were no intrusive granites in the Lower Road and considered the veins to have formed by lateral secretion during metamorphism. More

recently Jolly (1972), describing the geochemistry of vein occurrences at Luanshya, Muliashi and Chambeshi, concluded that; "lateral secretion of wall rock material in a closed system, metamorphosed to lower amphibolite grade is not adequate to explain the origin of the veins". He went on to suggest an external source for the fluids unrelated to metamorphism, and points to the young amphibolite intrusives in the area as evidence of magmatic activity. It would seem that there is either a discrepancy in the interpretation of field relationships and geochemistry or there are several generations of vein formation, a possibility which must be borne in mind when using vein samples for thermometry analysis.

Kruegen (1980) has shown that one way to prove a lateral secretion origin is to compare veining and host rock fluid inclusion chemistry. Unfortunately, fluid inclusions in the Ore-Shale are extremely rare, occurring mainly in detrital quartz. Fluid inclusion composition would therefore reflect the chemistry at their time of formation rendering such a comparison with vein inclusions spurious.

In order to investigate the origin of veins in the vicinity of the Ore-Shale, samples from both the Footwall and the Ore-Shale of the same vein sheet were analysed. The lack of underground workings in the Hangingwall meant that it was not possible to sample the vein

continuation. All the samples analysed were taken from veins of diameter less than 10 cms.

### 7.3.1 Vein Geochemistry

Attention was paid to the fluid inclusion phases, since these were less likely to suffer from any inhomogeneity effects, and be more representative of the vein forming fluids than bulk analysis of vein forming material.

A total of 14 doubly-polished thick sections were studied. It was observed that inclusions in the Ore-Shale had a mean solid content of between 25-35% (Plate 7.1a and b), compared with 5-15% in the Footwall samples.

All the samples showed evidence of necking and the formation of healed inclusion trails (Plate 7.1c, d and e), making temperature or pressure determination impossible (Dr. T. Sheppard, pers comm).

Crawford (1981) points out that decrepitation due to expansion of trapped fluid (resulting in necking), occurs where the pressure-temperature trajectory of the rock crosses the isochors for the fluid in the direction from lower to higher volume. Thus it seems probable that the veins have undergone a post-formational tectono-thermal event.



An S.E.M. examination of freshly broken clean quartz fragments reveals four types of inclusion filling. Identification was by a Link 850 energy dispersive analysing unit attached to the SEM.

(i) Pure quartz forming a coating on rug sidewalls. This is to be expected since the fluid will be saturated with respect to the host (Roedder, 1981).

(ii) Potassium and sodium chloride salts. These may occur as euhedral crystals (Plate 7.1f) but usually form mixed compounds.

These two types are probably end members produced as a result of necking.

(iii) Larger inclusions (greater than 20 microns) which usually show a number of phases, as in Plate 7.2. These were invariably potassium and sodium chlorides with alumino-silicates and occasional copper/cobalt salts.

(iv) Cryptocrystalline aggregates formed as a result of evaporation of water from the fluid phase of the inclusion as a result of pressure release during sample preparation.

Energy dispersive analysis indicates the presence of:- Na, Al, Si, S, U, K, Ca, Fe Cu and Co.

More accurate semi-quantitative analysis was performed using the method describe by Chryssoulis (1983). Basically this involved thermally decrepitating the inclusions onto the surface of a polished slice of the vein material, and analysing the resultant solute. The results are shown in Table 7.5.

Low analytical totals are to be expected for three reasons:

- (a) the decrepitation surface being analysed is uneven, resulting in energy loss due to backscatter;
- (b) the analysis is undertaken using a scanning mode (for homogenization reasons) and consequently the take off angle varies;
- (c) the surface being analysed is not solid but porous.

The cation totals (Table 7.6) have been normalised and plotted in Figure 7.6. From this it can be seen that the bulk chemistry of the fluid from both the Footwall and the Ore-Shale inclusions is similar, although in detail the fluids are different. The Footwall values are higher in Al and k content (Table 7.6) but have no Mg, Ba, Cu, Co or Zn.

Hydrocarbon inclusions, although rare, occur in both Ore-Shale and Footwall samples, and have been confirmed by long wave UV (458 Nm) excitation, Plate 7.3.

Threshold values for hydrocarbon migration are generally about 100°C (Leith and Rowsell, 1979) and are rarely as high as 147°C (Sajgo, 1979). This then gives a maximum temperature for the vein hydrocarbon inclusions.

Liquid/Gas phase geochemistry, the methodology of which is described in Appendix 6, was applied to five samples. Two of these were from the Footwall and two from the Ore-Shale of the same sheet vein system, from the south side of the South Orebody. The fifth sample was taken from a vein at approximately the same stratigraphic horizon in the Ore-Shale, one kilometer north of the other samples. The results from the analysis are shown in Figures A6.1 to A6.5. It can be clearly seen that the Footwall samples are very similar to each other but are different from those in the Ore-Shale which in turn show a remarkable similarity to each other.

The Footwall samples have a very low fluid content - 0.17 mg of water per gram of sample compared with 1.07 mg for the Ore-Shale samples, and have a higher CO<sub>2</sub>, CH<sub>4</sub> and N<sub>2</sub> content. This is clearly demonstrated by the H<sub>2</sub>O/CO<sub>2</sub> ratio which is 26 for the Footwall samples compared with



an average of 133 for the Ore-Shale samples. This suggests that at the time of vein formation, the Ore-Shale section was considerably wetter than the Footwall rocks, and that there was free flow of fluid laterally within the Ore-Shale.

Thus, although the samples belong to the same vein system, in terms of fluid inclusion chemistry, the composition of the vein forming fluids was different in the Footwall compared to the Ore-Shale. This, together with the macroscopic features already described, is proof of a lateral secretion origin for these veins. The occurrence of hydrocarbons suggests a formational temperature in the region of 120°C.

The evidence is in favour of the veins having formed by lateral migration of fluids during late diagenetic dewatering. The abundant necking and annealing, resulting in inclusion trails, confirm at least one post-formational tectons-thermal event.

#### 7.4 CONCLUSIONS

Electron microprobe analysis has shown that the U, Th and Nb whole rock contents can be explained in terms of trace element composition of zircon and rutile. Lead and arsenic were found to substitute in both chalcopyrite and bornite.

The strong association of copper with the detrital index elements suggests that copper was in solution with elements released during diagenetic breakdown. This was confirmed by electron microprobe analysis of authigenic feldspar overgrowths, which were found to contain significant amounts of copper.

Cobalt was found to be associated with manganese and strontium; elements shown to be associated with waters of marine composition at the time of Ore-Shale formation.

Thus, although it may not be considered determinant, the statistical analysis of the geochemical data suggests that copper and cobalt probably had different sources.

The fluid inclusion geochemistry has shown that veins cross-cutting the Ore-Shale owe their origin to lateral secretion. During the formation of the veins, the Ore-Shale was considerably wetter than the Footwall lithologies. It is therefore considered that vein formation took place during Ore-Shale dewatering. A formation temperature of approximately 120°C is indicated by the occurrence of hydrocarbon in the inclusions. This is compatible with vein formation during dewatering, and suggests a late diagenetic rather than metamorphic origin for the veins. The abundant examples of necking of inclusions are proof that the veins have undergone at

least one post formational tectono-thermal event, and preclude their use as a geothermometer.



## CHAPTER 8

### DISCUSSION AND CONCLUSIONS CONCERNING COPPERBELT ORE

#### DEPOSITION WITH PARTICULAR REFERENCE TO THE

#### KONKOLA BASIN

### 8.1 TECTONIC SETTING

The size and shape of Roan depositional basins were controlled by the syntaxis of N-NW (Ubendian approx. 1800my) and ENE (Irumide approx. 1310my) structural trends. These structural trends continued to influence basin development (discussed in Chapter 2) and affected the sedimentation pattern in the Konkola basin until after the deposition of the Ore-Shale (see Figure 2.6).

The idea that regional vertical tectonics controlled the Basement topography and influenced the development of Katangan depositional basins was proposed by Brock (1962, 1972). In 1961, Brock noted parallel north-westward alignments of orebodies on the Copperbelt and suggested that these lineaments possibly reflected the control of Basement structure in localising the orebodies. This linear distribution of orebodies and the way in which basin sediments rapidly pinch out against Basement highs led Raybould (1978a) to accept the importance of vertical tectonics, and to suggest that the early Katangan sedimentary basin was a young intercratonic rift. The linear alignment of orebodies can also be explained in

terms of a palaeo-shoreline as determined from facies analysis and palaeocurrent directions (Fleischer et al., 1976; Figure 2.2), but vertical tectonics was certainly locally important in controlling rapid facies variation. In reviewing the geotectonic environment of copper-cobalt mineralization, Annels (1984) concludes that the Copperbelt is the site of an ancient aulacogen. The evidence he cites includes the following: rapid facies variation not explainable in terms of purely sedimentary processes; the vertical stacking of ore deposits in a narrow zone which implies some degree of tectonic control; and the occurrence of thick amphibolite bodies in the footwall but mainly in the hangingwall of the Ore-Shale which are thought to reflect rift-associated magmatism.

Whether or not the case for the Copperbelt being an ancient rift system is proven is open to debate, but there is ample evidence for tectonic activity during Lower Roan sedimentation on a regional scale and within the Konkola basin.

## 8.2 EFFECTS OF METAMORPHISM

(with particular reference to isotopic composition)

At Konkola, metamorphism has resulted in the formation of new minerals and the destruction of original clays. Metamorphism has also resulted in the necking down and subsequent healing of quartz vein fluid inclusions,

making them unsuitable for geothermometry. There is no evidence of large scale migration of elements, in particular the stratigraphic cut-off in copper grade is preserved. The original morphological and chemical differences in lenticular carbonates have been retained, as have their isotopic variations. Sulphides show signs of recrystallization, but generally retain their original chemical and isotopic compositions.

An attempt to use the isotopic composition of co-existing silicate minerals and coexisting sulphide phases to determine their formation temperatures failed and indicates that isotopic re-equilibration has probably not taken place. Even whole rock Rb/Sr isotope analysis shows that re-equilibration was not complete.

In summary, metamorphism up to lower greenschist facies seems to have had little effect on the isotopic compositions of the carbonate, silicate or sulphide samples analysed.

### 8.3 PALAEOENVIRONMENT OF THE MINDOLA FORMATION AND THE COPPERBELT OREBODY MEMBER

Sedimentation in the Mindola Clastics Formation commenced with a period of fanglomerate growth, during which the Boulder Conglomerate, Pebble Conglomerate and Porous Conglomerate were deposited. The change in



conglomerate type with time was a consequence of either climatic variation or tectonic control. The depositional environment of the Footwall Quartzite is somewhat controversial but it was probably aeolian with a certain amount of marine reworking. The picture of marine water and the high evaporation rate expected with an aeolian environment is confirmed by the isotopic composition of carbonate cements in the Footwall Quartzite. The thickness of the Footwall Quartzite probably resulted from the combined effect of basin subsidence and possible basin margin faulting. The regular separation of fine and coarse sediment found in the Argillaceous Sandstone requires an aqueous medium, and a prograding shallow tidal environment is envisaged for its deposition.

The Kafue Arenite/Bancroft Quartzite Members contact is erosive and probably marks a Copperbelt-wide chronostratigraphic event. The sediments in all three units of the Kafue Arenites Member are similar, differing mainly in clast size. The contacts between the units are gradational, and all the units have a red colouration. Sedimentary features and the overall geometry of the units indicate that they are fan deposits of a semi-arid climate.

The contact between the Mindola Clastics and the Kitwe Formation (base of the Ore-Shale) is erosive. The Ore-Shale has been divided into five lithological units,

numbered A to E from the base upwards. Unit A marks the onset of a marine transgression and is interpreted as an intertidal mud with an algal mat component. Unit B was deposited during a period of continued regression. Units C and D are very similar and sedimentary features indicate that they formed during a regressive event. A tidal flat/supratidal environment is envisaged for their deposition. The top of unit D and unit E mark the return to deeper water conditions.

#### 8.4 DIAGENETIC EVENTS

A metasomatic origin for the Copperbelt Orebodies as proposed by Darnley (1960) and Vaes (1962) but is not compatible with the data presented in Chapters 4 and 6, and discussion now centres on whether the orebodies are of synsedimentary or of diagenetic origin. A synsedimentary origin was first proposed by Garlick (1961) and was based on the observed mineral zonation parallel to a proposed palaeoshore line and on the association of sulphides with sedimentary structures, such as concentrations of sulphides occurring in the troughs of ripples, the foresets of cross-bedded strata and in desiccation cracks (Garlick, 1961, 1967, 1972, 1981; Whyte and Green, 1971). Also, Clemmey (1974a) showed that the grade of mineralization of Nkana was parallel to palaeocurrent directions. All of these features could be explained by the sedimentary deposition of sulphides (supposedly

detrital bornite is recorded by Binda, 1975), but these processes would also concentrate heavy minerals including ilmenite, tourmaline and zircon.

The role of ilmenite breakdown (under reducing conditions) in fixing metal sulphides is well documented (Dimanche and Bartholomé, 1976; Brown and Chartrand, 1983). At Konkola the association of copper sulphides with titanium dioxide has been described (Chapter 4), and the strong positive correlation in some boreholes between copper and the detrital index elements (Zr, Ti, Nb) was seen in Chapter 7. It is suggested that many of the supposed synsedimentary concentrations of sulphide can be best explained by sulphide nucleation as a result of ilmenite breakdown under reducing conditions during diagenesis. Indeed many of the sulphides found in implied synsedimentary concentrations could not have been deposited in hydrodynamic equilibrium and could not be of simple detrital origin.

In the authors opinion, mineral zonation in many of the Copperbelt orebodies and in particular at Konkola, is not as clearly defined or simple as implied in the literature (see Mendelsohn, 1961; Fleischer et al., 1976). Zoning, where it is observed, is often reversed and may conflict with sedimentological evidence as noted by Renfro (1974). Rather than being a phenomenon peculiar to a synsedimentary origin, mineral zoning can be



explained by small changes in porewater Eh-pH at the time of sulphide formation (Vink, 1972).

A paragenetic sequence of diagenetic events affecting the copper-cobalt mineralised host rocks was presented in Chapter 4. The footwall rocks underwent a complex history of oxic diagenesis under semi-arid conditions before the onset of Ore-Shale deposition. Early diagenesis in the Ore-Shale was characterised by a reducing environment, and from that period on, the diagenetic history of the Ore-Shale and the footwall rocks was broadly similar. Feldspar overgrowths in the Ore-Shale were found to contain copper. A close association between the replacement of lenticle sulphate and the production of sulphide and associated silicates was observed, and shown to be pre-sediment compaction. Carbon and sulphur isotope data indicate that bacterial reduction of sulphate was responsible for the carbonate and sulphide produced during this replacement. The strong positive correlation between copper sulphide and carbonate carbon in whole rock samples confirms the importance of sulphate replacement in the mineralising process. The  $\delta^{34}\text{S}$  values of sulphides were seen to vary with regressive/transgressive events as determined from sedimentological evidence. This is interpreted as reflecting the availability of sulphate during sediment deposition.

The transgressive event which signalled the onset of

Ore-Shale deposition resulted in the pore space in the footwall rocks being saturated with marine water. The carbonates which subsequently formed (rhombohedral) were cobalt-rich and have isotopic compositions approximating to marine values. Within the Ore-Shale, the isotopic composition of the carbonates reflects the differing influence of groundwater and marine waters (which determine  $\delta^{18}\text{O}$ ) and of bicarbonate produced during bacterial sulphate reduction and marine waters (which determine  $\delta^{13}\text{C}$ ). The variation in  $\delta^{18}\text{O}$  and  $\delta^{13}\text{C}$  of the different carbonate groups (Footwall, Ore-Shale lenticle both rim and core) is also reflected in their Na and Sr content, high Na and Sr being associated with carbonate of inferred marine composition.

The copper content of carrollite has been shown by Craig et al. (1979) to be a function of  $a\text{S}_2$ . The vertical variation in copper content of carrollite within the Ore-Shale compared with the uniform values found in the samples from the footwall probably reflects the porosity difference of their host sediments, and in particular the poor degree of vertical diffusion in the Ore-Shale. This variation in  $a\text{S}_2$ , together with systematic carrollite compositional changes in nickel, and particularly iron (which mimics the iron compositional trend of the Ore-Shale) is considered further proof of the early diagenetic formation of this mineral.

The paragenetic sequence of sulphide formation indicates an early period of pyrite growth, the last stages of which were markedly cobaltian. This was followed by a minor copper mineralizing event which preceded the main phase of cobalt mineralization represented by carrollite. This mineralising event was followed by the formation of sulphides increasingly rich in copper. Lead and zinc occur in only trace amounts (up to 200 ppm) in whole rock analyses. Traces (up to 0.15%) of lead were found in chalcopyrite and bornite, otherwise no lead-bearing minerals were identified. Very minor amounts of sphalerite were seen, but no paragenetic relationship with the other sulphide minerals could be determined.

Petrographic observations suggest that most of the malachite from deeper mining levels (approximately 700m below surface) may be of diagenetic origin. Although fractionation data for malachite is not known, the variation in malachite isotope results (Figure 6.7) is not compatible with the samples analysed having formed from recent groundwaters. It is envisaged that as burial commenced, copper-rich pore water was expelled from the Ore-Shale and malachite was formed. The systematic enrichment in  $^{13}\text{C}$  displayed by the malachite samples may represent an increased contribution of fermentation-derived bicarbonate as burial progressed. Fermentation-derived carbonate can have  $\delta^{13}\text{C}$  values of +15 per mil



(Curtis, 1978), and is an active source of bicarbonate down to depths of approximately one kilometer. The progressive depletion in  $^{18}\text{O}$  of the malachite samples may simply reflect the increased depth of burial and thus temperature of formation of the later precipitated malachite.

Continued burial would result in mineralogical changes affecting mainly clay minerals. Because of the effect of metamorphism these changes cannot be followed in the Konkola Basin, but fortunately changes in clay mineralogy with depth have been well documented from other sedimentary basins.

Burst (1959) showed that phyllosilicate transformation is temperature dependant, and a change from smectite to illite and eventual chlorite formation is found with increasing depth. The transformation of smectite to illite is accompanied by a release of water. Powers (1967) demonstrated that the rate of clay alteration is temperature controlled and coincides with the same depth/temperature window as does the generation of liquid hydrocarbons. Burst (1969) confirmed the link between the smectite-illite transformation and oil generation and showed that the transformation or threshold temperature was in the region of  $90^{\circ}\text{C}$ . The smectite-illite conversion was demonstrated by Perry and Hower (1972) to be a two-step reaction which is all but complete

The effect of burial diagenesis on both the footwall rocks and the Ore-Shale is to alter some of their component minerals and release elements into pore water. In generalised terms, the footwall rocks pore water would be enriched in K and Al (from potassium feldspar breakdown) with respect to the Ore-Shale, and the Ore-Shale pore water would be enriched in Mg, Fe and Na (from clay transformations) with respect to the footwall rocks. Much silica would be released in pore water of both the footwall rocks and Ore-Shale, and silicification would be pervasive.

The occurrence of hydrocarbon in quartz veins, cross-cutting both the Ore-Shale and footwall rocks, suggests that their formation took place in the temperature range 90 - 140°C, and was probably related to the smectite-illite transformation. The geochemistry of fluid inclusions from these veins reflects the general enrichment of K/Al in the footwall rocks and Mg/Na in the Ore-Shale as predicted from the burial diagenetic reactions discussed above. The high H<sub>2</sub>O/CO<sub>2</sub> ratio of the inclusions in the part of the veins which cut the Ore-Shale (133 against 26 in the footwall rocks section) probably reflects the increased influence of the water released during smectite dehydration of the Ore-Shale. The similarity of fluid inclusion gas/liquid phase geochemistry within the Ore-Shale section of veins (even

when samples were almost a kilometer apart), and the difference from those of the footwall rocks section of the same vein system is striking, and indicates that little vertical (cross strata) fluid flow took place, while lateral movement within the Ore-Shale could take place with apparent ease.

The bulk of evidence presented, therefore, suggests a diagenetic origin for the copper-cobalt mineralization in the Konkola Basin.

#### 8.5 TRANSPORTATION AND SOURCE OF COPPER AND COBALT

Two consequences of suggesting a diagenetic rather than a syngedimentary origin for the Konkola Orebodies are to extend the time interval during which copper and cobalt could be introduced into the host lithologies, and to increase the variety of permissible copper-cobalt transporting methods.

Any model to explain the mode of copper-cobalt introduction into the sediments must take into account the following limiting parameters:

- (a) The sulphur used in metal fixation was derived from bacterial reduction of sulphate. The maximum temperature of sulphide formation would therefore be 100°C and was likely to be considerably less,



since bacteria work less efficiently at such elevated temperatures.

- (b) The sulphides were formed before appreciable sediment compaction took place. Using ratios of detrital minerals in carrollite crystals from footwall rocks suggests a porosity at the time of formation of some 60 - 70% (even higher in the Ore-Shale), and is equivalent to a depth of burial of under 30m (Baldwin, 1971).
- (c) During metal fixation, the environment was reducing and had a near-neutral pH. This probably rules out metal transportation by highly acidic solutions, or suggests a solution mixing model to reduce acidity to near neutral before metal fixation.

In summary, the copper and cobalt must have been introduced into the sediments during very early diagenesis.

#### 8.5.1 Transportation of Copper and Cobalt

Discussion will now be centred on the transportation of the major economic elements found on the Copperbelt; namely, Copper and Cobalt. These elements can be transported either as detrital grains or as aqueous species.

#### 8.5.1.(a) Detrital Transportation

A potential source of detrital copper is provided by the rocks of the Basement Complex. The presence of copper porphyry type deposits in the Basement rocks of the Copperbelt has been confirmed by Wakefield (1978). Voet and Freeman (1972) have recorded mineralization in the Basement which can reach concentrations as high as 4% copper over 4 metres thickness.

Detrital particles are potentially an important source of copper. Working on the Amazon and Yukon rivers Gibbs (1973) concluded that about 75% of the copper present was transported as crystalline detrital particles. Ashry (1973) obtained similar results from his studies on the Nile. Although sulphide minerals are not considered stable phases during aqueous transportation (Stendal, 1978), the occurrence of detrital concentrations of sulphides 145 kms from their source has been recorded by Clemmey, (1978). The occurrence of detrital bornite grains at Mufulira has been recorded by Binda (1975), but Bowen and Gunatilaka (1977) question the detrital origin of these grains and suggest that bornite was formed by diagenetic alteration of rounded iron oxide grains. Clemmey (1976) proposed that copper was transported from the Copperbelt Basement as detrital chrysocolla ( $\text{Cu SiO}_3 \cdot n\text{H}_2\text{O}$ ) and reduced to sulphide at the site of deposition

during early diagenesis. The weathering of copper porphyries has produced large associated detrital chrysocolla deposits in Chile (Newberg, 1967), and this may be an important means of transporting copper.

#### 8.5.1.(b) Transportation in Aqueous Systems

Metals can be transported in aqueous systems as organo-metallic complexes, as hydroxides of iron and manganese, adsorbed on clays and as soluble complexes (notably chloride complexes). Aqueous systems can be surface (essentially surface run off and marine) or subsurface. Transportation of metals in subsurface systems can be by either diffusion or infiltration (Brown, 1984). In the diffusion model, metals migrate along a chemical gradient within a stationary pore fluid, while infiltration involves the movement of metal-bearing solutions through a sediment. Mineralizing fluids may pass through a suitable depositing centre once (Brown, 1971; Renfro, 1974; Haynes and Mostaghel, 1982) or many times (the convective cell model). The convective cell model has been used to explain the deposition of major lead-zinc sediment-hosted ore deposits (Russell et al., 1981).

#### 8.5.2 Source of Copper and Cobalt

Metals can be derived by erosion of pre-existing



rocks (via detrital/solution systems) or from an igneous source or fluids derived from such. Alternatively, thermally driven aqueous cells can leach and transport metals over large distances.

#### 8.5.2.(a) The Basement Complex

The Basement Complex on the Copperbelt is known to contain copper porphyry-type deposits (Wakefield, 1978). Clemmey (1976) has calculated that the copper contained in all known Copperbelt ore deposits can be obtained by eroding to, a depth of 200m approximately 1% of the palaeoland-area, assuming it was mineralised to a grade of 1% copper. Alternatively, to put it in perspective, the Chuquicamata copper porphyry deposit (Chile) contains the equivalent of a quarter of the Copperbelt's known orebodies present and past metal reserves.

Erosion of a Basement which did not contain major metal concentrations could also supply metals to a depositary via the diagenetic breakdown of original clastic components. Rocks of red bed affiliation are considered particularly likely to transport copper in this manner. The close association of red beds and stratiform copper deposits in both time and space is well documented (Zambian Copperbelt - Garlick, 1972; Kupferschiefer - Rentszsch, 1974; White Pine - Brown, 1974; Adelaidean Orebodies of Australia - Rowlands, 1974; Copper deposits

of the Damaran Belt - Ruxton, 1981). Mafic minerals, amorphous iron oxides and even feldspars (Kucha, pers. comm.) found in red beds can contain trace amounts of copper which would be released into pore water during diagenetic alteration, and may subsequently migrate, via diffusion or infiltrations mechanisms, to form metal concentrations as suggested by Brown (1974, 1984).

Such an origin for the Copperbelt deposits is considered unlikely, since we have seen that, in red bed (footwall) rocks, diagenetic reactions were mainly complete before the formation of sulphides. Although copper may have been released into pore waters during diagenetic alteration, the occurrence of carbonates of marine isotopic composition associated with the formation of sulphides implies that there was little pre-existing pore water in the footwall rocks before this marine transgression.

In the case of mud rocks, metals adsorbed on smectites would be released into pore waters during the dehydration and conversion of smectite to illite. The increase in pore water volume may result (under ideal conditions) in the migration of mineralizing solutions towards the basin margin, by which time the solution temperature would be lower and metals carried could be fixed by bacterial sulphate reduction. Such a mineralizing process was probably not important on the

Copperbelt, indeed many of the ore deposits have no association with mud rocks.

In conclusion, erosion of the Basement complex (Wakefield, 1978; estimates some 2km was eroded during Lower Roan times) could explain, in terms of metal content, the observed copper deposits. Whether transportation of copper via detrital minerals (Binda, 1975; Whyte and Green, 1971; Clemmey, 1976) or via mineralized solutions/groundwaters (Van Eden, 1974; Renfro, 1974) was dominant cannot be ascertained, but the latter is considered more likely.

#### 8.5.2.(b) Igneous-Associated Sources

Although weathering and erosion of the Basement could liberate sufficient copper to account for the Copperbelt ore reserves, no occurrences of cobalt from Basement rocks are recorded. Davidson (1962) drew attention to this anomaly, and suggested that any discussion of ore genesis must take it into account. Annels (1974) pointed out the anomalous aerial distribution of cobalt. Other than in trace amounts, cobalt only occurs along the western Ore-Shale alignment (Figure 2.2) and none is found along the eastern alignment. Therefore, unless a very localised distribution of cobalt is implied, simple weathering and erosion of the Basement (Kafue Landmass) cannot explain the distribution of cobalt found in the ore deposits.



Annels (1974, 1983) also showed that the aerial distribution of amphibolite bodies and deposits containing cobalt overlapped, and that the amphibolites contained significant cobalt mineralization.

Simmonds (1980), after reviewing the cobalt mineralization on the Copperbelt, concluded that the similarity between Cu/Co and Co/Ni ratios of the ore deposits and of fluids derived from ferrogabbroic magma, suggested that the ultimate source of the copper and cobalt was from a deep-sealed basic intrusion aligned beneath the Copperbelt. Annels (1984) demonstrated that faulting was probably active during the time of Ore-Shale deposition, and suggested that seepages of magmatically-enriched hydrothermal solutions could be channelled along these faults, and metals were subsequently dispersed in the sedimentary environment to be fixed during diagenesis. This depositional model was further refined by Annels and Simmonds (1984) who suggested that cooling of the hydrothermal solutions by connate water and the differing solubility of the metals would result in precipitation of sulphides in a zonal fashion, and explain the carrollite compositional differences towards orebody fringers observed by Simmonds (1980). The model is attractive since it explains the occurrence of cobalt in the orebodies when none has yet been found in the Basement (the other potential source of metals). It also allows for the early introduction of mineralizing fluids into the

host sediments, necessary since the sulphides formed are pre-sediment-compaction. There are, however, a number of problems with the mineralization model proposed by Annels and Simmonds (1984):

- (1) The occurrence of extensive faulting during Ore-Shale deposition is not proven or generally accepted by most geologists working on the Copperbelt (Mendelsohn, 1961; Fleischer et al., 1976).
- (2) The model predicts that the richest mineralized areas would be near faults, and yet no such fault/ore grade association has yet been identified at any of the deposits, even though such a richly mineralised zone would result in the most intense mining activity.
- (3) The mineralizing solutions are likely to have been hot and acidic. Even allowing for cooling and meeting connate waters, Annels and Simmonds (1984) indicate that they think the temperature may have been too high for bacterial sulphate reduction. They suggest that inorganic sulphate reduction may have been important, whereas the evidence presented in this thesis indicates that it is not.
- (4) The majority of the amphibolite bodies occur in the

Upper Roan, well above and much later than the Lower Roan orebodies.

- (5) The large copper-cobalt reserves and the relatively small volume of amphibolite seem incompatible, even though the amphibolite is only an indicator of the amount of magmatic differentiation. Perhaps further amphibolite bodies will be discovered with time.
- (6) The model states that the source of copper and cobalt are the same. Why then is there no cobalt at Mufulira when there is abundant copper, and the mineralization is considered synchronous with the cobalt-bearing orebodies?
- (7) The occurrence of stratiform copper mineralization in the hangingwall rocks of the western alignment is relatively common and of regional extent (Binda and Mulgrew, 1974), but there is no associated cobalt mineralization, once again suggesting that copper and cobalt do not have the same source. Perhaps the degree of magmatic differentiation determines whether the mineralization is copper-bearing or copper- and cobalt-bearing? If this is the case, then the stratigraphic distribution of mineralization at, for example, Chingola would require several reversals of the differentiation



trend to explain the observed mineralization.

- (8) The Basement is known to contain copper porphyry-type deposits, yet the model dismisses the Basement as a source of copper in the orebodies and instead proposes a hypothetical basic magma as the primary source of copper and cobalt.

At Konkola, the whole-rock Co/Ni ratios are similar to those described by Simmonds (1980) and Annels and Simmonds (1984). However, based on isotopic and geochemical data, carbonates containing cobalt are of marine origin which implies a basinward source for the cobalt. The strong correlation found between cobalt and manganese indicates that cobalt was transported adsorbed on manganese hydroxides. It is proposed that cobalt was derived via differentiation of basic magma (as suggested by Annels, 1974, 1979) and debouched in the basin centre via a fault system (the phantom fault? - Figure 2.5 ). The solutions were chilled and the cobalt was transported by marine waters to the basin margin, adsorbed on manganese hydroxides. Copper is considered to have been derived from the Basement. The influence of groundwater on the isotopic composition of Ore-Shale carbonate, produced during sulphide formation suggests that the bulk of the copper was carried in solution by groundwater.

In conclusion, it is considered that the pene-

exhalative model proposed by Annels and Simmonds (1984) could adequately provide a source of cobalt, but a Basement origin for copper seems more probable. This two-phase model for mineralization permits the formation of copper and mixed copper-cobalt deposits and, by inference, implies that deposits of dominantly cobalt may be found towards the basin centre.

## CHAPTER 9

### INTRODUCTION, REGIONAL SETTING, SEDIMENTOLOGY AND PETROGRAPHY OF THE MARL SLATE

#### 9.1 INTRODUCTION

The remaining chapters of the thesis will be concerned with the mode of formation of the Marl Slate (the English equivalent of the Kupferschiefer, Sedgwick 1829), with particular reference to the contained sulphides.

The Marl Slate and the Kupferschiefer extend over an area of approximately 400,000 km<sup>2</sup> (Oszczepalski, 1982) stretching from England across the North Sea (where it is readily recognised in wireline logs because of its strong gamma-ray peak) through Holland, Germany and into Poland, see Figure 9.1. The Kupferschiefer has been mined in Germany (Mansfield area) for its copper, lead and zinc, and is currently a major source of these metals in Poland (Fore-Sudetic area). In England, although base metal "showings" are widespread in the Marl Slate, no intersections of economic interest have been recorded.

The ease with which the Marl Slate weathers effectively rules out the use of surface outcrop samples for either geochemical or isotopic analysis. Some difficulty was experienced in obtaining suitable fresh



material. This study is therefore mainly confined to the examination of three borehole cores from the Southern Permian Basin. Two of the cores are from block forty-nine of the North Sea (Borehole numbers 49-26-4 and J1000), the last core numbered D.C. was donated by the National Coal Board and came from south of Doncaster (GR, SE6721714791). The general approach to this study and the techniques used were the same as those employed in the Konkola Basin study. In this chapter, the pertinent pre-Marl Slate geology is very briefly surveyed; this is followed by a discussion of events associated with the major marine transgression which marks the onset of Marl Slate deposition. Marl Slate sedimentology and petrography are then briefly discussed.

## 9.2 PRE-MARL SLATE GEOLOGICAL SETTING

The Variscan Orogeny (approximately 400-800 my) was a structurally complex event, the results of which can be simplified into two tectonic styles, resulting from the movement of Laurasia and Gondwanaland to form the Pangean supercontinent (Ziegler, 1982a). The tectonic styles were a north-south compressive event resulting in a period of mountain building, and an east-west tensional event resulting from a change in the relative movement directions between Laurasia and Gondwanaland.

The consequence of this tectonic interplay in the

North Sea was the production of two east-west aligned basins, the North and South Permian basins which are separated from each other by the Mid-North Sea-Ringkøbing Fyn High. A complex system of grabens was also formed at that time including the Central, Horn, Viking and Oslo grabens.

Glennie (1984) has suggested that the North and South Permian basins were developed during the late Carboniferous, while Kent (1981) proposes, on the basis of Devonian marine incursions, that subsidence began as early as the Devonian. More detailed information has allowed Glennie (1984) to show that the Devonian marine sediments followed a structural trend possibly initiated during the closure of the Tornquist Sea and the formation of Laurasia during the mid-Devonian. The Central graben follows the same trend as the Devonian marine sediments and was possibly formed during the Hercynian by reactivation along this older structural trend.

The Permian of the Southern North Sea Basin is underlain by Carboniferous (Westphalian) rocks (Eames, 1975; Wills, 1973), which are the probable source rocks for the Rotliegendes gas fields (Van Wijhe et al., 1980), while the Northern basin is underlain by Old Red Sandstone (Ziegler, 1982b). The final phases of the Variscan orogeny were marked by a period of uplift and consequent erosion, particularly in the Westphalian. Thus, the

Permian sequence is normally separated from the Carboniferous by a substantial unconformity.

The lower Rotliegendes (basal Permian unit) are predominantly volcanic in character but include molasse sequences derived from newly-formed highland, and aeolian sandstones and lacustrine sediments. The volcanics range from basic to intermediate compositions. They are associated with faults and with graben systems and are volumetrically more important in the Southern Permian basin.

The upper Rotliegendes is essentially the same in both North Sea Permian basins, but has been studied in greater detail in the southern basin because of its importance as a gas reservoir. Here it consists of sediments of fluvial (Wadi), sabkha, lacustrine and aeolian environments, the character and distribution of which have been discussed in detail by Glennie (1972). The upper Rotliegendes sediments are generally coloured yellow (resulting in the English name Yellow Sands) or red, the latter colour being thought to be due to early diagenetic oxidation of iron-containing minerals and being indicative of desert conditions (Walker, 1967; Nemec and Poresky, 1977; and Turner, 1980). Smith (1984) implies that red colouration which is now unusual in the Yellow Sands was probably once more extensive, and that it was pre-sulphate and carbonate cement in age, and of early



diagenetic origin. The Yellow Sands are usually poorly cemented and the sand grains display rounded forms typical of aeolian sandstones, see Plate 9.1A. The upper part (approximately 50m) of the Rotliegendes (termed Weissliegend) is commonly grey in colour and is thought by Glennie and Buller (1983) to reflect the position of the Weissliegend above the water table (before the mid-Permian transgression) and thus its non-exposure to a suitable diagenetic reddening environment.

Continued erosion resulted in the lower Permian surface being a gently rolling peneplain (Smith et al., 1974). The directions of winds blowing across this surface have been deduced from the dune bedding and suggest an E-NE direction in the Southern Permian basin (Smith, 1970a; Glennie, 1972, 1982), although the situation can be locally complicated. The resultant topographic expression is a change of dune-style from barchans at the basin centre to NE-SW aligned seif-dunes at the basin margin, with dunes attaining a height of 50m or more, (see Figure 9.2 and Plate 9.1B).

### 9.3 MID-PERMIAN (ZECHSTEIN) MARINE TRANSGRESSION

As a result of the subsidence rate exceeding that of sedimentation, by the end of the lower Permian the surfaces of the north and south basins of the North Sea were approximately 240m below open sea water level (Smith,

1970b). The Zechstein transgression was almost certainly a consequence of a world-wide rise in sea level coinciding with the end of a period of Permian glaciation. Waters breached the barrier with the Boreal ocean (see Figure 9.1) and flooded the Rotliegendes desert basins (Smith, 1970b). This process was possibly aided by fracture systems induced during the late Carboniferous proto-Atlantic sea-floor spreading event (Russell, 1976).

Although the transgression was synchronous throughout the Zechstein basin, there is evidence (Plumhoff, 1966; and Peryt, 1976; both referred to in Smith, 1980) of brief periods of earlier flooding. The transgression was rapid; Glennie (1984) estimated that the entire Zechstein basin could have filled in six years. Smith (1979) also supports the idea of a rapid transgression. The transgression was erosive, probably more so in the northern basin nearer to the breach than in the southern basin. Marine reworking and scouring of the top of the Rotliegendes has been well documented (Smith, 1970a) and is particularly well displayed at Raisby Quarry (NZ 3436), where a reworked zone up to 0.5 metre thick occurs (see Plates 9.2A and 9.2B). Glennie and Buller (1983) report highly-deformed bedding which they attribute to soft-sediment deformation due to the escape of air trapped in the dunes following the rapid rise in water-level. Liquification and homogenization of the upper 27 metres of Rotliegendes during the Zechstein transgression has been



recorded by Glennie (1982) from North Sea Cores. The occurrence of an apparently algal-coated rounded carbonate-cemented clast in the Rotliegenden of the Doncaster core (Plate 9.3) suggests that sediment redistribution occurred during the transgression and also points to a possible earlier period of flooding. The marine fossil *Lingula* has been found 30 cms below the surface of the Rotliegenden (Bell et al., 1979) and again provides evidence that sediment erosion and redistribution occurred locally during the transgression.

#### 9.4 THE SEDIMENTOLOGY AND PETROGRAPHY OF THE MARL SLATE

##### 9.4.1 Water Depth and Marl Slate Thickness

The depth of water in the basin at the time of Marl Slate deposition has been estimated at less than 250 metres but more than 60 m in the north Durham area (Smith, 1970a) and was probably greater than this away from the basin margin. Based on the thickness of succeeding carbonates, Smith (1980) suggests that basinward water depths exceeded 200 metres. The water column is generally considered to have been stratified and was periodically anoxic (Pompeckj, 1914, 1920, Brongersma-Sanders, 1966; and Gibbons, 1983). The conditions leading to the occurrence of anoxic events have been described by Demaison and Moor (1980). The Marl Slate was deposited over an area of approximately 400,000 km<sup>2</sup> and ranges in



thickness from a few centimetres up to 6 metres but is generally in the region of 0.5 metres thick. Kautsch (1942) noted the influence of the underlying Rotliegendes topography on Marl Slate thickness, with the thickest accumulations occurring in hollows. Plate 9.1B shows the thickness of the Marl Slate decreasing over a dune crest of Rotliegendes Sandstone. Turner et al. (1978) produced an isopachyte map which revealed a NE-SW trend consistent with the basin-margin seif-dune orientation as deduced from palaeowind directions computed by Glennie and Buller (1983).

#### 9.4.2 Petrography of the Marl Slate

The Marl Slate is a dark grey to black well-laminated highly carbonaceous calcite/dolomite-rich shale. The lower part overlying the Rotliegendes is often sandy, while the upper part usually becomes more carbonate-rich, and grades into the overlying Lower Magnesian Limestone. The vertical sequence: sapropel; laminite; massive dolotone, can be repeated a number of times within the Marl Slate. Based on carbon and oxygen isotope data, Magaritz and Turner (1982) were able to show that such repetitions were not due to slumping. At outcrop the Marl Slate frequently weathers to a brown colour and can adopt a classic paper-shale fissility, thin (few mm) carbonate layers and lenses can also be seen (see Plate 9.4A). The Marl Slate is famous for its fossil fish and plants

(Westoll, 1941; Stonley, 1958; Bell et al., 1979) but there is no evidence of burrowing activity and a notable absence of any benthos. According to the classification proposed by Spears (1979), the Marl Slate would qualify as a fine to very fine shale.

In thin section, the lamination is seen to result from alternations of carbon-rich layers (occurring as discontinuous streaks) and carbonate/clay laminae (Plate 9.4B), the proportion of calcite to dolomite varying widely. The alternating carbonaceous and carbonate-rich laminae are 0.1 mm thick, and were considered by Hirst and Dunham (1963) to represent annual layering. They are consistent in number with a depositional time of 17,000 years as estimated by Oelsner (1959) for the Kupferschiefer. Fine horizons of quartz silt, often with coarse-grained sulphides (Plate 9.5A) occur towards the base of the Marl Slate. Carbonate micronodules (up to 0.5 mm) often with associated sulphide can be seen to deform bedding (see Plate 9.5B). Such nodules appear to be more common towards the basin margin and were not seen in cores from near the basin centre. The nodules have been shown by Turner et al. (1978) to contain bundles of length slow chalcedony, thought to indicate replacement of sulphate (Folk and Pittman, 1971; Siedlecka, 1972).

The two cores from the middle of the Southern Permian basin of the North Sea (J1000, 29 cms thick and 49/26-4,



41 cms thick) are typical black sapropels, and lack the well-developed laminations and increasing carbonate content typical of the upper sections of the cores described by Turner et al. (1978), and Turner and Magaritz (in press). Pyrite, mainly in the form of framboids, was the only sulphide seen in these two cores. The Doncaster core (D.C.; Figures 10.1 and 10.2) has a typical sapropelic base (161 cms) with three thin (6-10 cms) horizons of relatively massive organic-poor carbonate rich in ostracods (Plate 9.6A). Lamination in the sapropel becomes more distinct towards the top. This is succeeded by 36 cms of laminated organic-rich carbonate (see Plate 9.6B) with one horizon of laminated organic-rich calcite which contains rare ostracods. The total thickness of Marl Slate in the Doncaster core is 197 cms. Above the Marl Slate lies a zone (58 cms of which are examined in this study) of white carbonate (mainly calcite), grey carbonate (mainly dolomite) and sapropel horizons, intercalated on the centimeter scale, and termed in this thesis the Transition Zone. For logistic reasons only, the latter is considered part of the Marl Slate for the purpose of this thesis, although it is possibly equivalent to the Passage Beds of County Durham.

#### 9.4.3 Cathodoluminescence Observations on the Marl Slate and the Transition Zone

Cathodoluminescence studies reveal that calcites



within sapropelic horizons (Marl Slate and Transition Zone cores) are often slightly etched (see Plates 9.7A and 9.7C). Dolomite does not luminesce, probably because of its high iron content (as discussed in Chapter 10). Within calcite-rich units of the Transition Zone, calcite crystals are euhedral and frequently zoned (Plate 9.7B); although they coexist with dolomite. Similarly, within the dolomite-rich units, calcite shows no signs of etching, (see Plate 9.7D). These features indicate that calcite and dolomite may have formed in equilibrium, the lack of compositional variation (Chapter 10) between the two end-members also supports this view.

Although not commonly seen, a dolomitization event can also be recognised in the calcite-rich units of the Transition Zone core (notably sample DC109). From Plate 9.8A, it can be seen that the dolomite appears to have been nucleated around organic matter. An increase in porosity towards the edge of the dolomitizing front can be seen, and is reflected in the brighter luminescing patches of Plate 9.8A. Clustering of dolomite lenticles could possibly have resulted in the formation of thin dolomite horizons within a calcite matrix (see Plate 9.8B).

Veinlets containing nonluminescing saddle dolomite and pyrite, Plate 9.9, crosscut the lower part of the Transition Zone core.

#### 9.4.4 Sulphide Forms in the Marl Slate and the Transition Zone

By far the most abundant sulphide observed in the cores studied was pyrite, only minor amounts of chalcopyrite and sphalerite were found.

The processes involved in the formation of sedimentary pyrite are complex, and will not be discussed in detail here. They have been recently reviewed by Berner (1984). Briefly, sedimentary pyrite can form directly from reaction between iron and sulphur or via the monosulphide precursors, mackinawite or greigite (Goldhaber and Kaplan, 1974) see Figure 9.3. The occurrence of pyrite framboids is favoured by the formation of the spheroidal precursor greigite (Sweeney and Kaplan, 1973). Raiswell (1982) showed that pyrite texture is influenced by sediment and pore water chemistry, notably by the availability of iron. Raiswell (1982) concluded that a combination of abundant in situ reactive iron and  $H_2S$  would cause supersaturation with respect to pyrite and mackinawite. Preferential precipitation of mackinawite (for kinetic reasons) and its transformation to greigite would lead to the formation of framboidal pyrite. Decreasing availability of iron results in mackinawite becoming undersaturated while



pyrite remains saturated, leading to direct precipitation of euhedral pyrite.

A variety of sulphide forms occur within the Marl Slate. Plate 9.10A shows a sulphide spheroid with an overgrowth approaching cubic form. Energy dispersion analysis using the Scanning Electron Microscope yielded S/Fe ratios of 1.14 for the spheroid and 1.90 for the overgrowth. Despite the low analytical totals of approximately 80% (due partly to the gold coating used), it seems likely that the spheroid is greigite which typically has a spherical form (Sweeney and Kaplan, 1973). Framboids occur as single isolated grains (Plates 9.10B and 9.10C), as small groups of large spheres (Plate 9.10D) and as 'nests' of well-formed compound crystal framboids (Plates 9.10E and 9.10F). Euhedral crystals of pyrite (also occur and) are commonly associated with organic debris (Plates 9.10G and 9.10H). Euhedral crystals of pyrite appear to be paragenetically later than pyrite framboids. Pyrite framboids which display an euhedral overgrowth are occasionally seen (see Plate 9.11A), and may be an intermediate step between framboidal and euhedral forms. Chalcopyrite and sphalerite frequently enclose euhedral and framboidal pyrite and are apparently paragenetically later, see Plate 9.11B.

Within the Transition Zone core, pyrite in the sapropel is dominantly framboidal, whereas that in the calcite-rich units is euhedral and considerably less



abundant than in the sapropel. Pyrite form in the dolomite-rich units is a mixture of framboidal and euhedral, with the latter being most common.

## CHAPTER 10

### GEOCHEMISTRY OF THE MARL SLATE

#### 10.1 INTRODUCTION

The ease with which the Marl Slate weathers means that only data derived from fresh sub-surface samples can be relied upon to be geochemically representative. Since the bulk of Marl Slate sub-outcrop lies at depths of 500 - 2000 m, sampling difficulties have meant that geochemical data are sparse. To date there is no record of mineralisation reaching grades comparable to those that are mined in the Kupferschiefer of Europe.

In this chapter, after a brief review of previous work, the data on trace element geochemistry of three boreholes are presented. This is followed by an examination of the organic carbon, calcite, dolomite and quartz content, and carbonate composition of selected samples taken from the Doncaster Core. Finally, geochemical factors affecting pyrite formation are examined and discussed with special reference to the Marl Slate (Doncaster Core).

#### 10.2 PREVIOUS WORK

The first published study of the trace element composition of the Marl Slate was that of Deans (1950), who demonstrated the similarity in composition between the

Kupferschiefer, the Marl Slate and sapropelic shales in general. The work of Hirst and Dunham (1963) drew attention not only to trace element composition but also to vertical variation in trace and major element concentration, and they were able to show that such variations can be correlated between boreholes. They also showed that the concentration of Mo, Ni, Co and, to a lesser extent, Cu was inversely proportional to sedimentation rate, and correlated well with clay and organic carbon content. This led the authors to suggest that Mo, Ni, Co and possibly Cu were transported by being adsorbed on detrital clays and organic matter. Hirst and Dunham (1963) also implied that the rubidium and zirconium contents of the Marl Slate are of detrital origin, while manganese and strontium were probably precipitated as carbonate directly from seawater. The sources of Pb, Zn and to a lesser degree Cu were considered to be more problematical by these authors, who concluded that they were probably introduced into the basin via submarine springs.

Turner et al. (1978) studied a cored intersection of Marl Slate (D4) in detail and made a number of pertinent observations:-

- (a) A vertical Cu-Pb-Zn zonation exists in the Marl Slate and is the same as that described by Wedepohl (1964), and Jung and Knitzschke (1976) from the Kupferschiefer.



- (b) Sulphides occur in two distinct forms; as pyrite framboids and as lenses of pyrite, chalcopyrite, galena and sphalerite. The second type of sulphide is intimately linked with dolomite pseudomorphs after anhydrite.
- (c) The carbonate component of the core is dominantly dolomite, and this dolomite is calcium-rich.
- (d) Throughout the core, the variation in copper content correlates closely with that of quartz, and suggests a detrital source for that element.

Turner and Magaritz (in press) linked base metal (Cu and Zn) distribution in a Marl Slate core (VT8) to change in the  $\delta^{18}\text{O}$  values of associated carbonates. Negative shifts in  $\delta^{18}\text{O}$  were interpreted as indicative of freshwater influxes and correlate broadly with increases in detrital quartz and, to a lesser degree, with copper and zinc. The authors concluded that base metals (Cu and Zn) were introduced into the basin during periods of freshwater influx.

### 10.3 TRACE ELEMENT GEOCHEMISTRY

The techniques employed in sample preparation and the analytical method used (XRF) are discussed in Appendix 5. The trace element concentrations of samples from

individual boreholes are plotted in graphical form in figures A10.1 to A10.4, and are presented in Appendix 10. R-mode correlation matrices were constructed for all element pairs within individual boreholes and are shown in Tables A9.1 - A9.4 (Appendix 9). The mean trace element compositions for individual boreholes are compared to concentrations in an average black shale (as defined by Vine and Tourelot, 1970) in Table 10.1.

Geochemical variations within the Doncaster Core accurately reflect lithological changes, a feature particularly well displayed in the Transition Zone section (see Figure A10.4). Compared with the carbonate units, the sapropelic horizons are enriched in all elements except manganese, strontium and barium. The increase in Mn, Sr and Ba in the carbonate units reflects the substitution of these elements in carbonate minerals as originally observed by Hirst and Dunham (1963). Iron variation in the Transition Zone core similarly reflects carbonate composition, in particular the iron content of dolomite, as discussed in Section 10.5.

In the sapropelic part of the Marl Slate section of the Doncaster Core, several vertical trends in trace element composition can be observed (see Figure A10.3). Copper, cobalt, nickel and, to a lesser degree, lead and zinc show a systematic upward decrease in concentration. Copper, lead and zinc display the vertical zonation in concentration previously discussed. At the base of the



laminated carbonate section (which overlies the sapropel) all elements, except manganese and strontium, show a slight peak followed by an upward decline in concentration. Throughout the Marl Slate section of the Doncaster Core, quartz is strongly correlated with all elements except manganese and strontium (Table A9.3), and indeed manganese and strontium behave antipathetically with all other trace elements.

From Table 10.1 it can be seen that boreholes J1000 and 49-26-4, both of which are totally sapropelic, have very similar trace element compositions. The main difference is that borehole 49-26-4 has approximately double the iron and titanium concentration, and four times the manganese and half the strontium concentration of borehole J1000. The samples in both of these boreholes are enriched relative to the average black shale in all elements except rubidium and zinc. Vertical trends within these two boreholes are generally not well developed. However, borehole J1000 (Figure A10.1) does show an increase in Cu, Co, Ni and Zn concentration on passing upwards, whereas Pb and Fe display a decrease in concentration. This trend in base metal concentration is contrary to that seen in the Doncaster Core. Turner and Magaritz (in press) also noted that trace element trends in cores VT8 and D4 were not in agreement, even though the boreholes were only 3 km apart. The Doncaster Core displays the same trend (upward decrease in Cu, Pb and Zn concentration) as the D4 core while the J1000 and 49-26-4



cores show similar trends to the VT8 core of Turner and Magaritz.

Although they need to be taken into account in any genetic model, too much emphasis should not be placed on the observed base metal trends, since, in the cores examined, they reflect differences in concentration of relatively minor amounts of sulphide. Pyrite is by far the most abundant sulphide found in all the cores studied, and the iron content in each core displays a systematic decrease in concentration on passing upwards.

Ten samples from the base of the Doncaster Core were analysed for gold and platinum by neutron activation analysis. The platinum analyses were subject to interference from strontium rendering the analyses meaningless. The gold values were less than 10 parts per billion but were again subject to analytical error.

#### 10.4 VARIATION IN THE ORGANIC CARBON CONTENT OF THE DONCASTER CORE

The method used to determine organic carbon ( $C_{org}$ ) is described in Appendix 2. The sapropelic part of the Marl Slate core shows a steady increase in  $C_{org}$  from 1.5 to 6.0% on passing upwards with spikes of low concentration reflecting the influence of calcite-rich horizons. The upper laminated carbonate section of the core displays a rather rapid upwards decline in  $C_{org}$  content. The

antipathetic relationship between  $C_{org}$  and carbonate carbon ( $C_{carbonate}$ ) is well seen in Figure 10.1. The Transition Zone core reveals major, yet consistent variations and once again the antipathetic relationship between  $C_{org}$  and  $C_{carbonate}$  is well demonstrated, (see Figure 10.2). The sapropelic units have a mean  $C_{org}$  content of 2.01% compared with 4.3% for the Marl Slate saproprel, while the Transition Zone calcite-rich and dolomite-rich horizons contain, on average, 1.06% and 1.50% organic carbon respectively.

#### 10.5 CALCITE, DOLOMITE AND QUARTZ CONTENT AND CARBONATE COMPOSITION OF THE DONCASTER CORE

The calcite, dolomite and quartz contents of samples from the Doncaster Core were determined by quantitative X-ray Diffraction as described by Carver (1967). Within the Marl Slate section of the Doncaster Core, the percentage dolomite in the carbonate phase is highly variable, but also reflects lithological changes (see Figure 11.2). This mineralogical variation and its relationship to carbon and oxygen isotope values is further discussed in Chapter 11. The percentage quartz in the Marl Slate section varies from 19.6% to 7.5%. It is highest in the basal samples, but also mirrors lithological differences, being lower in carbonate-rich horizons. There is thus an antipathetic relationship between percentage quartz and percentage carbonate carbon (see Figure 10.1). In the Transition Zone of the Doncaster Core, the percentage

dolomite in the carbonate phase changes markedly with lithology, and also isotopic composition (see Figure 11.4). The quartz content is strongly antipathetic to total carbonate content (measured as %  $C_{\text{carbonate}}$ , see Figure 10.2). The quartz content is highest in the sapropelic horizons (mean value of 12.9%), with the carbonate horizons showing little variation and having a value of 6.6% in the calcite-rich units and 5.8% in the dolomite-rich units.

The percentages of carbonate that are dolomite and the compositions of the carbonate phases (calcite and dolomite) for different lithologies are shown in Table 10.2. The percentages of dolomite present in the carbonate phase of samples increases from the calcite-rich unit (15%) to the sapropel (80%) reaching a maximum in the dolomite-rich unit (92%).

The analytical totals are high (110%) for all the analysis (108 in total). This is almost certainly due to the breakdown of carbonate during analysis. Individual analyses of either calcite or dolomite are remarkably constant. To allow comparison of data, the results presented in Table 10.2 have been normalised and averaged. In all lithologies, calcite is extremely pure, being 98% to 99% calcium carbonate and containing only trace amounts of iron or manganese. Conversely, all of the dolomites analysed are ferroan dolomites (containing approx. 14%  $\text{FeCO}_3$  and contain traces (1-2%) of



manganese. The dolomites are also consistently rich in calcium.

## 10.6 DISCUSSION OF GEOCHEMICAL RESULTS

The most obvious feature common to all the borehole samples is that manganese, strontium and to a lesser degree barium, vary sympathetically and are generally antipathetic to all the other elements. As in Chapter 7, manganese, strontium and possibly barium are considered to be derived from marine water.

Element dendrograms have been produced from the samples obtained from each borehole (see Figure 10.3 to 10.5). Borehole 49-26-4 shows the above-mentioned feature well. In this instance, Mn and Sr correlate with copper and are clearly grouped separately from the other trace elements and silica, (see Figure 10.3). In borehole J1000, the elements Sr and Ba are clustered along with  $\delta^{18}O$  and the detrital index elements Zr, Ti, Nb, Rb and Th, and may reflect the influence of a freshwater influx.

Within the Transition Zone core, Mn, Sr, Ba and carbonate carbon are associated together (Figure 10.4a), reflecting the incorporation of these elements during the precipitation of carbonate. The remaining elements are grouped with quartz, pyritic sulphur ( $S_{py}$ ) and  $C_{org}$ , and possibly reflect the detrital origin of these elements, some of which may be adsorbed on organic carbon (and

clays) as originally suggested by Hirst and Dunham (1963). The Marl Slate section of the Doncaster Core is similar to the Transition Zone core, (see Figure 10.4b) but in addition to carbonate carbon, Ni and Zn are grouped with Mn and Sr.

Dendrogram analyses were also performed on the different lithological types in the Transition Zone core (see Figure 10.5). For the sapropelic units, once again Mn, Sr, Ba and C<sub>carbonate</sub> cluster together, but in this instance the group also includes C<sub>Org</sub>. The remaining elements are tightly grouped with quartz. Within the carbonate units, the element groupings are less clear. Nevertheless, in both the calcite-rich and the dolomite-rich horizons, Mn and Fe occur together as do Ba, Sr and Zn. These elements probably reflect carbonate composition, Mn and Fe are closely associated in all the dolomite samples analysed. The whole-rock concentrations of Ba, Sr and Zn are such that, even if these elements were present as carbonate, they would be below the detection limit of electron probe microanalysis. In both carbonate units, quartz is grouped with Ti, Rb and Ni and possibly reflects a detrital grouping.

#### 10.7 PYRITE FORMATION AND MARL SLATE GEOCHEMISTRY

Although this discussion is confined to the formation of pyrite, this simply reflects the greater degree to which pyrite formation has been studied. It is probable

that the underlying principles are equally valid for other sulphide minerals. Indeed, the occurrence of framboids with zinc as the major cation has been reported by Luther et al. (1980).

Sedimentary pyrite formation involves the bacterial reduction of sulphate to produce  $H_2S$  which is combined with available iron to form pyrite, often via an iron monosulphide precursor mineral. Organic matter is consumed during the reaction, which can be generalised as follows:-



Since this process occurs only in the absence of oxygen, an anoxic environment is required. During the formation of the Marl Slate, sedimentation was dominantly taking place under an anoxic water column (as discussed in Chapter 9). The other major requirements for pyrite formation are:-

- (i) a supply of Organic Matter
- (ii) a supply of Sulphate
- (iii) availability of Iron.

Organic matter is necessary since it is the food for sulphate-reducing bacteria. Since the oxidation of organic matter in the upper parts of the water column uses up oxygen, a good supply of organic matter also helps in



creating an anoxic environment (Demaison and Moore, 1980). If the organic matter metabolised during pyrite formation is a constant proportion of the total organic matter entering the sulphate reduction zone, then a linear correlation should exist between the sediment pyrite sulphur and organic carbon content (i.e. it should have a constant C/S ratio). Such a linear relationship has been shown to exist in modern sediments (Berner, 1970; Goldharber and Kaplan, 1974; Berner, 1982) and yields a C/S ratio of about 3.

Jørgensen (1978) has shown that up to 90% of the  $H_2S$  produced during sulphate reduction in sediments escapes to the overlying water column, and this is reflected in the high C/S ratio. If the overlying water column is oxic then some of the  $H_2S$  could be oxidised to sulphate and may once again enter into the reaction cycle, but would have a negligible effect on the C/S ratio. On the other hand, if the overlying water column is anoxic then the  $H_2S$  may react with available iron to form pyrite without a proportional consumption of organic matter. This would have a major influence on the C/S ratio and possibly result in regression lines with a positive intercept on the S axis, (see Figure 10.6). Such a situation was found by Leventhal (1983) for recent sediments in the Black Sea, and he suggested that such features could be used to identify ancient anoxic sedimentary environments. Berner and Raiswell (1983, 1984) further refined the model and showed that C/S ratios could be used to distinguish

between freshwater and marine sedimentary rocks, (see Figure 10.6). The C/S ratio of freshwater sediments reflects the lower concentration of sulphate in freshwaters compared to marine, and consequently the reduced potential for pyrite formation.

Seawater provides the major source of sulphate in marine sediments. If sulphate reduction occurs within the water column, the sulphate-reducing bacteria are in contact with what is essentially an infinite sulphate reservoir, and this would be reflected in the isotopic composition of any sulphide mineral formed (ie. open system fractionation as defined by Schwarcz and Burnie (1973) would be operative, and result in light isotopic compositions).

The availability of iron for sedimentary pyrite formation is dependant on the reactivity of the detrital iron minerals. Fine-grained iron hydroxides obviously react more readily than ilmenite or magnetite. To overcome this problem, Berner (1970) proposed that a measure of the iron available for pyrite formation could be defined as follows:-

$$\text{Degree of Pyritization (D.O.P.)} = \frac{\% \text{ Fe as pyrite}}{\% \text{ Fe as pyrite} + \% \text{ Fe HCl}}$$

where % Fe HCl is the amount of iron liberated on treatment with hot hydrochloric acid. If pyrite formation is



limited by iron then the DOP will approach 1. The effect of iron availability on the form of pyrite produced was discussed in section 9.4.4, and it was concluded that where iron availability is high then framboids are formed, and where iron availability is a limiting factor, euhedral pyrite is formed.

#### 10.7.1 C/S Ratios in the Marl Slate

Organic carbon and pyrite sulphur content were determined for samples from the Doncaster Core (Marl Slate and Transition Zone sections). The pyrite sulphur content was determined by quantitative measurement of the volume of SO<sub>2</sub> produced from whole rock samples during sample preparation for sulphur isotope analysis (see Appendix 3). A total of 29 samples were analysed from the Transition Zone section and 24 from the Marl Slate section.

The results of the analyses are plotted in Figure 10.7. The Marl Slate core section has a C/S ratio of 2.2 and a positive intercept of 0.93% on the S axis. If only the sapropelic samples are considered then the intercept on the S axis increases to 2.33% and the percentage pyritic sulphur is uncorrelated with the percentage organic matter. As explained above, such a result (positive intercept on the S axis) indicates that pyrite was forming in an anoxic water column. Even in the non-sapropelic samples from the Marl Slate core a positive



intercept of 0.77% S was found, so it would seem that throughout Marl Slate depositional times, pyrite was forming in an overlying anoxic water column and was most advanced during sapropelic deposition.

The Transition Zone section has a C/S ratio of 1.72 and a positive intercept on the organic carbon axis of 0.43% which implies that sulphate supply may have been a limiting factor in pyrite formation. When individual units within the Transition Zone are plotted, the data points are relatively scattered, but the best-fit straight line for the sapropelic unit has a positive intercept on the S axis of 1.24%, indicating pyrite formation in an anoxic water column.

#### 10.7.2 Degree of Pyritization in the Marl Slate

The degree of pyritization (DOP) in the Marl Slate section of the Doncaster Core, plotted against organic carbon content, is shown in Figure 10.8. The degree of pyritization was calculated by dividing the percentage pyritic sulphur by total iron as suggested by Raiswell (pers. comm.). Results obtained by this method would, in theory, tend to be lower than those determined by the method of Berner (1970), since iron from non acid-soluble minerals will be included in the divisor. The results yield a mean DOP of 0.83 for the Marl Slate which increases to 0.93 if the non-sapropelic samples (laminated carbonate and calcite horizons) are excluded. Such a

degree of pyritization (0.83) is extremely high and suggests that iron availability may have been a limiting factor in pyrite formation. It is interesting to note that slow sedimentation rates, such as those found under anoxic conditions would maximise the amount of pyrite formed since more time would be allowed for slowly reacting iron compounds to react with  $H_2S$ . Thus, the high DOP and low sedimentation rate suggests that, in this case, the limit to sulphide formation was not simply availability of iron minerals of suitable reactivity, but availability of iron (in any form) or any other cation.

Had there been an external source of metals capable of forming sulphides then the data suggest that there was ample  $H_2S$  available for sulphide precipitation. Within the Transition Zone, the DOP of the sapropelic horizons approaches 1. The DOP of the carbonate units reflects the composition of the carbonate phases. It may not be valid to apply the idea of iron availability in such cases, particularly when the  $C_{org}$  content is also relatively low. However, in the calcite-rich units (92% of the carbonate phase is pure calcite) the DOP approaches 1. Dolomite-rich horizons have a DOP of approximately 0.25, reflecting the iron content of the dolomite which averages 15% iron carbonate.



### 10.7.3 Pyrite Compositional Variations Within the Marl Slate

Pyrite compositional variations within the Doncaster Core are shown in Table 10.3. The most obvious feature is that all of the pyrites analysed contain traces of lead, with a concentration of up to 0.70% in the sapropel units. The analytical totals of samples from the Transition Zone sapropel unit are low. This is probably a consequence of the intermixing of carbonate matrix within these fine grained framboids. This feature cannot, however, explain the anomalous composition of these pyrites, namely the occurrence of Zn, Ni, Cu and Mn, since the content of these elements in the carbonate matrix is low (see XRF results). The manganese content is particularly anomalous and difficult to explain since it reaches a level of 0.55%.

Pyrites from the Marl Slate sapropel contain, in addition to lead, traces of copper and nickel up to 0.68%, but lack the manganese impurity of the pyrites from the Transition Zone sapropels. Pyrites from calcite-rich and dolomite-rich units of the Transition Zone are similar, with the lead content of the dolomite-associated pyrite possibly being slightly higher than that associated with the calcite-rich units.

Veinlets which crosscut carbonate units of the Transition Zone contain saddle dolomite, pyrite, and trace



amounts of sphalerite. The pyrite within the veins is coarse grained, but towards the vein margins becomes coarsely intergrown with the matrix carbonate. The pyrite from the marginal area contains lead and arsenic up to 0.41%, and is the only pyrite analysed which contains arsenic.

#### 10.8 SUMMARY

A strong lithological control of both mineralogical and trace element compositions is evident in all the cores examined. The elements Mn, Sr, Ba and, to a lesser extent, Zn are grouped together statistically and probably substitute in the carbonate lattice, although their concentration is such that they are often below the detection limit of the electron-microprobe. The remaining trace elements correlate with quartz and C<sub>org</sub>.

Within the Transition Zone core, the percentage dolomite in the rock carbonate increases from 15 in the calcite-rich units to 80 in the sapropelic horizons to 92 in the dolomite-rich units. In the Marl Slate section (Doncaster Core) the calcite/dolomite ratio varies widely. In all lithologies the composition of the carbonate minerals is remarkably uniform, as shown below:-

Calcite (n=48)	Ca <sub>0.99</sub>	Mg <sub>-</sub>	Fe <sub>0.01</sub>	Mn <sub>0.01</sub>	C <sub>03</sub>
Dolomite (n=59)	Ca <sub>0.59</sub>	Mg <sub>0.25</sub>	Fe <sub>0.15</sub>	Mn <sub>0.01</sub>	C <sub>03</sub>

The constant chemical composition of calcite or dolomite, irrespective of the extent of their association or lithological occurrence suggests that replacement was not active and that both minerals are primary.

Base metal concentrations passing upwards through the core vary between different boreholes and often show reverse trends even in boreholes less than 3 km apart. However, it should be remembered that the observed base metal trends reflect differences in concentration of relatively minor amounts of sulphide in the borehole cores studied. Variations in the concentrations of major elements and minerals (quartz, iron,  $C_{org}$  and Clay) are similar in all boreholes examined in this and previous studies.

In the Marl Slate section of the Doncaster Core, the C/S ratio and the positive intercept on the pyrite sulphur axis (0.93% for the total core and 2.33% for the sapropelic section) indicate that pyrite formation took place in an anoxic water column. The degree of pyritization (0.83) indicates that iron availability was a limiting factor to pyrite growth within the Marl Slate. In the Transition Zone core, the positive intercept on the  $C_{org}$  axis of the C/S plot suggests that sulphate supply was a limiting control on pyrite formation, although the sapropelic units maintain a positive intercept of 1.3% S. The degree of pyritization indicates that the availability

of iron was limiting in calcite-rich and sapropelic horizons, but was abundant in the dolomite-rich units.

Pyrite compositional data reveal that all pyrite contains minor amounts of lead which increases to 0.70% in the sapropels. The pyrite from sapropels also contains traces of Cu, Zn and Ni. Pyrites from Transition Zone sapropels also contain manganese up to 0.52%. Other than the lead already mentioned, pyrite from the carbonate units contains no extraneous elements. Pyrites from vein margins which crosscut the upper carbonate units of the Transition Zone core contain arsenic, not found in the matrix pyrites, and thus ruling out a lateral secretion origin for vein pyrite.



## CHAPTER 11

### STABLE ISOTOPE RESULTS FROM THE MARL SLATE

#### 11.1 INTRODUCTION

The first published extensive isotope study of a single sedimentary unit in ancient rocks is the work on the Kupferschiefer by Marowsky (1969); English summaries of which can be found in Maynard (1980) and Wedepohl (1980). Although this classic work is not concerned with the Marl Slate but with its German equivalent (Kupferschiefer), the number of analyses performed present such a large database, including the only available sulphur isotope (sulphide) values, that it deserves summary.

Marowsky (1969) showed that within the Kupferschiefer there is no appreciable lateral change in sulphur isotope values, but that there was an upward enrichment in  $^{34}\text{S}$  of up to 15 per mil. Limiting sulphate supply was not considered responsible for this change, nor can it be explained by change in sedimentation rate (which would affect the fractionation factor) since regular varves occur, and the sedimentation period was short (Oelsner, 1959).

Marowsky (1969) interpreted the sulphur isotope shift as reflecting the water body becoming cut off from the open sea, and consequently enriched in  $^{34}\text{S}$  as sulphide

formation continued, and also established that pyrite was isotopically lighter ( $\delta^{34}\text{S}$  from -30 to -40 per mil) than copper, lead or zinc sulphides ( $\delta^{34}\text{S}$  from -25 to -36 per mil). Consequently pyrite could not have been formed in equilibrium with these sulphides since in an equilibrium assemblage pyrite should contain the isotopically heavier sulphur. Wedepohl (1980), to explain this anomaly, suggested that pyrite formed in a different environment than the copper, lead and zinc sulphides. The  $\delta^{13}\text{C}$  values of carbonate minerals from the Kupferschiefer were shown to exhibit an upward enrichment in  $^{13}\text{C}$  (Marowsky, 1969). He also observed that calcite-rich horizons tended to be depleted in  $^{18}\text{O}$ , and to a lesser extent in  $^{13}\text{C}$ , compared with dolomite-rich horizons, although there was a spread of data in both cases.

To date, all isotope studies of the Marl Slate have been confined to the determination of carbonate  $\delta^{13}\text{C}$  and  $\delta^{18}\text{O}$  values. Due to the potential contamination effect of weathering, only samples from borehole cores have been analysed. The first isotope study of the Marl slate was that of Magaritz et al. (1981). In this study, the authors established a vertical enrichment of  $^{13}\text{C}$  of between 2 and 4 per mil from Marl Slate cores D4 and D7, and from two German Kupferschiefer cores. The  $\delta^{18}\text{O}$  values display similar trends. The samples from Germany were mainly calcite while the English ones were primarily dolomite. This mineralogical difference does not appear to alter isotope trends, although the actual  $\delta^{13}\text{C}$  values



are higher in the Marl Slate than in the Kupferschiefer cores. The results of a more detailed study on borehole core VT8 were given by Margaritz and Turner (1982). The VT8 core displays a  $^{13}\text{C}$  enrichment of 2.8 per mil from the base to the top of the Marl Slate. Data from Magaritz and Schulze (1980) indicate that  $^{13}\text{C}$  enrichment continues to the top of the third Zechstein Cycle. The  $\delta^{13}\text{C}$  and  $\delta^{18}\text{O}$  trends in the VT8 core are poorly correlated (Magaritz and Turner, 1982), and the  $\delta^{18}\text{O}$  pattern exhibits spikes of very low values. A correlation between change in  $\delta^{18}\text{O}$  and lithology was also recorded and taken to indicate that isotope changes are primary and not the result of later recrystallization. A detailed geochemical examination of the VT8 core (Turner and Magaritz, In Press) revealed that vertical  $^{13}\text{C}$  enrichment is accompanied by a decrease in organic carbon content. The low  $\delta^{18}\text{O}$  spikes coincided with an increase in sample quartz and iron content, which the authors suggest reflects periods of freshwater influx.

In the present study, stable isotope analyses were performed on carbonate phases from boreholes J1000 and the Marl Slate and Transition Zone sections of the Doncaster Core (see location map, Figure 9.1). In addition, sulphur isotope analyses were conducted on both sections of the Doncaster Core. Dolomite and calcite occurs in variable proportions in the samples analysed, but the fine grain size of their intergrowth did not permit their separation. A total of 116 carbonate and 62 sulphide



samples were analysed. The method of sample preparation and analysis is discussed in Appendix 4 for carbonates, and Appendix 3 for sulphides. Lack of sufficient sulphate did not permit the determination of the isotopic composition of Permian seawater, and where appropriate the  $\delta^{34}\text{S}$  value of +11 per mil from Holser and Kaplan (1966) and Claypool et al. (1980) is used.

## 11.2 CARBON AND OXYGEN ISOTOPE RESULTS FROM BOREHOLE J1000

A total of 12 samples were analysed, the results are shown in Table 11.1 and are plotted in Figure 11.1. The core is sapropelic throughout and contains less than 10% carbonate. The small amount of sample available for analysis resulted in analytical difficulties, and the uppermost sample is of unreliable accuracy. The most marked features of the results are the strong positive correlation between  $\delta^{18}\text{O}$  and  $\delta^{13}\text{C}$ , and the marked depletion in  $^{18}\text{O}$  and  $^{13}\text{C}$  in the basal few centimetres of the core. The depletion in  $^{13}\text{C}$  of about 4 per mil at the base may simply reflect the incorporation into carbonate of isotopically light carbon derived from the oxidation of organic matter during the initial transgression. The basal depletion in  $^{18}\text{O}$  and the vertical return to values of around zero per mil probably reflects a return to marine seawater values after an initial 'freshwater' influx.

### 11.3 STABLE ISOTOPE RESULTS FROM THE MARL SLATE SECTION OF THE DONCASTER CORE

The core was sampled at two centimetre intervals throughout its length, and every second sample was isotopically analysed. Occasionally, particularly when crossing lithological boundaries, additional samples were analysed. For practical reasons fewer sulphur isotope analyses were undertaken than carbonate analyses. The results of the analysis are shown in Table 11.2, and are plotted in Figure 11.2.

#### 11.3.1 Carbon Isotope Results

The basal 8 cms of sapropelic section of the core is depleted in  $^{13}\text{C}$  by 3.5 per mil. Four other  $^{13}\text{C}$  depleted spikes are observed and correspond to calcite-rich horizons. These calcite-rich horizons contain ostracods (Plate 9.6A) and are geochemically characterised by depletion in elements of presumed detrital origin (Ti, Zr, Rb and Fe) or with quartz and are enriched in Mn and Sr, see Figure 10.1. The central section of the core displays remarkably uniform  $\delta^{13}\text{C}$  values of between 2.6 and 3.2 per mil over a length of 80 cms. The  $\delta^{13}\text{C}$  values do not strongly correlate with organic carbon content (see Figure 10.1). For comparative purposes, the number of points plotted in Figure 10.1 is limited by the number of sulphur isotope analyses. Superimposed on the  $^{13}\text{C}$  depleted spikes already mentioned there is a steady upward enrichment in

$^{13}\text{C}$ . Using this data, two equations can be derived to relate  $^{13}\text{C}$  enrichment with height above base (which is equivalent to time), both of which are significant at the 99.9% confidence level. The equations derived are;

$$\delta^{13}\text{C} = 1.7 + \text{Ht (m)} \quad (1)$$

$$\delta^{13}\text{C} = 2.3 + 0.65 \text{ Ht (m)} \quad (2)$$

The first equation uses all the data points, and in determining the second, all the data points from the negative spikes were removed from the calculation. This is equivalent to an enrichment in  $^{13}\text{C}$  over the Marl Slate depositional period (  $\approx$  17000 years, Oelsner, 1959) of 1.3 to 2.0 per mil, the latter value derived using all of the data points.

The results of two analyses of calcite vug material collected from Quarrington Quarry are also shown in Table 11.2, and these clearly show the contaminating effect of meteoric waters.

#### 11.3.2 Oxygen Isotope Results

Samples from the basal 8 cms of core show a depletion of  $^{18}\text{O}$ , (Figure 11.2). Similarly the  $\delta^{18}\text{O}$  values display negative spikes corresponding to the calcite-rich units discussed in the previous section. In this respect the  $\delta^{13}\text{C}$  and  $\delta^{18}\text{O}$  values have similar trends, implying a



degree of lithological control. However, a significant departure from this sympathetic relationship is the large (approximately 3 per mil) negative "belly" of  $\delta^{18}\text{O}$  values in the central sapropelic section of the core. The  $\delta^{18}\text{O}$  values are negatively correlated (at the 99.9% C.L.) with the organic carbon content of samples (Figure 10.1 and Table A9.3). In terms of geochemistry, the  $\delta^{18}\text{O}$  values are not significantly correlated with the detrital index elements (Ti, Zr, Rb and Fe) or with quartz, and are negatively correlated with Sr, high Sr values being associated with areas of  $^{18}\text{O}$  depletion (see Table A9.3). A more remarkable correlation is that between  $\delta^{18}\text{O}$  and the percentage dolomite in the sample carbonate phase (see Figure 11.2), high percentage dolomite being associated with  $^{18}\text{O}$  enrichment. As a consequence of carbonate chemistry, (Table 10.2) areas of  $^{18}\text{O}$  enrichment are enriched in Mn, as confirmed by the positive correlation between these parameters (see Table A9.3).

#### 11.3.3 Sulphur Isotope Results

Only one sample from the underlying Rotliegend was analysed, and this yielded a mean  $\delta^{34}\text{S}$  value of -2.5 per mil (Table 11.2). Since whole-rock samples were analysed, polished thin sections were prepared from many samples to ensure that pyrite was the only significant sulphide present. Results from trace element geochemistry were used to confirm this observation. No sulphate was observed in any thin sections of analysed material. The

Marl Slate  $\delta^{34}\text{S}$  values range from -36.7 to -29.1 per mil and have an average value of -32.7 per mil. The  $\delta^{34}\text{S}$  values do show an upward vertical trend to more  $^{34}\text{S}$  enriched values, although this trend is not well developed, (Figure 11.2). The only significantly (at the 95% C.L.) correlated parameter with  $\delta^{34}\text{S}$  is the amount of carbonate in the sample (see Table A9.3), high carbonate content (equivalent to carbonate carbon) being associated with  $^{34}\text{S}$  enriched pyrite. One sulphate sample (barytes) found filling vugs in the Marl Slate at Quarrington Quarry yielded a  $\delta^{34}\text{S}$  value of +11.6 per mil which is in keeping with the Permian marine water sulphate value given by Claypool et al. (1980).

#### 11.4 DISCUSSION OF THE STABLE ISOTOPE RESULTS FROM THE MARL SLATE SECTION OF THE DONCASTER CORE

It is suggested that the depletion in  $^{13}\text{C}$  over the basal 8 cms of core is due to the incorporation into carbonate phases of isotopically light carbon derived from the oxidation of organic matter during the transgression. If, as explained in Chapter 9, the Zechstein transgression was caused by a change in water level resulting from the end of a period of glaciation, one would expect water released from such a source to be isotopically light, relative to normal marine water (see Section 5.4.2). This would explain the initial  $^{18}\text{O}$  depleted values seen at the base of Marl Slate cores.



The four horizons of calcium-rich organic laminate are coincident with zones of  $^{13}\text{C}$  and  $^{18}\text{O}$  depletion in the isotope record, indicating a degree of lithological control, and implying a lack of post-depositional alteration. These carbonate-rich horizons have a low detrital element content which suggests a marine rather than a detrital origin for the carbonate.

A positive correlation between high organic carbon content and  $^{13}\text{C}$  depletion was found by Turner and Magaritz (in press) in samples from the VT8 core. Such a relationship may be an artefact of analysis, where isotopically light organic-derived  $\text{CO}_2$  released during sample reaction with orthophosphoric acid could mix with carbonate derived  $\text{CO}_2$ , resulting in a lowering of the true  $\delta^{13}\text{C}$  value. For this reason, organic matter was removed before analysis of all the carbonate samples isotopically analysed in this study (see Appendix 4). The resultant  $\delta^{13}\text{C}$  values are positively correlated (though not strongly) with organic carbon, high organic carbon content being associated with  $^{13}\text{C}$  enrichment. This is the reverse of the relationship found by Turner and Magaritz (in press) but in keeping with the findings of Vergnaud-Grazzini et al. (1977), Weissert et al. (1979) and Scholle and Arthur (1980), who observed that  $^{13}\text{C}$  enrichment of carbonate minerals accompanied periods of organic-rich sedimentation. The burial of large amounts of organic matter effectively 'locks-up' isotopically light carbon and results in carbonates formed during such periods being



$^{13}\text{C}$  enriched. The Permian was a period of high burial rate of organic matter as demonstrated by Garrels and Lerman (1981) and Berner and Raiswell (1983). Consequently, this model may explain the overall  $^{13}\text{C}$  enrichment found in the Marl Slate section of the Doncaster Core, and other Marl Slate cores as discussed in Section 11.1. Indeed,  $^{13}\text{C}$  enrichment of Permian carbonates is well documented and of world-wide extent; in Australia by Compston (1960), in Japan by Osaki (1973), in Arctic Canada by Davies (1977) and in the United States by Kirkland and Evans (1976) and Magaritz et al. (1983).

Possibly the most remarkable feature of the results is the almost perfect relationship between the isotopic variations and the percentage dolomite in the carbonate phase of the samples. The poor correlation between  $\delta^{18}\text{O}$  and  $\delta^{13}\text{C}$  and the detrital index elements (Zr, Ti, Rb) and quartz suggests that we are not dealing with freshwater influx. The intimate admixture of calcite and dolomite, the lack of replacement of calcite by dolomite and the purity and consistency of the composition of the carbonate phases (Chapter 10) combined with the lithostratigraphic control of the isotopic composition previously discussed, effectively rules out a secondary origin for the dolomite in these samples. The data from Figure 11.3 establish that if the calcite and dolomite formed in equilibrium, then in comparison the calcite would be depleted in  $^{18}\text{O}$  by 3.8 per mil and in  $^{13}\text{C}$  by 1.5 per mil. This depletion is less than that suggested by

Northrop and Clayton (1966), O'Neil and Epstein (1966) and Sheppard and Schwarcz (1970) but in general agreement with more recent studies by Fritz and Smith (1970) and Mathews and Katz (1977). This lends further support to the suggestion that the dolomite in this core is primary and formed in equilibrium with calcite.

The  $\delta^{34}\text{S}$  values of pyrite are isotopically light, having a mean value of -32.7 per mil, and are very different from the value of -2.5 per mil from the underlying Rotliegendes, which appears to be of detrital origin, see Plate 9.11C. Using a mean Permian sulphate value of +11 per mil gives a fractionation factor for the Marl Slate samples of almost 44 per mil. This fractionation factor and the limited range of  $\delta^{34}\text{S}$  values are typical of those found in euxinic basins in which there is abundant supply of sulphate and in which open system fractionation was evident (see Schwarcz and Burnie, 1973). The upward trend towards sulphide  $^{34}\text{S}$  enrichment probably reflects a minor  $^{34}\text{S}$  enrichment in seawater sulphate as originally suggested by Marowsky (1969).

The calcite/sulphide filled vugs from surface exposures (Quarrington Quarry) have  $\delta^{18}\text{O}$  and  $\delta^{13}\text{C}$  values which clearly show the effects of contamination by meteoric waters. However, the sphalerite extracted from one of the vugs (Plate 9.9B) yielded a  $\delta^{34}\text{S}$  value which is in accord with a primary origin, as was the sulphate sample.



## 11.5 STABLE ISOTOPE RESULTS FROM THE TRANSITION ZONE SECTION OF THE DONCASTER CORE

In order to determine if there was any isotopic variation associated with the rapid changes in lithology, this section of core was sampled approximately every two centimetres, and each sample was isotopically analysed. The results of the analysis are shown in Table 11.3 and are plotted in Figure 11.4.

### 11.5.1 Carbon Isotope Results

As with the samples from the Marl Slate core section, all the  $\delta^{13}\text{C}$  values in the Transition Zone core are enriched in  $^{13}\text{C}$  with respect to normal marine carbonates. The  $\delta^{13}\text{C}$  values display a marked variation with rock type, the calcite-rich horizons being the least  $^{13}\text{C}$  enriched, (see Table 11.3). Superimposed on this lithological variation is a vertical trend towards  $^{13}\text{C}$  enrichment, similar to that seen in the Marl Slate.

From Figure A9.4 it can be seen that the  $\delta^{13}\text{C}$  values are not correlated with either the detrital index elements (Zr, Ti, Rb) or quartz.

### 11.5.2 Oxygen Isotope Results

As with the carbon isotope results, the oxygen



isotope values distinguish clearly between different lithologies, the depletion in  $^{18}\text{O}$  increasing from the sapropel to the dolomite-rich to the calcite-rich horizons. Superimposed on this variation there appears to be an upward trend towards  $^{18}\text{O}$  enriched values. In terms of geochemistry, the  $\delta^{18}\text{O}$  values are strongly positively correlated with the detrital index elements (Zr, Ti, Rb) and quartz, higher concentrations of these being associated with  $^{18}\text{O}$  enrichment (see Figures 10.2 and A10.2 and Table A9.4).

One dolomite sample (see Plate 9.9A), from a mineralised cross-cutting vein, was analysed and found to be depleted in  $^{18}\text{O}$  by approximately 3.5 per mil compared with the matrix in which it occurred.

### 11.5.3 Sulphur Isotope Results

The sulphur isotope values show the greatest variation with lithology of all the isotopes studied (see Figure 11.4), ranging from an average  $\delta^{34}\text{S}$  value of -15.0 per mil in the calcite rich units to -29.1 per mil in the sapropelic units. These variations are remarkably large and consistent considering that they occur over sediment thicknesses in the order of a few centimetres. The  $\delta^{34}\text{S}$  values are strongly negatively correlated with quartz and all trace elements except strontium and barium (see Figure 10.2 and Table A9.4). Pyrite taken from a vein cross-cutting sample 104 was depleted in  $\delta^{34}\text{S}$  by

1.8 per mil compared with pyrite from sample 104.

#### 11.6 DISCUSSION OF THE STABLE ISOTOPE RESULTS FROM THE TRANSITION ZONE OF THE DONCASTER CORE

The most striking feature of the results obtained from the Transition Zone core is the marked variation in the isotopic composition of the different lithologies. This is particularly so when one considers that the differences, which are often very large, occur over a thickness of a few centimetres. This is extremely convincing evidence that the isotopic compositions are primary features and have not been significantly altered by later diagenetic events. This is substantiated in Figure 11.5 where  $\delta^{18}\text{O}$  is plotted against  $\delta^{13}\text{C}$  in terms of lithology. The trend towards  $\delta^{18}\text{O}$  and  $\delta^{13}\text{C}$  enrichment from the calcite-rich to the sapropelic horizons can be seen. Similarly in Figure 11.6,  $^{34}\text{S}$  depletion can be seen to accompany progressive  $^{18}\text{O}$  enrichment from the calcite-rich, through the dolomite-rich to the sapropelic horizons. To a large degree, the isotopic variation of carbon and oxygen can be explained in terms of carbonate mineralogy. As in the case of the Marl Slate section, calcite-rich samples are depleted in  $^{13}\text{C}$  and  $^{18}\text{O}$  with respect to the dolomite-rich samples (see Figure 11.4).

The change in  $\delta^{34}\text{S}$  values is somewhat more problematic. It is difficult to visualise circumstances



in which the isotopic composition of the marine water sulphate reservoir could vary with the rapidity and cyclicity necessary to explain the observed changes in  $\delta^{34}\text{S}$ . The dilution of the sulphate reservoir, as a consequence of freshwater influx could explain variation in the  $\delta^{34}\text{S}$  values of the sulphides ultimately produced. However, if such a mechanism was active, periods of freshwater influx (mirrored in  $^{13}\text{C}$  and  $^{18}\text{O}$  depletion) should have a strong positive correlation with high detrital input. Since the opposite is found to be the case, dilution of the sulphate reservoir by freshwater influx is not thought to be responsible for the change in pyrite  $\delta^{34}\text{S}$  values seen. Similarly, fluctuation in the supply of iron or organic matter could not be responsible for the variation in the observed  $\delta^{34}\text{S}$  values.

Assuming a relatively constant  $\delta^{34}\text{S}$  value of the reservoir sulphate (there has been some vertical  $^{34}\text{S}$  enrichment - see below), the pyrite  $\delta^{34}\text{S}$  values within the calcite rich and sapropelic horizons represent a fractionation factor of 29.6 per mil and 43.7 per mil respectively. This corresponds to a change from partially open (calcite-rich) to open (sapropel) system fractionation as defined by Schwarcz and Burnie (1973). The fractionation factors take into account the 3.6 per mil enrichment in  $^{34}\text{S}$  of the sulphate reservoir as discussed below.

It is proposed that the sulphur isotope record is



simply the combined effect of partially open system fractionation of sulphides within the sediment, and fully open system fractionation of sulphides produced in the overlying anoxic water column. Thus, the sapropelic samples have a component of sulphide formed in the anoxic water column (open-system) and sulphide formed within the sediment (partially open system) while, in the calcite-rich units, sulphide formation was limited to within the sediment. The dolomite-rich horizons are visualised as being intermediate between these two extremes. One consequence of this model which will be discussed later, is that calcite formation occurred in an oxic water column while dolomite formed in an anoxic water column or at the oxic/anoxic interface.

If it is assumed (as discussed in Section 11.1) that the sulphate-sulphide fractionation factor remained constant within similar lithologies, then pyrite  $\delta^{34}\text{S}$  values can be used to reflect changes in the isotopic composition of the reservoir sulphate. It can be seen from Tables 11.2 and 11.3 that the  $^{34}\text{S}$  enrichment of sulphate observed during Marl Slate formation continued during Transition Zone deposition. This is confirmed by the isotopic composition of pyrite from sapropelic horizons, within the Marl Slate these range from -36.7 per mil to -29.8 per mil (average -32.7 per mil) and in the Transition Zone range from -31.5 per mil to -27.1 per mil with an average value of -29.1 per mil. There is, thus, an estimated 3.6 per mil enrichment in  $^{34}\text{S}$  of the sulphate

reservoir from Marl Slate to Transition Zone times. This trend towards isotopically heavier sulphate with time is a consequence of progressive enrichment in  $^{34}\text{S}$  of a sulphate reservoir of fixed size as isotopically light sulphur is extracted from the reservoir in the form of sulphides. This is a good example of the "reservoir effect" (see Figure 5.1).

The probable causes of the general  $^{13}\text{C}$  enrichment of the carbonates and their continued upward  $^{13}\text{C}$  enrichment trend, have been explained in Section 11.6.

The one sample of saddle dolomite from a vein that was isotopically analysed yielded a  $\delta^{18}\text{O}$  value, of -8.18 per mil which is depleted in  $^{18}\text{O}$  by 3.4 per mil relative to the matrix carbonate in which it occurred. If the saddle dolomite formed in equilibrium with marine derived water, the  $\delta^{18}\text{O}$  value corresponds to an increase in formation temperature of  $79^{\circ}\text{C}$  compared with the matrix carbonate. This is in agreement with the observations of Radke and Mathis (1980) who established that saddle dolomite formed in the temperature range  $60 - 150^{\circ}\text{C}$ .

#### 11.7 SUMMARY AND CONCLUSIONS

The contaminating effect of meteoric water can be clearly seen in the isotopic composition of the two Quarrington Quarry carbonate samples (see Table 11.2 and Plate 9.9B). As a consequence of this potential



contamination, all isotopic studies of the Marl Slate and the Kupferschiefer have been carried out on borehole samples.

Carbonates from the basal section of the Marl Slate core are highly depleted in  $^{13}\text{C}$  and  $^{18}\text{O}$ , this can be seen particularly well in the J1000 core (see Figure 11.1). The depletion in  $^{13}\text{C}$  is interpreted as being due to the incorporation, into carbonate phases of isotopically light carbon, derived from the oxidation of organic matter. The  $^{18}\text{O}$  depletion reflects the non-marine, isotopic composition (partially glacially derived and therefore isotopically light) of the early transgression waters.

The Marl Slate cores display a remarkably strong and consistent lithological control on all isotope parameters. In all the cores studied, carbonate samples are enriched in  $^{13}\text{C}$  with respect to normal marine carbonates, and show an upward trend towards  $^{13}\text{C}$  enrichment. An enrichment in  $^{13}\text{C}$  of between 1.3 per mil and 2 per mil was found in the Marl Slate section of the Doncaster Core. The vertical enrichment in  $^{13}\text{C}$  was also evident in the Transition Zone core, and may continue until the third cycle Zechstein carbonate (Magaritz and Schulze, 1980). This  $^{13}\text{C}$  enrichment is characteristic of the Permian and can be explained in terms of a world-wide balance between burial of organic matter, which locks up isotopically light carbon, and the simultaneous production of carbonate which is consequently  $^{13}\text{C}$  enriched.



Turner and Magaritz (in press) show that spikes of  $^{18}\text{O}$  depletion in the carbonates of the VT8 core correspond to an increase in detrital elements and quartz, which they attributed to the influence of freshwater influx events. No such correlation was found in the Marl Slate section of the Doncaster core, indeed, although not well correlated, the opposite trend was observed. In the Transition Zone core,  $^{18}\text{O}$  and  $^{13}\text{C}$  depletion in the carbonate isotope record is strongly correlated with periods of low detrital input. It is suggested that the concentration of detrital phases is probably a function of sedimentation rate.

The most significant parameter to correlate with carbonate  $\delta^{18}\text{O}$  and  $\delta^{13}\text{C}$  values is the percentage dolomite in the carbonate phase. Bivariant scatter and least squares fit plots for the percentage dolomite in the carbonate phase against  $\delta^{13}\text{C}$  and  $\delta^{18}\text{O}$  for the Marl Slate section of the Doncaster Core give fraction factors between calcite and dolomite in agreement with recent experimental work. This strongly suggests that the calcite and dolomite formed in equilibrium. Previous workers have also noticed that calcite rich-cores are depleted in  $^{13}\text{C}$  and  $^{18}\text{O}$  relative to dolomite-rich cores (Marowsky, 1969; Magaritz and Turner, 1981), although no detailed comparative data on the relative proportion of calcite and dolomite are recorded.

Sulphides in the Marl Slate are isotopically light,

values in the range -30 per mil to -40 per mil being typical for pyrite. Marowsky (1969) established that copper, lead and zinc sulphides were isotopically lighter than pyrite, and consequently did not form in equilibrium with it. The range in  $\delta^{34}\text{S}$  values found in the Marl Slate are indicative of open system fractionation in which there is an abundant supply of sulphate. An upward trend towards  $^{34}\text{S}$  enrichment was observed in the Marl Slate cores. The most likely explanation for this trend is the progressive enrichment in  $^{34}\text{S}$  of a fixed sulphate reservoir, as isotopically light sulphur is removed in precipitated sulphides.

The  $\delta^{34}\text{S}$  values of pyrite within the Transition Zone core display large and systematic changes with lithology. These rapid variations are interpreted as the combined effects of partially open and open system fractionation. Sapropelic samples have a large component of pyrite formed in an anoxic water column (open system), and some sulphide formed within the sediment (partially open system) and are thus isotopically lighter than pyrite from calcite-rich horizons which formed only within the sediment. Pyrite, from dolomite-rich horizons, is considered to be intermediate between these two extremes. One consequence of this model is that calcite formed within an oxic water layer and dolomite formed within an anoxic water column or in the area of the anoxic/oxic interface. Obviously some dolomite will form within the sediment during bacterial reduction of

sulphate, as has been indicated by Turner et al. (1978) and this may explain the spread of data in Figure 11.3. A model for Marl Slate deposition combining petrological, geochemical and isotope data will be presented in the next chapter.



## CHAPTER 12

### THE MARL SLATE : DISCUSSION AND CONCLUSIONS

#### 12.1 SUMMARY

In this chapter, data from the previous three chapters are reviewed, and used to propose a model for Marl Slate formation. Consequences of the proposed model are then briefly discussed in the context of potential base metal mineralization.

##### 12.1.1 Marl Slate Regional Setting and Petrography

By the mid-Permian, the Northern and Southern basins of the North Sea were already developed, and had subsided to a level approximately 250 m below open sea level. As a consequence of a world-wide rise in sea level, resulting from glacial melting, water breached the barrier with the Boreal ocean and flooded the Southern Permian basin (Smith, 1970b). The transgression was rapid, possibly taking as little as six years (Glennie, 1984), and probably aided by fracture systems induced during the late Carboniferous proto-Atlantic sea-floor spreading event. Some reworking of Rotliegendes sediments took place during the transgression. With time a stratified water column roughly 250 m deep at the basin centre developed and this had an anoxic base (Pompeckj, 1914, 1920; Brongersma-Sanders, 1966; and Gibbons, 1983).

A black sapropelic shale (the Marl Slate) was deposited. In the basin margin areas, the thickness of the Marl Slate reflects the topography of the underlying Rotliegendes, resulting in isopachyte trends (SW-NE) paralleling those of self-dune alignments (Turner et al. 1978). In general, the slightly siliceous sapropelic base of the Marl Slate gives way upwards to a well-laminated bituminous carbonate and finally to a massive dolostone. Several repetitions of this cycle may be present, and are not due to slumping (Magaritz and Turner, 1982). The alternating carbonaceous and carbonate-rich laminae in the Marl Slate are approximately 0.1 mm thick and were considered by Hirst and Dunham (1963) to represent annual layering. Oelsner (1959), on the same basis, had previously estimated a depositional time of 17,000 years for the Kupferschiefer. Füchtbaur (1972) has suggested that, if allowance is made for periods of non-deposition, the duration of Kupferschiefer sedimentation may have been as much as 60,000 years. In one of the cores studied in detail (Doncaster Core), the Marl Slate is succeeded by a zone (Transition Zone) of white carbonate (mainly calcite) grey carbonate (mainly dolomite) and sapropelic horizons intercalated on the centimetre scale. This Transition Zone core has proven to be an extremely useful indicator of the environmental conditions of Marl Slate deposition.



### 12.1.2 Geochemical Observations

The first published study of trace element concentrations in the Marl Slate was that of Deans (1950), who demonstrated the similarity in composition between the Kupferschiefer, the Marl Slate and black shales in general. In their work, Hirst and Dunham (1963) showed that Ni, Co and possibly Cu were associated with organic matter, while Zr and Rb were considered to be of detrital origin, Mn and Sr of marine origin and Pb and Zn possibly introduced via submarine springs. Turner et al. (1978) demonstrated a strong correlation between copper and quartz concentration, and suggested a detrital origin for that element. Based on isotopic evidence (negative  $\delta^{18}\text{O}$  spikes), Turner and Magaritz (in press) suggested that Cu and Zn were introduced by freshwater influx. In this study Mn, Sr, Ba and possibly Zn are shown to be of probable marine origin, the elements in fact substituting in the carbonate lattice. This may also be the case in the VT8 case, where Turner and Magaritz showed a much better correlation between these elements in the upper (carbonate-rich) part of the core. The remaining trace elements correlate (positively) to various degrees with quartz and  $\text{C}_{\text{org}}$  concentrations. This may reflect a detrital origin or may simply be a function of lithology or sedimentation rate. The lack of a positive correlation or, in the case of the Transition Zone Core, a strong antipathetic relationship between carbonate  $^{18}\text{O}$  depletion (used by Turner and Magaritz (in press) as being



indicative of a freshwater influx) and the detrital index elements (Zr, Ti, Rb) and quartz, suggests that freshwater influx was probably not the major source of base metals.

Variation in the concentration of trace elements with depth was first observed by Hirst and Dunham (1963). A copper-lead-zinc zonation was shown to exist (Turner et al., 1978; D4 core), which is the same as that described by Wedepohl (1964) and Jung and Knitzschki (1976) for the Kupferschiefer.

Further studies (Turner and Magaritz, in press; and this study) have shown that trends in base metal concentration as a function of depth do not correlate between boreholes, even when the boreholes are close together, (3 kms in the case of the VT8 and D4 cores of Turner and Magaritz). A number of other parameters vary between boreholes. Although overall isotopic trends are common to all boreholes, there are obvious local departures; also, the repetitions of lithology seen in the VT8 core by Magaritz and Turner (1982) have not been seen in other cores. This lack of correlation in various parameters between boreholes indicates the importance of local controls (notably the topography) on Marl Slate formation; it may even be that there were a number of separate but interconnected depositional basins.

The quartz content of the Marl Slate (Doncaster Core) varies between 7 and 19.6%, and is highest in the samples

nearer to the base. A similar trend was observed by Turner and Magaritz (in press), and probably reflects the incorporation of Rotliegendes quartz during the initial transgression. Samples from the Doncaster Core were systematically analysed for their proportion of calcite and dolomite. Within the Marl Slate section, the percentage dolomite in the carbonate phase is highly variable, but this also reflects lithological changes. In the Transition Zone section of the Doncaster Core, the percentage dolomite in the carbonate phase changes markedly with lithology, being 15% in the calcite-rich horizons, 80% in the sapropels and 92% in the dolomite-rich horizons.

Organic carbon versus pyrite sulphur plots for the Marl Slate section of the Doncaster Core and the sapropelic horizons of the Transition Zone core, have positive intercepts on the sulphur axis. The excess of  $S_{py}$  to  $C_{org}$  indicates that much of the pyrite formed in an anoxic water column (Leventhal, 1983).

The Degree of Pyritization (DOP) is a measure of the amount of iron available for pyrite formation. The value of 0.83 for the Marl Slate (Doncaster Core) is extremely high and implies that iron availability was a limiting control on pyrite formation. Within the Transition Zone core, the calcite-rich and sapropel horizons have high DOP values, while the dolomite-rich values are very low, showing that there was high iron availability during



pyrite growth in the dolomite horizons.

### 12.1.3 Isotopic Observations

Carbonates in the basal few centimetres of all the Marl Slate cores examined display a marked depletion in  $^{18}\text{O}$  and  $^{13}\text{C}$ . The  $^{13}\text{C}$  depletion is attributed to the incorporation into carbonates of isotopically light carbon derived from the oxidation of organic matter. The depletion in  $^{18}\text{O}$  reflects the non-marine composition of the early formation waters. Both of these features are consistent with the sedimentological evidence of a rapid and, in part, erosive transgression involving isotopically light water, much of which was derived from glacial melting.

Carbonates in all the cores studied are enriched in  $^{13}\text{C}$  relative to normal marine carbonates and display an upward (stratigraphic) trend towards continued  $^{13}\text{C}$  enrichment. This  $^{13}\text{C}$  enrichment is characteristic of the Permian period, and can be explained in terms of the world-wide balance in the carbon cycle, where burial of large amounts of organic matter 'locked-up' isotopically light carbon and the simultaneously produced carbonate was  $^{13}\text{C}$  enriched.

Previous workers (Marowsky, 1969; Magaritz and Turner, 1981) have noted that calcite-rich cores are depleted in  $^{13}\text{C}$  and  $^{18}\text{O}$  compared with dolomite-rich cores,



although no detailed data on the relative proportions of calcite and dolomite were given. In the Doncaster Core, the percentage dolomite in the carbonate phase was the most significant parameter to correlate with the  $\delta^{13}\text{C}$  and  $\delta^{18}\text{O}$  values. Least squares plots for the percentage dolomite in the carbonate phase and  $\delta^{13}\text{C}$  and  $\delta^{18}\text{O}$ , give fractionation factors between calcite and dolomite in agreement with recent experimental work. This strongly suggests that the calcite and dolomite in the Marl Slate (Doncaster Core) formed in equilibrium.

Sulphides from the Marl Slate are isotopically light, values in the range -30 per mil to -40 per mil being typical for pyrite. Using a mean seawater sulphate value of +11 per mil (Claypool et al., 1980) gives a fractionation factor of 44 per mil. This fractionation factor and the limited range of  $\delta^{34}\text{S}$  values are indicative of open system fractionation (Schwarz and Burnie, 1973) where there is an abundant sulphate reservoir.

Marowsky (1969) established that copper, lead and zinc sulphides within the Marl Slate are isotopically heavier than pyrite. Consequently, pyrite did not form in equilibrium with these sulphides since, in an equilibrium assemblage, pyrite should be the isotopically heavier sulphide phase.

The pyrite  $\delta^{34}\text{S}$  values display an upward enrichment

in  $^{34}\text{S}$  of approximately 15 per mil in the cores studied by Marowsky (1969) and about 8 per mil in this study. A change in fractionation factor to explain this variation is considered unlikely on sedimentological grounds, and can be effectively ruled out since Marowsky (1969) showed that sulphate  $\delta^{34}\text{S}$  values display a similar upward enrichment in  $^{34}\text{S}$ . The most likely explanation for the observed trend is the enrichment in  $^{34}\text{S}$  of a large but fixed size sulphate reservoir, as isotopically light sulphur is removed in precipitated sulphides.

Two pyrite samples from the Rotliegend, taken from about 1 cm below the base of the Marl Slate, yielded a mean  $\delta^{34}\text{S}$  value of -2.5 per mil, which is markedly different from those within the Marl Slate.

As with the Marl Slate, the  $\delta^{13}\text{C}$ ,  $\delta^{18}\text{O}$  and  $\delta^{34}\text{S}$  values in the Transition Zone core show a remarkable degree of lithological control, the calcite-rich horizons being the most depleted in  $^{13}\text{C}$  and  $^{18}\text{O}$  and the most enriched in  $^{34}\text{S}$ . The variation in isotope values with lithology are systematic, often large, and occur over a stratigraphic thickness of a few centimetres. This is convincing proof that the isotopic compositions and trends are a primary feature and have not been significantly altered by diagenetic, or later events.

The pyrite  $\delta^{34}\text{S}$  values for the calcite-rich and sapropelic horizons represent a fractionation of 29.6 per



mil and 43.7 per mil respectively, and probably correspond to a change from partially open system (calcite-rich) to open system (sapropel) fractionation. It is proposed that the pyrite  $\delta^{34}\text{S}$  values record the combined effects of fully open system fractionation for pyrite produced in the anoxic water column, and partially open system fractionation for pyrite produced within the sediment where pore-water and diffusion would supply the sulphate. Thus, sapropelic pyrite would have a component of sulphide formed within the anoxic water column (framboidal form) and a component formed within the sediment (euhedra and euhedral overgrowths) while, in the calcite-rich horizons, sulphide formation was limited to within the sediment.

#### 12.1.4 Textural and Compositional Observations

The deduced sulphide paragenetic sequence is: framboidal pyrite formation followed by euhedral pyrite formation, with euhedral overgrowths on framboids being a possible intermediate stage. The last sulphides to form were those of copper, lead and zinc. The small amounts of these sulphides in the cores studied did not allow a relative paragenetic age determination between them to be made. Turner et al. (1978) suggested that lead and zinc sulphides were early diagenetic pseudomorphs after sulphate. These sulphides would therefore have formed within the sediment and consequently would be paragenetically later than pyrite framboids which formed



dominantly in an anoxic water column. Confirmation that pyrite and the other base metal sulphides did not form in equilibrium and probably formed in different environments, was provided by the isotope data of Marowsky (1969). However, the sulphur isotope values found in this study suggest that the base metal sulphides, although not in isotopic equilibrium with the bulk of the pyrite (i.e. framboid), may have formed in equilibrium with the isotopically heavier euhedral pyrite.

Framboidal pyrite is by far the most abundant pyrite form in the Marl Slate and in the sapropelic horizons of the Transition Zone core. Within the calcite-rich horizons of the Transition Zone core, euhedral pyrite is by far the dominant pyrite form, while in the dolomite-rich horizons framboidal pyrite is more common than euhedral pyrite. Raiswell (1982) has shown that pyrite form is a function of iron availability, with low availability of iron favouring the formation of euhedral pyrite. Iron availability was thus low in the calcite-rich horizons of the Transition Zone core, as confirmed by its high DOP. The high percentage of framboidal pyrite in the sapropelic horizons suggests that iron availability in the sapropel was high, an apparent contradiction with the DOP value of 0.83. However, it must be remembered that the DOP value reflects the final availability of iron within a sediment, i.e. the end product of a number of ages of pyrite growth. It is probable that iron availability was high during framboidal pyrite formation,

but was reduced during subsequent sulphide formation resulting in the high DOP value observed.

These two factors (DOP and textural form) imply that euhedral and framboidal pyrite formed in different environments. It is suggested that pyrite framboid formation took place dominantly within the anoxic water column, while euhedral pyrite growth was restricted to formation within the sediment column.

Pyrite compositional differences are shown in Table 10.3. Two features are apparent: (a) All the pyrites analysed contain lead, with the higher concentrations being associated with pyrite from sapropelic horizons; (b) pyrites from sapropelic horizons contain significant amounts of Cu, Zn and Ni and, in addition, pyrite from the Transition Zone sapropel has high (up to 0.55%) concentrations of manganese. Pyrite from late cross-cutting veins is compositionally different from matrix pyrite in that it contains arsenic. A lateral secretion origin for vein pyrite is therefore not envisaged.

The intimate and fine scale of calcite and dolomite intergrowth meant that conventional staining techniques were not always successful in distinguishing between carbonate phases. Cathodoluminescence studies allowed the form of the calcite grains to be examined. Dolomite does not luminesce, probably as a consequence of its high iron content. It was observed that calcite from sapropelic



samples and, to a lesser extent, from the dolomite-rich horizons, was etched; whereas within the calcite-rich horizons, calcite formed euhedral crystals which were often zoned. This implies that the calcite and dolomite formed in differing environments, possibly at different levels within a stratified water column. The compositional differences between the calcite and dolomite phases, (particularly with respect to iron) and the consistency of composition of each phase, suggests that dolomite did not form by replacement of calcite. The micro- and macro-textural, and the isotopic data also substantiate this conclusion.

#### 12.1.5 Conclusions

One of the keys to understanding the Marl Slate depositional environment is a knowledge of the environmental parameters influencing the deposition of the different lithologies found within, and associated with the Marl Slate. In this respect, the Transition Zone section of the Doncaster Core has been extremely useful. The features characteristic of the different lithologies are summarised in Table 12.1. In the table the sapropelic horizons include both the Marl Slate and the sapropelic units of the Transition Zone core.

There are a number of features which appear to be common to all lithologies:-



- (a) All carbonate  $\delta^{13}\text{C}$  values are enriched in  $^{13}\text{C}$  with respect to marine carbonates.
- (b) Superimposed on the general  $^{13}\text{C}$  enrichment and the initial  $^{13}\text{C}$  and  $^{18}\text{O}$  depletion, the  $\delta^{18}\text{O}$  and  $\delta^{13}\text{C}$  values can be interpreted in terms of changes in carbonate mineralogy. There is some departure from a perfect correlation between percentage dolomite in the carbonate phase and  $\delta^{18}\text{O}$  and  $\delta^{13}\text{C}$  values. This is probably caused by later dolomite produced by:
- (i) late bacterial sulphate reduction associated with copper, lead and zinc formation;
  - (ii) the minor amounts of dolomite found associated with organic matter in calcite-rich horizons.
- (c) In all lithologies, and independent of the percentage dolomite in the carbonate phase, the compositions of calcite and dolomite remain remarkably constant.
- (d) There is no correlation between spikes of  $^{18}\text{O}$  depletion and an increase in sediment detrital components. This implies that there were no major periods of freshwater influx.

It is obvious from Table 12.1 that the calcite-rich and sapropelic horizons were formed in different environments, with the dolomite-rich horizons being intermediate between the two. Characteristic features indicate that the sapropelic sediments accumulated below an anoxic water-column (positive  $S_{py}$  intercept), with much pyrite forming within the anoxic layer. Within the anoxic water-column, pyrite framboids formed in an environment of high sulphate availability (large fractionation factor), and high iron availability (framboidal texture, DOP). Paragenetically later euhedral pyrite and minor amounts of copper and zinc sulphides 'mopped-up' the remaining available iron. The slight etching of calcite grains found in the sapropelic samples, implies that calcite was relatively unstable and was corroded in passing through the anoxic water layer. Calcite-rich sediments must have formed in the anoxic water layer which was relatively deficient in sulphate (negative  $S_{py}$  intercept, lower fractionation factor) and deficient in iron, during pyrite formation (pyrite form, DOP). In the calcite-rich horizons, pyrite formation must have taken place after sediment deposition. The sulphate reservoir was smaller (a combination of porewater-derived and diffusion-derived sulphate) than for sapropel framboid formation (open to seawater sulphate), as is reflected in the different  $\delta^{34}S$  values for the pyrites. The dolomite-rich sediments exhibit features intermediate between the sapropel and calcite-rich sediments, but must have had a very high availability of iron during pyrite formation, as evidenced



by the low DOP.

#### 12.2.1 PROPOSED MODEL FOR MARL SLATE FORMATION

The proposed model for Marl Slate deposition is shown in Figure 12.1A and B. The water column, during Marl Slate deposition, was stratified (as previously discussed) which resulted in the existence of two separate geochemical environments; one oxic and the other anoxic. The geochemical, sedimentological and mineralogical record of stratified lakes has been studied by a number of authors including Muller and Forstner (1973), Degens and Hecky (1974) and Degens and Ross (1974). In 1976, Degens and Stoffers (1976) showed that the oxic water layer in the Black Sea was characterised by the formation of calcite, mainly biogenic and euhedral forms. In East African lakes, the carbonate formed in oxic water layers can be manganese- or magnesium-rich (Degens and Hecky, 1974; Degens and Stoffers, 1976). It was shown by Brewer and Spencer (1974) that, in the Black Sea, the oxic/anoxic boundary is a zone of chemical anomaly (see Figure 12.2). Particulate manganese and iron reach peak concentrations just above the oxic/anoxic boundary, whereas the concentrations of dissolved manganese and iron reach peaks at or just below this boundary. The concentration of particulate manganese and iron is a consequence of the diffusion of these elements from the anoxic to the oxic water layer and their consequent fixation as oxides. A similar process is active in Lake



Kiva (Degens and Hecky, 1974), but carbonates form instead of oxides.

Until recently it has been generally accepted that dolomite formation requires a high  $Mg^{2+}/Ca^{2+}$  ratio (Folk and Land, 1975). However, dolomite has been found forming from pore fluids of low  $Mg^{2+}/Ca^{2+}$  ratio (Garrison et al, 1984). Recent experimental studies (Baker and Kastner, 1981) have shown that the essential condition for dolomite formation is not necessarily a high  $Mg^{2+}/Ca^{2+}$  ratio, but a low concentration of sulphate, and this has been confirmed by Gunatilaka et al. (1984). One consequence of this is that dolomite formation would be favoured in sites of sulphate reduction. Pyrite formation may commence at the top of the anoxic water layer, indeed Jannasch et al. (1974) have shown that two maxima of sulphate reduction occur, one near the top of the sediment layer and the other in the neighbourhood of the oxic/anoxic boundary. It is proposed here that dolomite formation could take place in a zone about the oxic/anoxic boundary, where the sulphate concentration would be lowered as a consequence of pyrite formation. This may also explain the high iron content of the dolomites. From the carbonate composition data, it is suggested that manganese migration was greater than iron, since all the carbonates analysed contain manganese. Dolomite would also form preferentially during sulphate reduction during diagenesis within the sediment.

Calcite formed in the oxic and dolomite formed in the

anoxic boundary layer on falling through the anoxic water column, would be unstable and liable to dissolution, as is found to be the case. The degree of etching would depend on the residence time within the anoxic layer and consequently on its thickness and on the sedimentation rate.

Sapropelic units are a result of sedimentation under an anoxic water column. Pyrite framboids form in the anoxic water in contact with a large sulphate reservoir (seawater) and will consequently be isotopically light. Although initially there would be high availability of iron (see Figure 12.1), this would decrease with depth below the oxic/anoxic boundary and would be least below the sediment/water interface. During sapropel formation, the anoxic water layer would be expected to be relatively thick. As a result, the preservation of carbonate would be lower in the sapropel ( $3.7\% C_{\text{carbonate}}$ ) than it would be in the case of sedimentation within the oxic (calcite-rich) or oxic/anoxic boundary (dolomite-rich) where the percentage  $C_{\text{carbonate}}$  is 10.3.

A change in sediment-type deposited at a locality would simply reflect oscillations in the oxic/anoxic boundary (see Figure 12.1B). A raising of the water level (b) would be reflected in the deposition of an organic-rich facies low in carbonate but with abundant sulphide. A lowering (c) in the water level would, depending on amount, result in the deposition of either iron-rich



dolomite with minor pyrite (framboidal and euhedral) or calcite-rich sediments with minor euhedral pyrite. The euhedral dolomite in both instances would form within the sediment during early diagenesis.

This model explains all the features discussed in section 12.1, and also the cyclicity of sedimentation seen in the Transition Zone core. Changes in water level could be caused by tectonic activity, evaporation (which would thin the oxic layer and promote calcite precipitation), inflow of normal marine or fresh-waters, or inflow of saline or cold waters over the mid-North Sea high.

### 12.3 IMPLICATIONS OF THE PROPOSED MODEL TO MARL SLATE MINERALISATION

Sulphide within the Marl Slate was formed as a consequence of bacterial reduction of sulphate. In the cores studied, there was abundant organic matter and an ample supply of sulphate for this process to proceed. Conditions ideal for sulphide formation probably occurred over most of the Zechstein Basin during Marl Slate deposition. However, textural evidence (euhedral pyrite forms) and the high Degree of Pyritization indicate that an inadequate supply of metal was the limiting control in sulphide formation within the sapropelic Marl Slate. Economic concentrations of sulphide will, therefore, only be found in areas associated with high metal input.



There are a number of potential sites of high base metal input, and these will now be discussed from a viewpoint of potential mineralising source;

(a) Detrital Input

A simple detrital origin for Marl Slate sulphide can be dismissed because of the form of pyrite (mainly framboidal and obviously not mechanically transported), and because of the large difference in isotopic composition of detrital pyrite found in the Rotliegend and the Marl Slate pyrite. A source of base metals adsorbed on clays or organic matter or in solution in freshwater influxes associated with detrital input, as suggested by Turner and Magaritz (in press), cannot be totally dismissed. Such a source is, however, thought unlikely, since there is no correlation between high detrital input and  $^{18}\text{O}$  depletion in carbonate phases as the model requires. Also, as pointed out by Richter-Bernburg (1941) with reference to the Kupferschiefer, it is unlikely that the denudation of the hinterland over such a short sedimentation period could explain the large concentration of accumulated metals.

(b) Marine Waters

Brongersma-Sanders (1965) suggested that upwelling along continental margins can result in currents rich in organic matter and base metals which, on precipitation,

can form sediments rich in metals and organic matter. Such a process would result in metal zonation roughly parallel to the palaeoshoreline, which is not found to be the case (Rentzsch, 1974). Also, Wedepohl (1964) has demonstrated that normal seawater is incapable of accounting for the base metal concentration of the Kupferschiefer, even allowing for reasonable amounts of water renewal.

(c) Magmatic (fault-controlled) Sources

Ekiert (1960) has shown that basic magmatic differentiates of Lower Permian age were copper-rich, and has suggested that metal-rich hydrothermal solutions emanating from these magmas could pass directly into marine waters. Alternatively, the hydrothermal fluids could be channelled along fault/fracture systems and be precipitated as sulphides in the vicinity of the Kupferschiefer sediments where hydrogen sulphide was present. The relative solubilities of the base metals would explain their vertical and lateral zonation. Hirst and Dunham (1963) have suggested submarine springs as the most likely source of copper, lead and zinc, with these metals being transported, adsorbed on organic matter in seawater. Harwood (1980) has implied that, if the source of metals was seawater-enriched due to rifting and vulcanism, then an even distribution of metals would be expected, which is clearly not the case.



However, this study has shown that conditions for metal precipitation as sulphide prevailed throughout the basin, and metal-rich solutions, debouched into the anoxic water layer or into the organic-rich sediment, would be rapidly precipitated as sulphides. An even distribution of metals would therefore not be expected. Moreover, recent studies on the first cycle Zechstein carbonate (Harwood and Smith, 1982) have shown that base metal mineral occurrences in this formation are coincident with the intersection of Permian (EZ1 Ca) outcrop and cross-cutting structures in the pre-Permian basement. The inference is that the pre-Permian basement structures may have acted as channels for mineralising solutions. No information (because of outcrop) is available on mineralisation in the underlying Marl Slate.

(d) Groundwaters

Areas of oxic leaching directly underlying the Kupferschiefer (Rote Fäule) and associated with areas of rich mineralisation, were described by Kautzsch (1942). It is generally agreed (Jung and Knitzschke, 1976) that the Rote Fäule represents areas of groundwater migration, and that the metal-rich zones were the product of an interaction between solutions of different Eh and pH; the metals being supplied by high Eh - low pH groundwaters and reacting with low Eh - high pH waters in the vicinity of the Kupferschiefer (or Marl Slate). The strong lateral mineral zonation, noted by Rentzsch (1974) around the Rote



Fäule, can then be explained in terms of changing Eh-pH conditions as groundwater travels into deeper parts of the basin.

It is not possible, from this study of the relatively unmineralised samples from the Marl Slate, to determine the source of base metals in the Marl Slate and Kupferschiefer. However, a combination of groundwater-derived and/or fault-controlled low temperature hydrothermal fluids of magmatic origin seems the most likely source of metals.

## REFERENCES

- Ali, A. D., and Turner, P., 1982. Authigenic K-feldspar in the Bromsgrove Sandstone Formation (Triassic) of central England. *Jour. Sed. Pet.*, V. 52, No. 1, p. 187-197.
- Anderson, A. T., 1967. The dimensions of oxygen isotope equilibrium attainment during prograde metamorphism. *Jour. Geol.*, V. 75, p. 323-332.
- Annels, A. E., 1974. Some aspects of the stratiform ore deposits on the Zambian Copperbelt and their genetic significance. In *Giese ment Stratiformes et Provinces Cupriferes*, Cent. Soc. Belg. Liege, p. 235-254.
- Annels, A. E., 1979. The genetic relevance of recent studies at Mufulira Mine, Zambia. *Ann. de la Soc. Geo. Belg.*, V. 102, p. 431-449.
- Annels, A. E., 1984. The Geotectonic environment of Zambian copper-cobalt mineralization. *Jour. Geol. Soc. Lond.*, V. 141, p. 279-289.
- Annels, A. E., and Simmonds, J. R., 1984. Cobalt in the Zambian Copperbelt. *Precamb. Res.*, V. 25, p. 75-98.
- Annels, A. E., Vaughan, D. J., and Craig, R. J., 1983. Conditions of ore mineral formation in certain Zambian Copperbelt deposits with special reference to the role of cobalt. *Min. Dep.*, V. 18, p. 71-88.
- Ashry, M. M., 1973. Occurrence of Li, B, Ca and Zn in some Egyptian sediments. *Geochim. Cosmochim. Acta.*, V. 37, p. 2449-2458.
- Baas Becking, L. G. M., Kaplan, I. R., and Moore, D., 1960. Limits of the natural environment in terms of pH and oxidation-reduction potentials. *Jour. Geol.*, V. 68, No. 3, p. 243-283.
- Bagnold, R. A., 1941. *The physics of blown sand and desert dunes*. Methuen, London.
- Baker, P. A., and Kastner, M., 1981. Constraints on the formation of sedimentary dolomite. *Science*, V. 213, p. 214-216.
- Baldwin, B., 1971. Ways of deciphering compacted sediments. *Jour. Sed. Pet.*, V. 41, p. 293-301.
- Barnes, S. J., and Sawyer, E. W., 1980. An alternative model for the Damaran mobile belt: ocean crust subduction and continental convergence. *Precamb. Res.*, V. 13, p. 297-336.



Barr, M. W. C., 1974. The pre Karroo geology of the Rufunsa area with special reference to structure and metamorphism. Unpub. Ph.D. Thesis, University of Leeds.

Barr, M. W. C., Cahen, L., and Ledent, D., 1978. Geochemistry of syntectonic granites from Central Zambia: Lusaka Granite and Granite, NE of Rufunsa. *Ann. de la Soc. Geol. Belg.* V. 100, p. 49-54.

Bartholome, P., 1974. On the diagenetic formation of ores in sedimentary beds, with special reference to the Komoto ore deposit. *Gisement Stratiformes et Provinces Cupriferes*, Cent. Soc. Belg. Liege, p. 203-214.

Bateman, A. M., 1930. Ores of the Northern Rhodesian Copperbelt. *Econ. Geol.*, V. 25, p. 365-418.

Bateman, A., and Jensen, M. L., 1956. Notes on the origin of the Rhodesian Copper deposits; Isotopic composition of the sulfides. *Econ. Geol.*, V. 51, p. 555-564.

Becker, R. M., and Clayton, R. N., 1976. Oxygen isotope study of the Precambrian Banded Iron formation, Hamersley Range, Western Australia. *Geochim. Cosmochim. Acta.*, V.40, p. 1153-1165.

Bell, J., Holden, T. H., Pettigrew, T. H., and Sedman, K. W., 1979. The Marl Slate and Basal Permian breccia at Middridge, Co. Durham. *Proc. Yorks. Geol. Soc.*, V. 42, P. 3, p. 439-460.

Benmore, R. A., 1983. Stable isotope and geochemical evidence for the origin of phosphorites. Unpub. Ph.D. Thesis, University of London.

Berner, R. A., 1970. Sedimentary pyrite formation. *Am. Jour. Sci.*, V. 268, p. 1-23.

Berner, R. A., 1982, Burial of organic carbon and pyrite sulphur in the modern ocean: its geochemical and environmental significance. *Am. Jour. Sci.*, V. 282, p. 451-473.

Berner, R. A., 1984. Sedimentary pyrite formation: An update. *Geochim. Cosmochim. Acta.*, V. 48, No. 4, p. 605-615.

Berner, R. A., and Raiswell, R., 1983. Burial of organic carbon and pyrite sulphur in sediments over Phanerozoic time: a new theory. *Geochim. Cosmochim. Acta.*, V. 47, p. 855-862.

Berner, R. A., and Raiswell, R., 1984. C/S method for distinguishing freshwater from marine rocks. *Geology*, V. 12, p. 365-368.



Binda, P. L., 1975. Detrital bornite in the Late Precambrian B greywacke of Mufulira Zambia. Min. Dep., V. 10, p. 101-107.

Binda, P. L., and Mulgrew, J. R., 1974. Stratigraphy of copper occurrences in the Zambian Copperbelt. Gisement Stratiformes et Provinces Cupiferes., Cent. Soc., Belg., Liege, p. 215-233.

Birnbaum, S. J., and Wireman, J. W., 1984. Bacterial sulfate reduction and pH: implications for early diagenesis. Chem. Geol., V. 43, p. 143-149.

Blatt, H., Middleton, G., and Murry, R., 1972. Origin of Sedimentary Rocks. Prentice-Hall.

Bluck, B. J., 1964. Sedimentation of an aluvial fan in southern Nevada. Jour. Sed. Petrol., V. 34, p. 395-400.

Bluck, B. J., 1967. Deposition of some Upper Old Red Sandstone conglomerates in the Clyde area: A study in the significance of bedding. Scott. Jour. of Geol., V. 3, p. 139-167.

Boles, J. R., and Franks, S. G., 1979. Clay diagenesis in the Wilcox sandstones of southwest Texas: implications of smectite diagenesis on sandstone cementation. Jour. Sed. Pet., V. 49, p. 55-70.

Bonhomme, M. G., and Bertrand-Sarfati, J., 1982. Correlation of Proterozoic sediments of Western and Central Africa and South America based upon radiochronological and palaeontological data. Precamb. Res., V. 18, p. 171-194.

Bottinga, Y. and Savoy, M., 1973. Comments on oxygen isotope geothermometry. Earth Planet Sci. Lett., V. 20, No. 2, p. 250-265.

Bowen, R., and Gunatilaka, A., 1977. Copper: its geology and economics. Applied Science Publishers, p. 267.

Brett, R., and Yund, R. A., 1964. Sulphur-rich bornites. Am. Mineralogist, V. 49, p. 1084-1097.

Brewer, P. G., and Spencer, D. W., 1974. Distribution of some trace elements in Black Sea and their flux between dissolved and particulate phases. In: The Black Sea; Geology, Chemistry and Biology. Eds.: E. T. Degens, and D. A. Ross, Am. Ass. Pet. Geol. Memoir 20, p. 137-143.

Briden, J. C., 1976. Applications of palaeomagnetism to Proterozoic tectonics. Phil. Trans. R. Soc., Lond., V. A280, p. 405-416.

- Brock, B. B., 1961. Structure - Chapter 4. In the Geology of the Northern Rhodesian Copperbelt. Edited by F. Mendlesohn, MacDonald, London.
- Brock, B. B., 1962. On the structure and sedimentation of the Katanga Basin. In J. Lombard and P. Nicolini (Eds.), Stratiform Copper Deposits in Africa, 2., Assoc. African Geol. Surv., Paris.
- Brock, B. B., 1972. A Global Approach to Geology. Balkema Press, Cape Town., p. 208.
- Brongersma-Sanders, M., 1966. Metals of Kupferschiefer supplied by normal sea water. Geol. Rundschav., V. 55, p. 365-375.
- Brown, A. C., 1971. Zoning in the White Pine copper deposit, Ontonagon County, Michigan. Eco. Geol., V. 66, p. 543-573.
- Brown, A. C., 1974. The copper province of Northern Michigan, U.S.A. Gisements Stratiformes et Provinces Cupriferes, Cent. Geol. Soc. Belg. Liege., p. 317-330.
- Brown, A. C., 1978. Stratiform copper deposits - evidence for their post sedimentary origin. Min. Sci. Eng., V. 10, No. 3, p. 172-181.
- Brown, A. C., 1981. The timing of mineralization in stratiform copper deposits. In: Handbook of Strar-bound and Stratiform Ore Deposits, Ed. K. H. Wolf, Elsevier, Amsterdam, p. 1-33.
- Brown, A. C., 1984. Alternative sources of metals for stratiform copper deposits. Precamb. Res., V. 25, p. 61-74.
- Brown, A. C., and Bartholomé, P., 1972. Inhomogenities in cobaltiferous pyrite from the Chibuluma Cu-Co Deposit, Zambia. Min. Dep., V. 7, p. 100-105.
- Brown, A. C., and Chartrand, F. M., 1983. Stratiform copper deposits and interactions with co-existing atmospheres, hydrospheres, biospheres and lithospheres. Precamb. Res., V. 20, p. 533-542.
- Bruce, C. H., 1984. Smectite dehydration - Its relation to structural development and hydrocarbon accumulation in Northern Gulf of Mexico Basin. Am. Assoc. Geol. Bull., V. 68, p. 673-683.
- Burst, J. F., 1959. Post diagenetic clay mineral environmental relationships in the Gulf Coast Eocene. Proc. 6th Natl. Conf. Clays and Clay Minerals, Pergamon Press, p. 327-331.



Burst, J. F., 1969. Diagenesis of Gulf Coast Clayey sediments and its possible relation to petroleum migration. *Am. Assoc. Petrol. Geol. Bull.*, v. 53, p. 73-93.

Cahen, L., 1974. Geological background to the copper-bearing strata of southern Shaba (Zaire). *Gisement Stratiformes et Provinces Cuprifères*, Cent. Soc. Belg. Liege, p. 57-77.

Cahen, L., Delhal, J., Grogler, N. and Pasteels, P., 1970a. The age of the Roan Antelope and Mufulira granites (Copperbelt of Zambia). *Ann. Mus. R. Afr. Centr. Tervuren, Belg.*, V. 8, No. 64, p. 15-37.

Cahen, L., Delhal, J., Ledent, D. and Pasteels, P., 1970b. Isotopic data relative to the age and petrogenesis of dome-forming granites in the Copperbelt of Zambia and S. E. Katanga. *Ann. Mus. R. Afr. Centr. Tervuren, Belg.*, V. 8, No. 65, p. 69-97.

Cahen, L., and Eberhardt, P., 1961. Recherches sur l'âge absolu des minéralisations uranifères du Katanga et de Rhodesie du Nord. *Ann. Mus. R. Afr. Centr. Tervuren, Belg.*, V. 8, No. 41, p. 1-53.

Cahen, L., and Snelling, N. J., 1984. The geochronology and evolution of Africa. Clarendon Press, Oxford.

Cahen, L., and Snelling, N. J., 1971. Données radiométriques nouvelles par la méthode potassium-argon. Existence d'une importante élévation post-tectonique de la température dans les couches Katangiennes du Sud du Katanga et du Copperbelt de la Zambia. *Ann. de la Soc. Geol. Belg.*, V. 94, p. 199-209.

Cailteux, J., 1974. Les sulfures du gisement cuprifère stratiforme de Musoshi, Shaba, Zaire. *Gisement Stratiformes et Provinces Cuprifères*, Cent. Soc. Belg. Liege, p. 267-276.

Carroll, D., 1960. Ilmenite alteration under reducing conditions in unconsolidated sediments. *Econ. Geol.* V.55, p. 618-619.

Carver, R. E., 1967. Procedures in sedimentary petrology. Wiley, Interscience, New York.

Chambers, A., and Trudinger, P. A., 1979. Microbiological formation of stable sulfur isotopes. A review and critique. *Geomicrobiology*, V. 1, p. 249-293.

Chrysosoulis, S., and Wilkinson, N., 1983. High silver content of fluid inclusions in quartz from Guadalcazar Granite, San Luis Potosi, Mexico; A contribution to ore genesis. *Econ. Geol.*, V. 79, p. 302-319.



Claypool, G. E., Holser, W. T., Kaplan, I. R., Sakai, H., and Zak, I., 1980. The age curves of sulphur and oxygen isotopes in marine sulphate and their mutual interpretation. *Chem. Geol.*, V. 28, p. 199-260.

Claypool, G., Presley, B. J., and Kaplan, I. R., 1973. Gas analysis in sediment samples from legs 10, 11, 13, 14, 15, 18 and 19. *Init. Rep. D.S.D.P.*, V. 19, p. 879-884.

Clayton, R., and Mayeda, T., 1963. The use of Bromine Pentafluoride in the extraction of Oxygen in Oxides and Silicates for isotopic analysis. *Geochim. Cosmochim. Acta.*, V. 27, p. 43-57.

Clemmey, H., 1978. Implications of recent copper sulphide placer concentration in Chile. *T.I.M.M.*, V. 87, p. B32.

Clemmey, H., 1976. Aspects of stratigraphy, sedimentology and ore genesis on the Zambian Copperbelt, with special reference to Rokana Mine. Unpub. Ph.D. Thesis, University of Leeds.

Clemmey, H., 1974a. Sedimentary geology of a late Precambrian copper deposit at Kitwe Zambia. *Gisement Stratiformes at Province Cupriferes*, *Cent. Geol. Soc. Belg. Liege*, p.255-265.

Clemmey, H., 1974b. Correlation of the coarse clastics formation (Footwall Formation) in the Chambishi-Nkana basin and Mufulira. *10th Ann. Rep. Res. Inst. African Geol.*, Leeds University, p. 24-29.

Cliff, R. A., and Clemmey, H., 1976. Rb-Sr age of pegmatitic muscovite from Mindola Mine, Zambian copperbelt. *Ann. Rep. Res. Inst. African Geol. Leeds University*, p. 68.

Clutten, J. M., 1974. Geological guide to Konkola Division. Unpub. Company Report, Z.C.C.M. Limited.

Cohen, C. J., 1939. Comprehensive report on Konkola. Referred to in *Sedimentology of the Feldspathic Quartzite - Nchanga Open Pit*. Southworth, C., Unpub. Company Report, Z.C.C.M. Limited, Chingola Division, 1980.

Coleman, M. L., 1980. Corrections for mass spectrometer analysis of SO<sub>2</sub>. *Stable Isotope Report 45*, Geochemistry and Petrology Division, British Geological Survey.

Coleman, M. L., 1977. Sulphur isotopes in petrology. *Jour. Geol. Soc. Lond.*, V. 133, P. 6, p. 593-608.

Coleman, M. L., and More, M. P., 1978. Direct reduction of sulphates to sulphur dioxide for isotopic analysis. *Anal. Chem.*, V. 50, p. 1594-1595.



Collinson, J., 1978a. Alluvial sediments. In *Sedimentary Facies and Environment*, Edited by H. Reading, Blackwell Scientific Publications.

Collinson, J., 1978b. Deserts. In *Sedimentary Environment and Facies*. Edited by H. Reading, Blackwell Scientific Publications.

Compston, W., 1960. The carbon isotope composition of certain marine invertebrates and coals from the Australian Permian. *Geochim. Cosmochim. Acta.*, V. 18, p. 1-22.

Coward, M. P., and Daly, M. C., 1984. Crustal lineaments and shear in Africa: Their relationships to plate movements. *Precamb. Res.*, V. 24, p. 27-45.

Craig, H., 1965. The measurement of oxygen isotope paleotemperatures. In *stable isotopes in oceanographic studies and paleotemperatures*. Consiglio Nazionale dell Ricerche, Pisa., p. 3-24.

Craig, H., 1957. Isotopic standards for carbon and oxygen correction factors for mass spectrometer analysis of  $\text{CO}_2$ . *Geochim. Cosmochim. Acta.*, V. 12, p. 133-149.

Craig, H., 1953. The geochemistry of the stable carbon isotopes. *Geochim. Cosmochim. Acta.*, V. 3, p. 53-92.

Craig, J. R., Vaughan, D. J., and Higgins, J. B., 1979. Phase relations in the Cu-Co-S system and mineral associations of the carrollite ( $\text{CuCO}_2\text{S}_4$ ) - Linnaeite ( $\text{Co}_3\text{S}_4$ ) series. *Eco. Geol.*, V. 74, p. 657-671.

Crawford, M. L., 1981. Fluid inclusions in metamorphic rocks - Low and medium grade. In *short course in Fluid Inclusions, Applications to Petrology*, Edited by L. S. Hollister and M. L. Crawford, Min. Assoc. Canada, p. 157-176.

Curtis, C. D., 1978. Possible links between sandstone diagenesis and depth-related geochemical reactions occurring in enclosing mudstones. *Jour. Geol. Soc. Lond.*, V. 135, p. 107-119.

Curtis, C. D., 1977. Sedimentary geochemistry: environments and processes dominated by involvement of an aqueous phase. *Phil. Trans. R. Soc. London*, V. A286, p. 353-371.

Dana, E. S., 1951. The system of mineralogy. Vol. 2. John Wiley and Sons, p. 254.

Dansgaard, W., 1964. Stable isotopes in precipitation. *Tellus*, V. 16, p. 436-468.



Dawson, A. L., 1977. Notes on references to the geochemistry and mineralogy of Copperbelt rocks and ores. Unpub. Company Report No. PD/GC/77/09. R.C.M. Ltd.

Darnley, A. G., 1960. Petrology of some Rhodesian Copperbelt orebodies and associated rocks. T.I.M.M., V. 69, p. 137-173.

Darnley, A. G., and Killingworth, P. J., 1962. Identification of carrollite from Chibuluma by X-ray scanning microanalyser. T.I.M.M., V. 72, p. 165-167.

Davidson, C. F., 1962. On the Co:Ni ratio in ore deposits. Min. Mag., V. 106, p. 78-85.

Davies, G. R., 1977. Former magnesian calcite and aragonite submarine cement in upper Palaeozoic reefs of the Canadian Arctic. A Summary. Geology, V. 5, p. 11-15.

Davis, J. B., and Kirkland, B. W., 1970. Native sulphur deposition in the Castile formation, Gulberson County, Texas. Econ. Geol., V. 65, p. 107-117.

Deans, T., 1950. The Kupferschiefer and the associated lead-zinc mineralization in the Permian of Silesia, Germany and England. Rept. XVIII Int. Geol. Cong., V. 7, p. 340-352.

Dechow, E., and Jensen, M. L., 1965. Sulphur isotopes of some central African sulphide deposits. Eco. Geol., V. 60, p. 894-941.

Deer, W. A., Howie, R. A., and Zussman, J., 1977. An introduction to the rock forming minerals. Longman, p.14.

Degens, E. T., and Stoffers, P., 1976. Stratified waters as a key to the past. Nature, Vol. 263, p. 22-27.

Degens, E. T., and Hecky, R. E., 1974. Paleoclimatic reconstruction of late pleistocene and Molocene based on biogenic sediments from the Black Sea and a tropical African Lake. Colloqu. Int. C.N.R.S., V. 219, p. 13-24.

Degens, E. T. and Ross, D. A., 1974. The Black Sea: Geology, Chemistry and Biology. Am. Assoc. Pet. Geol. Mem. 20.

Degens, E. T. and Epstein, S., 1964. Oxygen and carbon isotope ratios in coexisting calcites and dolomites from recent and ancient sediments. Geochim. Cosmochim. Acta., V. 28, p. 23-44.

Deines, P., 1970. Mass spectrometer correction factors for the determination of small isotopic variations of carbon and oxygen. Int. J. Mass. Spectron. Ion. Phys., V. 4, p. 283-295.



Demaison, G. J., and Moore, G. T., 1980. Anoxic environments and oil source bed genesis. Am. Assoc. Petrol. Geol. Bull., V. 64, p. 1179-1208.

Dhannoun, H. Y., and Fyfe, W. S., 1972. Reaction rates of hydrocarbons and anhydrite. Progr. Exper. Petrol., N.E.R.C. Publ. Ser. D., p. 69-71.

Diederix, D., 1977. The geology of the Nchanga Mining Licence Area. Unpub. Company Report, Z.C.C.M. Limited.

Dimanche, F., and Bartholomé, P., 1976. The alteration of ilmenite in sediments. Min. Sci. Eng., V. 8, No. 3, p. 187-202.

Drysdall, A. R., Johnson, R. L., Moore, T. A., and Thieme, J. G., 1972. Outline of the geology of Zambia. Geol. Mijnbouw., V. 50, p. 265-276.

Duncumb, P., and Reed, S. J. B., 1968. Quantitative electron probe micro-analysis. N.B.S. Spec., Pub. 298, p. 133-154.

Eames, T. D., 1975. Coal rank and gas source relationships - Rotliegendes reservoirs. In: Petroleum and the Continental Shelf of North-West Europe, Edited by M. R. Brookfield, App. Sci., Pub. Barking, P. 191-201.

Eckelmann, W. R., Broecker, W. S., Whitlock, D. W., and Allsup, J. R., 1962. Implications of carbon isotope composition of total organic carbon of some recent sediments and ancient oils. Am. Assoc. Petrol. Geol. Bull., V. 46, p. 699-704.

Ekiert, F., 1960. Neue Anschauungen über die Herkunft des in den Sedimenten des Unteren Zechsteins auftretenden Kupfers. Freiberg. Forschungsh., C. 79, p. 190-201.

Emrich, K., Ehhalt, D. H., and Vogel, J. C., 1970. Carbon isotope fractionation during the precipitation of calcium carbonate. Earth Planet Sci. Lett., V. 8, p. 363-371.

Engel, A. E. J., Itson, S. D., Engel, C. G., Stickney, D. M., and Cray, E. J., 1974. Crystal evolution and global tectonics: A petrographic view. Bull. Geol. Soc. Am., V. 85, p. 843-858.

Epstein, S., and Maydea, T. K., 1953. Variations of the  $^{18}\text{O}/^{16}\text{O}$  ratio in natural waters. Geochim. Cosmochim. Acta., V. 4, p. 213-221.

Epstein, S., Graf, D. L., and Degens, E. T., 1963. Oxygen isotope studies on the origin of dolomites. In Isotopic and Cosmic Chemistry, Edited by H. Craig, G. J. Wasserburg and S. L. Miller, North Holland, p. 169-180.



Fairchild, I. J., 1983. Chemical controls of cathodoluminescence of natural dolomites and calcites: new data and review. *Sedimentology*, V. 30, p. 579-583.

Faure, G., 1977. Chapter 20, Carbon. In *Principles of Isotope Geology*, John Wiley and Sons, p. 379-380.

Fleischer, V. D., Garlick, W. G., and Haldane, R., 1976. Geology of the Zambian Copperbelt. In: *Handbook of Strata-bound and stratiform ore deposits*. Ed. K. H. Wolf., Elsevier Sci. Pub. Co. Amsterdam, p. 223-352.

Folk, R. L., and Land, L. S., 1975. Mg/Ca ratio and salinity, two controls over crystallization of dolomite. *Am. Assoc. Petrol. Geol. Bull.* V. 59, p. 60-68.

Folk, R. L., and Pittman, J. S., 1971. Length slow chalcedony: a new testament for vanished evaporites. *Jour. Sed. Pet.*, V. 41, p. 1045-1058.

Francois, A., 1974. Stratigraphic, tectonique et mineralisation dans l'arc cuprifere du Shaba (Republique du Zaire). *Gisements Stratiformes et Provinces Cupriferes*, Cent. Soc. Belg. Liege, p. 79-101.

Friedman, G. M., 1975. The making and unmaking of limestones and the downs and ups of porosity. *Jour. Sed. Pet.*, V. 45, p. 379-398.

Friedman, I., and Hall, W. A., 1963. Fractionation of  $^{18}\text{O}/^{16}\text{O}$  between coexisting calcite and dolomite. *Jour. Geol.*, V. 71, p. 238-243.

Fritz, P., and Smith, D., 1970. The isotopic composition of secondary dolomite. *Geochim. Cosmochim. Acta.*, V. 34, p. 1161-1173.

Froelich, P. N., Klinkhammer, G. P., Bender, M. L., Luedtke, N. A., Heath, G. R., Cullen, D., Dauphin, P., Hammond, D., Hartman, B. and Maynard, V., 1979. Early oxidation of organic matter in pelagic sediments of the eastern equatorial Atlantic: Suboxic Diagenesis. *Geochim. Cosmochim. Acta.*, V. 43, p. 1075-1090.

Fuchtbauer, H., 1972. Carbonate sedimentation and subsidence in the Zechstein basin (Northern Germany). In: *Recent Developments in Carbonate Sedimentology in Central Europe*. Editors: G. Muller and G. M. Friedman, Springer, Berlin, p. 196-204.

Garlick, W. G., 1981. Sabkhas, slumping and compaction at Mufulira, Zambia. *Eco. Geol.*, V. 76, p. 1817-1847.



Garlick, W. G., 1972. Sedimentary environment of Zambian Copper deposition. *Geologie en Mijnbouw.*, V. 51, No. 3, p. 271-289.

Garlick, W. G., 1967. Special features and sedimentary facies of stratiform sulphide deposits in arenites. *Proc. 15th Inter. Univ. Geol. Cong. Leicester*, p. 107-169.

Garlick, W. G., 1964. Criteria for recognition of syngenetic sedimentary mineral deposits and veins formed by their remobilisation. *Proc. Aust. Inst. Min. Met.*, p. 1-25.

Garlick, W. G., 1961. In the geology of the Northern Rhodesian Copperbelt. Edited by F. Mendelsohn. MacDonal and Co., London.

Garlick, W. G., and Brummer, J. J., 1951. The age of the granites of the Northern Rhodesian Copperbelt. *Econ. Geol.*, V. 46, p. 478-497.

Garlick, W. G., and Fleischer, V. D., 1972. Sedimentary environment of Zambian copper deposition. *Geologie en Mijnbouw.*, V. 51, No. 3, p. 277-299.

Garrard, P., 1972. The geology of the Chingola Area, Zambia. Unpub. Ph.D. Thesis, University of London, Imperial College.

Garrard, P., 1965. Chingola, Kalulushi and Ndola (Rural) Districts, Chingola Sheet. *Ann. Rep. for 1964, Geol. Surv. Zambia*, p. 2-3.

Garrels, R. M., and Christ, C. L., 1965. Minerals, solutions and equilibria. Pub. Harper and Row, New York.

Garrels, R. M., and Lerman, A., 1981. Phanerozoic cycles of sedimentary carbon and sulphur. *Proc. Natl. Acad. Sci.*, V. 78, p. 4652-4656.

Garrison, R. E., Kastner, M., and Zenger, D. H., 1984. Dolomites of the Monterey Formation and other organic rich units. *Soc. Econ. Paleontol. Min. Pract. Sect. Spec. Pub.*

Gat, J. R., 1971. Comments on the stable isotope method in regional ground water investigation. *Water Resour. Res.*, V. 7, p. 980-991.

Gibbs, R. J., 1973. Mechanisms of trace metal transport in rivers. *Science*, Vol. 180, p. 71-73.

Gibbons, M. J., 1983. The depositional environment and petroleum geochemistry of the Marl Slate - Kupferschiefer. Abstract from Marine Petroleum Source Rocks Conf., Burlington House, May 1983.



- Glennie, K. W., 1984. The structural framework and pre-Permian history of the North Sea. In: Introduction to Petroleum Geology of the North Sea, Edited by K. W. Glennie, Blackwell Sci. Pub., p. 17-39.
- Glennie, K. W., 1982. Early Permian (Rotliegendes) palaeowinds of the North Sea. Sed. Geol., V. 34, p. 245-265.
- Glennie, K. W., 1972. Permian Rotliegendes of North-West Europe interpreted in light of modern desert sedimentation studies. Am. Assoc. Petrol. Geol. Bull., V. 56, p. 1048-1071.
- Glennie, K. W., and Buller, A. T., 1983. The Permian Weisslied of N. W. Europe: the partial deformation of aeolian dune sands caused by the Zechstein transgression. Sed. Geol., V. 35, p. 43-81.
- Goldharber, M. B., and Kaplan, I. R., 1974. The sulphur cycle: In the sea. Edited by E. D. Goldberg. John Wiley and Son, V. 5, p. 569-655,
- Goldrich, S. S., 1938. A study in rock weathering. Jour. Geol., V. 46., p. 17-58.
- Goreau, T. J., 1977. Seasonal variations of coral skeletal chemistry, physiological and environmental controls of stable isotopes and trace metals in *Monopastrea amularis*. Proc. Royal. Soc. Lond., V. B196, No. 1124, p. 291-315.
- Gunatilaka, A., Saleh, A., Al-Temmami, A., and Nassar, N., 1984. Occurrence of subtidal dolomite in a hypersaline lagoon, Kuwait. Nature, V. 311, p. 450-452.
- Hall, A. J., 1982. Gypsum as a precursor to pyrrhotite in metamorphic rocks. Min. Dep., V. 17, p. 401-409.
- Harrison, A. G., and Thode, H. G., 1957. The kinetic isotope effect in the chemical reduction of sulphate. Trans. Faraday Soc., V. 53, p. 1648-1651.
- Hartmann, M., and Nielsen, H., 1969.  $\delta^{34}\text{S}$  Werts in rezenten Meeressedimenten und ihre Deutung am Beispiel einiger sedimentprofile ausder westlichen Ostsee. Geol. Rundschau, V. 58, p. 612-655.
- Hartnady, C. J., 1978. Tectonic evolution of the south eastern part of the Hakos-Auas Mountain zone in the Damara Orogenic Belt. 14th and 15th Ann. Rep. Precamb. Res. Unit. Univ. Cape Town, p. 171-182.
- Harwood, G. M., 1980. Calcitized anhydrite and associated sulphides in the English Zechstein First Cycle Carbonate (EZ1 Ca). Contr. Sedimentology, No. 9, p. 61-72.



Harwood, G. M., and Smith, F. W., 1982. Mineralization in Permian carbonates of the Yorkshire Province. English Zechstein 82 Conf. Abstract, Nottingham.

Haynes, S. J., and Mostaghel, M. A., 1982. Present day precipitation of lead and zinc from groundwaters. Min. Dep., V. 17, p. 213-228.

Heggie, D., and Lewis, T., 1984. Cobalt in pore waters of marine sediments. Nature, V. 311, p. 453-454.

Hickman, A. C. J., 1974. Polyphase deformation at Luanshya Mine. Rep. Geol. Surv. Zambia, No. 12.

Hirst, D. M. and Dunham, K. C., 1963. Chemistry and petrography of the Marl Slate of S. E. Durham, England. Econ. Geol., V. 58, p. 912-940.

Hoefs, J., 1980. Stable isotope geochemistry. Springer-Verlag, Berlin.

Holser, W. T., 1979. Rotliegendes Evaporites, Lower Permian of Northwestern Europe. Erdöl und Kohle und Erdgas petrochemie, V. 32, P. 4, p. 159-162.

Holser, W. T., 1977. Catastrophic chemical events in the history of the ocean. Nature, V. 267, p. 403-408.

Holser, W. T., and Kaplan, J. R., 1966. Isotope geochemistry of sedimentary sulphates. Chem. Geol., V. 1, p. 93-135.

Hower, J., Eslinger, E. V., Hower, M. E., and Perry, E. A., 1976. Mechanism of burial metamorphism of argillaceous sediment 1: Mineralogic and chemical evidence. Bull. Geol. Soc. Am., V. 78, p. 1125-1136.

Hubert, J., and Reed, A., 1978. Red bed diagenesis in the East Berlin Formation, Newark Group, Connecticut Valley. Jour. Sed. Pet., V. 48, p. 175-184.

Hudson, J. D., 1977. Stable isotopes and limestone lithification. Jour. Geol. Soc. Lond., V. 133, p. 637-660.

Irwin, H., 1979. Isotopic analysis of organic material from the Kimmeridge Clay. Stable Isotope Unit, Stable Isotope Report No. 32, Geochemistry and Petrology Division, British Geological Survey.

Irwin, H., 1978. Isotopic analysis of pyrite from the Kimmeridge Clay. Stable Isotope Unit, Stable Isotope Report No. 31, Geochemistry and Petrology Division, British Geological Survey.

Irwin, H., Curtis, C. D., and Coleman, M. L., 1977. Isotopic evidence for the source of diagenetic carbonates formed during burial of organic-rich sediments. *Nature*, V. 269, p. 209-213.

Jannasch, H. W., Truper, H. G., and Tuttle, J. H., 1974. Microbial sulfur cycle in Black Sea. In: *The Black Sea; Geology, Chemistry and Biology*. Eds. E. T. Degens and D. A. Ross, *Am. Ass. Pet. Geol. Memoir* 20, p. 419-425.

Jensen, M. L., and Dechow, E., 1962. The bearing of sulphur isotopes on the origin of the Rhodesian copper deposits. *Trans. Geol. Soc. S. Afr.*, V. 65, P. 1, p. 2-17.

Jolly, J. L. W., 1972. Recent contributions to Copperbelt geochemistry. *Geol. Mijnbouw.*, V. 51, p. 329-337.

Jordaan, J., 1961. Nkana. In *the Geology of the Northern Rhodesian Copperbelt*. Edited by F. Mendelsohn, MacDonald, London.

Jørgensen, B. B., 1978. A comparison of methods for the quantification of bacterial sulphate reduction in coastal marine sediments III. Estimation from chemical and bacteriological field data. *Geomicrobiol. J.*, V. 1, p. 49-64.

Jung, W., and Knitzschke, G., 1976. Kupferschiefer in the German Democratic Republic (GDR) with special reference to the Kupferschiefer deposits in the Southeast Harz Foreland. In: *Handbook of Stratabound and Stratiform Ore Deposits*, Ed. K. H. Wolf, Elsevier, Amsterdam.

Kaplan, I. R., Emery, K. O., and Rittenberg, S. C., 1963. The distribution and isotopic abundance of sulfur in recent sediments off southern California. *Geochim. Cosmochim. Acta.*, V. 27, p. 297-331.

Kaplan, I. R., and Rittenberg, S. C., 1964. Microbiological fractionation of sulfur isotopes. *Jour. Gen. Microbiol.*, V. 34, p. 195-212.

Kastner, M., 1971. Authigenic feldspar in carbonate rocks. *Am. Mineralogist*, V. 56, p. 1403-1442.

Kastner, M., and Siever, R., 1979. Low temperature feldspars in sedimentary rocks. *Am. Jour. Sci.*, V. 279, p. 435-479.

Katz, A., and Mathews, A., 1977. The dolomitization of  $\text{CaCO}_3$ , an experimental study at 252-259°C. *Geochim. Cosmochim. Acta.*, V. 51, p. 297-308.



Kautzsch, E., 1942. Untersuchungsergebnisse über die Meallverteilung im Kupferschiefer. Arch. Lagerst-Forsch. H74, 425, Berlin.

Keith, M. L., and Weber, J. N., 1964. Carbon and oxygen isotope composition of selected limestones and fossils. Geochim. Cosmochim. Acta., V. 32, p. 71-91.

Kemp, A. L. W., and Thode, H. G., 1968. The mechanism of the bacterial reduction of sulfate and sulfide from isotope fractionation studies. Geochim. Cosmochim. Acta., V. 32, p. 71-91.

Kent, P. E., 1981. The history of the North Atlantic margin in a world setting. In: Geology of the North Atlantic borderlands, Canadian Society of Petroleum Geologists, Memoir 7, p. 1-10.

Kessler, L. G., 1978. Diagenetic sequence in ancient sandstones deposited under desert climatic conditions. J. Geol. Soc. Lond., V. 135, p. 41-51.

Kinsman, D. J. J., 1966. Gypsum and anhydrite of recent age, Trucial Coast, Persian Gulf. In: Second Symp. on Salt., Edited by J. L. Rau, No. Ohio. Geol. Soc. Cleveland, Ohio, p. 302-326.

Kirkland, D. W., and Evans, R., 1976. Origin of limestone Buttes, Gypsum Plain, Culberson County, Texas. Am. Assoc. Petrol. Geol. Bull., V. 60, p. 2005-2018.

Knauth, L. P., and Epstein, S., 1976. Hydrogen and oxygen isotope ratios in nodular and bedded charts. Geochim. Cosmochim. Acta., V. 40, p. 1095-1108.

Korowski, S. P., 1978. Mineralogical, petrological and chemical investigations of 67 Chibuluma East drillcore samples. Unpub. Company Report No. RDK/112/78, R.C.M. Limited.

Kroner, A., 1977. Precambrian mobile belts of Southern and Eastern Africa - ancient sutures or sites of ensialic mobility? A case for crustal evolution towards plate tectonics. Tectonophysics, V. 40, p. 101-135.

Kroner, A., 1976. Proterozoic crustal evolution in parts of Southern Africa and the evidence for extensive sialic crust since the end of the Archaean. Phil. Trans. R. Soc. Lond., V. 280, p. 541-565.

Kruelen, R., 1980. CO<sub>2</sub> rich fluids during regional metamorphism on Naxos (Greece), carbon isotopes and fluid inclusions. Am. Jour. Sci., V. 280, p. 745-771.

Lambert, I. B., Donnelly, T. H., and Rowlands, N. J., 1984. Genesis of Late Proterozoic Copper Mineralisation, Copper Claim, South Australia. *Eco. Geol.*, V. 79, p. 461-476.

Lambert, I. B., Donnelly, T. H., and Rowlands, N. J., 1980. Genesis of Upper Proterozoic stratbound copper mineralisation, Kapunda, South Australia. *Min. Dep.*, V. 15, p. 1-18.

Land, L. S., 1973. Contemporaneous dolomitization of Middle Pleistocene reefs by meteoric water; North Jamaica. *Bull. Marine Science*, V. 23, p. 64-92.

Leith, M. J. and Rowsell, D.M., 1979. Burial history and temperature depth conditions for hydrocarbon generation and migration on the Agulhas Bank, South Africa. *Geol. Soc. S. Af. Spec. Pub.* 6, p. 205-217.

Leventhal, J. S., 1983. An interpretation of carbon and sulfur relationships in Black Sea sediments as indicators of environments of deposition. *Geochim. Cosmochim. Acta.*, V. 47, p. 133-137.

Link, M. H., and Osborne, R. H., 1978. Lacustrine facies in the Pliocene Ridge Basin Group: Ridge Basin California. In: *Modern and Ancient Lake Sediments*, Eds. A. Matter and M. Tucker, Blackwell Scientific Press, p. 167-185.

Luther, G. W., Meyerson, A. L., Krajewski, J. J., and Hires, R., 1980. Metal sulfides in estuarine sediments. *Jour. Sed. Pet.*, V. 50, No. 4, p. 1117-1120.

Magaritz, M., Anderson, R.Y., Holser, W. T., Saltzman, E. S., and Garber, J., 1983. Isotope shifts in the late Permian of the Delaware Basin, Texas, precisely timed by varved sediments. *Earth Planet Sci. Lett.*, V. 66, p. 111-124.

Magaritz, M., and Turner, P., 1981. Carbon isotope change at the base of the Upper Permian Zechstein sequence. *Geol. Jour.*, V. 16, p. 243-254.

Magaritz, M., and Schulze, K. H., 1980. Carbon isotope anomaly of the Permian period. In: *The Zechstein Basin of Europe*, Eds. Fuchtbauer, H. and Peryt, T., Cont. Sedimentology, Schweizerburtische Verlagsbuch, Stuttgart, p. 269-277.

Magaritz, M., and Turner, P., 1982. Carbon cycle changes of the Zechstein Sea: isotopic transition zone in the Marl Slate. *Nature*. V. 297, No. 5865, p. 389-390.



- Magaritz, M., Turner, P., and Kåding, K. C., 1981. Carbon isotope change at the base of the Upper Permian Zechstein sequence. *Geol. Jour.*, V. 16, p. 243-254.
- Marowsky, G., 1969. Schwefel-Kohlenstoff, und Sauerstoff-Isotopenuntersuchungen am Kupferschiefer als Beitrag zur genetischen Deutung. *Contr. Min. Pet.*, V. 22, p. 290-333.
- Mason, C. F., 1968. Footwall development at No. 1 Shaft. Unpub. Company Report, Z.C.C.M. Limited, Konkola Division.
- Mathews, A., and Katz, A., 1977. Oxygen isotope fractionation during dolomitization of calcium carbonate. *Geochim. Cosmochim. Acta.*, V. 41, p. 1431-1438.
- Maynard, J. B., 1980. Sulphur isotopes of iron sulphides in Devonian-Mississippian shales of the Appalachian basin: control by rate of sedimentation. *Am. Jour. Sci.*, V. 280, p. 772-786.
- Mendelsohn, F., 1961. The Geology of the Northern Rhodesian Copperbelt. MacDonald, London.
- Mulgrew, J. R., 1968. Recent information on the stratigraphy of the rocks of the Katanga System, derived from drilling in the area between Bancroft and Konkola. Unpub. Company Report, Z.C.C.M. Limited, Konkola Division.
- Muller, G., and Forstner, U., 1973. Recent iron ore formation in Lake Malawi, Africa. *Min. Dep.* V. 8, p. 278-290.
- Murray, J. W., 1975. The interaction of cobalt with hydrous-manganese dioxide. *Geochim. Cosmochim. Acta.*, V. 39, p. 635-642.
- MacGregor, J. A., 1964. The Lumwana Copper deposit in Zambia. Unpub. Ph.D. Thesis, Rhodes University, S. Africa.
- McCrea, J. M., 1950. The isotopic chemistry of carbonates and a paleotemperature scale. *Jour. Chem. Phys.*, V. 18, p. 849-857.
- McCready, R. G. L., Kaplan, I. R., and Din, G. A., 1974. Fractionation of sulfur isotopes by the yeast *Saccharomyces cerevisiae*. *Geochim. Cosmochim. Acta.*, V. 38, p. 1239-1253.
- McGowen, J. H., and Groat, C. G., 1971. Van Horn Sandstone: an alluvial fan model for mineral exploration. Report of Investigations, V. 72, p. 57. Bureau of Eco. Geol., Univ. of Texas, Austin.



- McKinnon, D. and Smit, N. J., 1961. Nchanga. In the Geology of the Northern Rhodesian Copperbelt. Edited by F. Mendlesohn. MacDonald, London.
- McWilliams, M. O. and Kröner, A., 1981. Paleomagnetism and tectonic evolution of the Pan-African Damaran Belt, Southern Africa. Jour. Geophys. Res., V. 86, p. 5147-5162.
- Naish, E. J. H., 1973. The pattern of sedimentation in the Ore Shale formation at Z.C.C.M. Limited - Konkola Division. Unpub. Company Report, Z.C.C.M. Limited, Konkola Division.
- Naish, E. J. H., 1972. Paleogeographic reconstruction of the Kirila Bombwe Area relating to Ore Shale sedimentation. Unpub. Company Report, Z.C.C.M. Limited, Konkola Division.
- Nakai, N., and Jensen, M. L., 1964. The kinetic isotope effect in the bacterial reduction and oxidation of sulfur. Geochim. Cosmochim. Acta., V. 28, p. 1893-1912.
- Nemec, W., and Poreski, S. J., 1977. Weissleigendes Sandstones: A transition from fluvial-aeolian to shallow marine sedimentation (Permian of the Fore-Sudetic Monocline). Ann. Geol. Soc. Pol., V. 47, p. 513-544.
- Newberg, D. W., 1967. Geochemical implications of chrysocolla bearing alluvial gravels. Econ. Geol., V. 62, p. 932-956.
- Nickel, E., 1978. The present status of cathodeluminescence as a tool in sedimentology. Min. Sci. Eng., V. 10, No. 2, p. 73-100.
- Nilsen, T. H., 1982. Alluvial Fan Deposits. In Sandstone Depositional Environments, Ed. P. A. Scholle and D. Spearing, A.A.P.G., Memoir 31.
- Nissenbaum, A., Presley, J. B., and Kaplan, I. R., 1972. Early diagenesis in a reducing fjord, Saanich inlet, British Columbia. Geochim. Cosmochim. Acta., V. 36, p. 1007-1027.
- Northrop, D. A., and Clayton, R. N., 1966. Oxygen isotope fractionation in systems containing dolomite. Jour. Geol., V. 74, p. 174-196.
- Oelsner, O., 1959. Bemerkungen zur Herkunft der Metalle in Kupferschiefer. Freiberg Forschungsh., V. C, 58, p. 106-113.
- Ohmoto, H., 1972. Systematics of sulphur and carbon isotopes in hydrothermal ore deposits. Econ. Geol., V. 67, p. 551-578.



- Ohmoto, H., and Rye, R. O., 1974. Hydrogen and oxygen isotopic compositions of fluid inclusions in the Kuroko Deposits Japan. *Eco. Geol.*, V. 69, p. 947-953.
- Osaki, S., 1973. Carbon and oxygen isotopic composition of Tertiary and Permian dolomite in Japan. *Geochem. Jour.*, V. 6., p. 463-477.
- Oszczepalski, S., 1982. Copper shale of southwestern Poland - its palaeoenvironments and mineralization. abstract of the English Zechstein Conference 1982, Nottingham.
- O'Neil, J. R., Clayton, R. N. and Mayeda, T. K., 1969. Oxygen isotope fractionation in divalent metal carbonates. *J. Chem. Phys.*, V. 51, p. 5549-5558.
- O'Neil, J. R., and Epstein, S., 1966. Oxygen isotope fractionation in the system dolomite-calcite - CO<sub>2</sub>. *Science*, V. 152, p. 198-201.
- Perry, E. A., and Hower, J., 1972. Late-stage dehydration in deeply buried pelitic sediments. *Am. Assoc. Petrol. Geol. Bull.*, B. 56, p. 2013-2021.
- Perry, E. C., and Tan, F. C., 1972. Significance of oxygen and carbon isotope determinations in early Precambrian charts and carbonate rocks of southern Africa. *Bull. Geol. Soc. Am.*, V. 83, p. 647-663.
- Peryt, T. M., 1976. Ingresja Morza Turynskiego (Gorhy Perm) Na Obszarze Monokliny Przedsudeckiej. *Rocznik Polskiego Towarzystwa Geologicznego.*, V. 46, p. 455-465.
- Piper, J. D. A., 1982. The Precambrian paleomagnetic record: the case for the Proterozoic supercontinent. *Earth Planet Sci. Lett.*, V. 58, p. 61-89.
- Piper, J. D. A., 1976. Paleomagnetic evidence for a Proterozoic super-continent. *Phil. Trans. R. Soc. Lond.*, V. 280, p. 469-490.
- Plumhoff, J., 1966. Marines Ober-Rotliegendes (Perm) in Zentrum des nordwestdeutschen Rotliegend-Beckens. *Erdöl u. Kohle*, V. 19, p. 713-720.
- Pompeckj, J. F., 1920. Kupferschiefer und Kupferschiefer Meer. *Z. Dtsch. Geol. Ges., Monatsber.*, V. 72, p. 329-339.
- Pompeckj, J. F., 1914. Das Mer des Kupferschiefers. *Branca-Festschrift, Leipzig*, p. 444-494.
- Powers, M. C., 1967. Fluid release mechanisms in compacting marine mud rocks and their importance in oil migration. *Am. Assoc. Petrol. Geol. Bull.*, V. 51, p. 1240-1254.



Presley, B. J., and Kaplan, I. R., 1968. Chagnes in dissolved sulphate and carboante from interstitial water of near-shore sediments. *Geochim. Cosmochim. Acta.*, V. 32, p. 1037-1048.

Preston, J. C., 1975. A theory of breccia formation in the south side of the Kirila Bombwe South Orebody. Unpub. Company Report, Z.C.C.M. Limited.

Radke, B. M., and Mathis, R. L., 1980. On the formation and occurrence of saddle dolomite. *Jour. Sed. Pet.*, V. 50, No. 4, p. 1149-1168.

Raiswell, R., 1982. Pyrite texture, isotopic composition and the availability of iron. *Am. Jour. Sci.*, V. 282, p. 1244-1263.

Ralston, I. T., 1961. Contribution to the symposium on the stratiform copper deposits in Africa. *Proc. of the Symp. on recent Dev. in the Occ of copper in stratiform copper dep. in Africa*, 2nd part tectonics, Lusaka.

Raybould, J. G., 1978a. Tectonic controls on Proterozoic stratiform copper mineralisation. *T.I.M.M.* V. 87, p. 79-86.

Raybould, J. G., 1978b. Duplication and related structures of the Kirila Bombwe South orebody. Unpub. Company Report, Z.C.C.M. Limited.

Raybould, J. G., 1978c. Cobalt distribution and mode of occurrence at Konkola Division. Unpub. Company Report, Z.C.C.M. Limited.

Rees, C. E., 1973. A steady state model for sulphur isotope fractionation in bacterial reduction processes. *Geochim. Cosmochim. Acta.*, V. 37, p. 1141-1162.

Rees, C. E., Jenkins, W. J., and Monster, J., 1978. The sulphur isotopic composition of ocean water sulphate. *Geochim. Cosmochim. Acta.*, V. 42, p. 377-381.

Renfro, A. R., 1974. Genesis of evaporite associated stratiform metaliferous deposits - A sabkha process. *Eco. Geol.*, V. 69, p. 33-45.

Rentzsch, J., 1974. The Kupferschiefer in comparison with the deposits of hte Zambian Copperbelt. *Gisement Stratiformes et Preovinces Cupriferes*. *Cent. Geol. Soc. Belg. Liege*, p. 1-34.

Richter-Bernburg, G., 1941. Geological relationships in the metal-bearing Kupferschiefer. *Arch. F. Lagerstättenforsch, N.F.*, No. 73.



Robinson, B. W., 1975. Carbon and oxygen isotopic equilibrium in hydrothermal calcites. *Geochem. Jour.*, V. 9, p. 43-49.

Robinson, B. W., and Kusabke, M., 1975. Quantitative preparation of SO<sub>2</sub> for <sup>34</sup>S/<sup>32</sup>S analysis from sulphides by combustion with cuprous oxide. *Analy. Chem.*, V. 47, No. 7, p. 1179-1181.

Roedder, E., 1981. Origin of fluid inclusions and changes that occur after trapping. In *Short Course in Fluid Inclusions, Applications to Petrology*. Edited by L. S. Hollister and M. L. Crawford, Min. Assoc. Canada, p. 101-129.

Rowlands, N. J., 1974. The geology of some Adelfidean stratiform copper occurrences. *Gisement Stratiformes et Provinces Cuprifères*, Cent. Geol. Soc., Belg., Liege, p. 419-427.

Rugman, G. M., 1977. Cobalt mineralisation in the Chambishi-Nkana basin. Unpub. Company Report, Z.C.C.M. Limited.

Russell, M. J., 1976. A possible Lower Permian age for the onset of ocean floor spreading in the northern North Atlantic. *Scott. Jour. Geol.*, V. 12, No.4, p. 315-323.

Russell, M. J., Solomon, M., and Walshe, J. L., 1981. The genesis of sediment-hosted exhalative zinc and lead deposits. *Min. Dep.*, V. 16, p. 113-127.

Ruxton, P., 1981. The sedimentology and diagenesis of copper bearing rocks of the southern margin of the Damara Orogenic Belt, Namibia and Botswana. Unpub. Ph.D. Thesis, University of Leeds.

Ryder, T. D., Fouch, T. D., and Elison, J. H., 1976. Early Tertiary sedimentation in western Uinta Basin, Utah. *Geol. Soc. Am. Bull.*, V. 87, No. 4, p. 496-512.

Rye, R. O., Schuiling, R. D., Rye, D. M., and Jansen, J. B. H., 1976. Carbon, hydrogen and oxygen isotope studies of the regional metamorphic complex at Naxos, Greece. *Geochim. Cosmochim. Acta.*, V. 40, p. 1031-1049.

Sackett, W. M., Eadie, B. J., and Exner, M. E., 1973. Stable isotope composition of organic carbon in recent Antarctic sediments. *Adv. in Organic Geochem.*, p. 661-671.

Sajgo, 1979. Hydrocarbon generation in a Neogene sequence (S. E. Hungary). In *Advances in Organic Geochemistry, Physics and Chemistry of the Earth*, V. 12, Edited by A. F. Douglas and J. R. Maxwell. Pergamon Press.



- Sakai, H., 1968. Isotopic properties of sulphur compounds in hydrothermal systems. *Geochem. Jour.*, V. 2, p. 29-49.
- Scholle, P. A., and Arthur, M. A., 1980. Carbon isotope fluctuations in Cretaceous pelagic limestones: Potential stratigraphic and petroleum exploration tool. *Am. Assoc. Petrol. Geol. Bull.*, V. 64, p. 67-87.
- Schumm, S. A., 1977. *The fluvial system*. John Wiley and Sons, p. 246-293.
- Schwarcz, H. P., and Burnie, S. W., 1973. Influence of sedimentary environment on sulfur isotope ratios in clastic rocks: A review. *Min. Dep.*, V. 8, p. 264-277.
- Schwellnus, J. E. G., 1961a. Bancroft-Nchanga Area. In *The Geology of the Northern Rhodesian Copperbelt*. Edited by F. Mendelsohn. MacDonald, London.
- Schwellnus, J. E., 1961b. A brief report on the geology and structure of Bancroft Mines. Unpub. Company Report, Z.C.C.M. Limited, Konkola Division.
- Sedgwick, A., 1829. On the geological relations and internal structure of the Magnesian Limestone, and the lower portions of the New Red Sandstone series in their range through Nottinghamshire, Derbyshire, Yorkshire and Durham, to the southern extremity of Northumberland. *Trans. Geol. Soc. Lond.*, V. 3, p. 37-124.
- Shackleton, R. M., 1976. Pan African structures. *Phil. Trans. R. Soc. Lond.*, VA280, p. 491-497.
- Shackleton, N. J., and Kennett, J. P., 1975. Paleotemperature history of the Cenozoic and the initiation of Antarctic glaciation, oxygen and carbon isotope analysis in DSDP Sites 277, 279 and 281. In *Initial Rep. D.S.D.P.*, Editors Kennett, J. P. and Houtz, R. E., v. 29, p. 743-756, U. S. Govt. Printing Office, Washington.
- Shearman, D. J., 1982. Evaporites of coastal sabkhas. In *Marine Evaporites*, Edited by W. E. Dean and B. C. Schreiber, S. E. P.M. Short Course No. 4, p. 6-43.
- Shearman, D. J., and Fuller, J. G., 1969. Anhydrite diagenesis, calcitization, and organic laminites, Winnipegosis Formation, Middle Devonian, Saskatchewan. *Bul. Canadian Pet. Geol.*, V. 17, No. 4, p. 496-525.
- Sheppard, R. A., and Gurde, A. J., 1973. Boron bearing potassium feldspar of authigenic origin in closed basin deposits. *U.S.G.S. J. Res.*, V. 1, p. 377-382.



Sheppard, S. M. F., and Schwarcz, H. P., 1970. Fractionation of carbon and oxygen isotopes and magnesium between coexisting calcite and dolomite. *Contrib. Min. Petrol.*, V. 26, p. 161-172.

Sibley, D. F., 1980. Climatic control of dolomitization, Seroe Domi (Pliocene), Bonaire, N. A.. In *Concepts and Models of Dolomitization*. Edited by D. Zenger, J. Dunham, and R. L. Ethington, Soc. Econ. Pleon. Min. Spec. Publ. No. 28, p. 247-258.

Siedlecka, A., 1972. Length slow chalcedony and relicts of sulphates: evidence of evaporitic environments in the Upper Carboniferous and Permian beds of Bear Island, Svalbard. *Jour. Sed. Petrol.*, V. 42, p. 812-816.

Smejkal, V., Hladikova, J., and Pisa, M., 1971. Izotopicke slozenc nekterych zilnych kalcitv a dolomitu. *Cas. Min. Geol.*, V. 16, p. 423-434.

Simmonds, J. R., 1980. Significance of the Baluba orebodies with respect to Zambian copper-cobalt mineralisation. Unpub. Ph.D. Thesis, University College, Cardiff.

Smith, D. B., 1984. Red basal Permian sands: a new discovery in National Coal Board boreholes off Sunderland, North-East England. *Proc. Yorks. Geol. Soc.*, V. 44, P. 4, No. 3, p. 497-500.

Smith, D. B., 1980. The evolution of the English Zechstein basin. In: *Contr. Sedimentology*, Ed. T. Peryt, V. 9, p. 7-34.

Smith, D. B., 1979. Rapid marine transgressions nad regression of the Upper Permian Zechstein sea. *Jour. Geol. Soc. Lond.*, V. 136, P. 2, p. 155-157.

Smith D. B., 1970a. Permian and Trias. In: *Geology of Durham County*: edited by G. Hickling, Trans. Nat. Hist. Soc. Northumb., V. 41, p. 66-91.

Smith D. B. 1970b. The Paleography of the English Zechstein. In: *Third Symposium on Salt*, Eds.: J. L. Rau and L. F. Dellwig, Northern Ohio Geol. Soc., Cleveland, Ohio, p. 20-23.

Smith D. B., Brunstrom, R. G. W., Manning, P. I., Simpson, S., and Shotton, F. W., 1974. A correlation of Permian rocks in the British Isles. *Jour. Geol. Soc. Lond.*, V. 130, p. 1-45.

Smith, J. V., and Stenstrom, R. C., 1965. Electron-excited luminescence as a petrologic tool. *Jour. Geol.*, V. 73, p. 627-635.



Snelling, N., Hamilton, E. I., Drysdale, A. R., and Stillman, C. J., 1964. A review of age determinations from Northern Rhodesia. *Eco. Geol.*, V. 59, p. 961-981.

Southworth, C., 1980. Sedimentology of the Feldspathic Quartzite - Nchanga Open Pit, South face between 18E-30½E. Unpub. Company Report, Z.C.C.M. Limited, Chingola Division.

Spears, D. A., 1979. Towards a classification of shale. *Jour. Geol. Soc. Lond.*, V. 137, P. 2, p. 125-129.

Stablein, N. K., and Dapples, E. C., 1977. Feldspars of the Tunnel City Group (Cambrian), Western Wisconsin. *Jour. Sed. Pet.*, V. 47, p. 1512-1538.

Steel, R. J., 1976. Devonian basins of Western Norway - Sedimentary response to tectonism and to varying tectonic context. *Tectonophysics*, V. 36, p. 207-224.

Steel, R. J., 1974. New Red Sandstone floodplain and piedmont sedimentation in the Hebridean Province. *Jour. Sed. Petrol.*, V. 44, p. 336-357.

Stendal, H., 1978. Geochemical copper prospecting by use of inorganic drainage sediment sampling in Central East Greenland. *T.I.M.M.*, V. 88, P. 5.

Stonely, H. M. M., 1958. The upper Permian flora of England. *Bull. Br. Mus. Nat. Hist. (Geology)*, V. 3, p. 295-337.

Sweatman, T. R., and Long, J. V. P., 1969. Quantitative electron-probe microanalysis of rock-forming minerals. *Jour. Petrol.*, V. 10, p. 332-379.

Sweeney, M. A., 1979. The economic viability of mining mineralised footwall ground at No. 1 shaft. Unpub. Company Report, Z.C.C.M. Limited, Konkola Division.

Sweeney, R. E. and Kaplan, I. R., 1973. Pyrite framboid formation: Laboratory synthesis and marine sediments. *Eco. Geol.*, V. 68, p. 618-634.

Taylor, H. P., 1974. The application of oxygen and hydrogen isotope studies to problems of hydrothermal alterations and ore deposition. *Econ. Geol.*, V. 69, p. 843.

Taylor, H. P., and O'Neil, J. R., 1977. Stable isotope studies of metasomatic Ca-Fe-Al-Si skarns and associated metamorphic and igneous rocks, Osgood Mountains, Nevada. *Contr. Min. Pet.*, V. 63, p. 1-49.



Thode, H. G., and Monster, J., 1965. Sulfur isotope geochemistry of petroleum, evaporites and ancient seas. In: Fluids in Subsurface Environments. Edited by A. Young and J. E. Galley, A. A. P. Geol., Mem. 4, p. 367-377.

Trudinger, P. A., and Chambers, L. A., 1973. Reversibility of bacterial sulfate reduction and its relevance to isotopic fractionation. Geochim. Cosmochim. Acta., V. 37, p. 1775-1778.

Turner, P., 1980. Continental red beds. Developments in Sedimentology 29, Elsevier, Amsterdam.

Turner, P., and Magaritz, M. (in press). Chemical and isotopic studies of a Marl Slate core (V78): influence of freshwater influx into the Zechstein Sea. English Zechstein and Related Basins, Ed: D. Smith, Geol. Soc. Lond., Spec. Pub.

Turner, P., Vaughan, D. J., and Whitehouse, K. I., 1978. Dolomitization and the mineralization of the Marl Slate (N. E. England). Min. Dep., V. 13, p. 245-258.

Unrug, R., 1983. The Lufilian Arc: A microplate in the Pan-African Collision Zone of the Congo and the Kalahari craton. Precamb. Res., V. 21, p. 181-196.

Urey, H. C., 1947. The Thermodynamic properties of isotopic substances. Jour. Chem. Soc., p. 562-581.

Vaes, J. F., 1962. A study of the metamorphism of the Roan sediments at the Musoshi copper deposit and its consequences. Musee. R. Oe L'Af. Cent. Tervuren, Belg., Ser. 8, P. 43, p. 1-30.

Van Eden, J. G., 1974. Depositional and diagenetic environments related to sulphide mineralization, Mufulira, Zambia. Econ. Geol., V. 69, p. 59-79.

Van Wijhe, D. H., Lutz, M., and Kaasschieter, J. P. H., 1980. The Rotliegend in the Netherlands and its gas accumulations. Geol. Mijnbouw., V. 59, p. 3-24.

Veizer, J., and Hoefs, J., 1976. The nature of  $O^{18}/O^{16}$  and  $C^{13}/C^{12}$  secular trends in sedimentary carbonate rocks. Geochim. Cosmochim. Acta., V. 40, p. 1387-1395.

Veizer, J., Hober, W. T., and Wilgus, C.K., 1980. Correlation of  $^{13}C/^{12}C$  and  $^{34}S/^{32}S$  secular variations. Geochim. Cosmochim. Acta., V. 44, p. 579-587.

Vergnaud-Grazzini, C., Ryan, W. B. F., and Cita, M. B., 1977. Stable isotope fractionation climatic change and episodic stagnation in the eastern Mediterranean during the late Quaternary. Marine Micropaleor., V. 2, p. 353-370.



- Vine, J. D., and Toutelot, E., 1970. Geochemistry of Black Shale Deposits - A Summary Report. *Eco. Geol.*, V. 65, p. 253-272.
- Vink, B. W., 1972. Sulphide mineral zoning in the Baluba Orebody, Zambia. *Geol. Mijnbouw.*, V. 51, No. 3, p. 309-315.
- Visser, C., 1974. Mineralogical, petrological and chemical investigations of thirty Chibuluma West drillcore samples. Unpub. Company Report No. RDF/92/74, R.C.M. Limited.
- Voet, H. W., and Freeman, P. V., 1972. Copper orebodies in the basal Lower Roan meta-sediments of the Chingola open pit area Zambian Copperbelt. *Geol. Mijnbouw.*, V. 51., No. 3, p. 299-309.
- Vogel, J. C., and Urk, H. Van., 1975. Isotopic composition of groundwater in semi-arid regions of southern Africa. *Jour. Hydrol.*, V. 25, p. 23-26.
- Wakefield, J., 1978. Samba: a deformed porphyry-type copper deposit in the basement of the Zambian Copperbelt. *T.I.M.M.*, V. 87, p. B43-52.
- Walker, T. R., 1976. Diagenetic origin of continental red beds. In: *The continental Permian in Central, West and South Europe*, H. Flake (Ed.), p. 240-282.
- Walker, T. R., 1967. Formation of red beds in modern and ancient deserts. *Geol. Soc. Am. Bull.*, V. 78, P. 3, p. 353-368.
- Walker, T. R., Waugh, B., and Grone, A. J., 1978. Diagenesis in first cycle desert alluvium of Cenozoic age, Southwestern United States and Northwestern Mexico. *Bull. Geol. Soc. Am.*, V. 89, p. 19-32.
- Waugh, B., 1978. Authigenic K-feldspar in British Permo-Triassic Sandstones. *Jour. Geol. Soc. Lond.*, V. 135, p. 51-56.
- Waugh, B., 1970. Formation of quartz overgrowths in the Pentrich Sandstone (Lower Permian) of northwest England as revealed by scanning electron microscopy. *Sedimentology*, V. 14, p. 309-320.
- Weber, J. M., Deines, P., Weber, P.H., and Baker, P. A., 1976. Depth related changes in the  $^{13}\text{C}/^{12}\text{C}$  ratio of skeletal carbonate deposited by the Caribbean reef-frame building coral *Montastrea Annualris* further implications of a model for stable isotope fractionation by scleractinian corals. *Geochim. Cosmochim. Acta.*, V. 40, p. 31-39.



Wedepohl, K. H., 1980. The geochemistry of the Kupferschiefer bed in central Europe. European Copper Deposits, Belgrad, p. 129-135.

Wedepohl, K. H., 1978. Handbook of Geochemistry, Springer-Verlag, p. 1613-6.

Wedepohl, K. H., 1964. Untersuchungen am Kupferschiefer in Nordwestdeutschland; ein Beitrag zur Deutung der Genese bituminöser Sedimente. Geochim. Cosmochim. Acta., V. 28, p. 305-364.

Weissert, H., McKenzie, J., and Hochuli, P., 1979. Cyclic anoxic events in the early Cretaceous Tethys Ocean. Geology, V. 7, p. 147-151.

Westoll, T. S., 1941. The Permian fishes *Dorypterus* and *Lekanichthys*. Proc. Zool. Soc. Lond., V. B111, p. 39-58.

Wills, L. J., 1973. A palaeogeological map of the Palaeozoic floor below the Permian and Mesozoic formations in England and Wales. Geol. Soc. Lond., Memoir. 7, p. 1-23.

Whyte, R., and Green, M., 1971. Geology and paleogeography of Chibulima West Orebody. Econ. Geol., V. 66, p. 411-424.

Yakowitz, H., Myklebust, R. L., and Heinrich, K. F. J., 1973. Frame: An on line correction procedure for quantitative electron probe microanalysis. N.B.S. Tech. Note 796.

Ziegler, P. A., 1982a. Faulting and graben formation in western and central Europe. Phil. Trans. R. Soc. Lond., V. 305A, p. 113-143.

Ziegler, P. A., 1982b. Geological atlas of Western and Central Europe. Elsevier, Amsterdam, p. 130.